Scale-up of a High-Technology Manufacturing Startup: Improving Product Reliability Through Systematic Failure Analysis and Accelerated Life Testing

by

Ali Shabbir

B.A.Sc. Mechanical Engineering,
University of Waterloo (2014)

Submitted to the Department of Mechanical Engineering
in partial fulfillment of the requirements for the degree of

Master of Engineering in Manufacturing

at the

MASSACHUSETTS INSTITUTE OF TECHNOLOGY

September 2015

Signature redacted

Author .....
Department of Mechanical Engineering
August 7, 2015

Signature redacted

Certified by .....
David E. Hardt
Ralph E. and Eloise F. Cross Professor of Mechanical Engineering
Thesis Supervisor

Signature redacted

Accepted by .....
David E. Hardt
Chairman, Department Committee on Graduate Theses

Scale-up of a High-Technology Manufacturing Startup: Improving Product Reliability Through Systematic Failure Analysis and Accelerated Life Testing

by
Ali Shabbir

Submitted to the Department of Mechanical Engineering
on August 7, 2015, in partial fulfillment of the
requirements for the degree of
Master of Engineering in Manufacturing

Abstract

Ensuring product reliability is a key driver of success during the scale-up of a high-technology manufacturing startup. Reliability impacts the company image and its financial health, however most manufacturing startups do not have a solid understanding of their product's reliability. The purpose of this thesis is to introduce systematic failure analysis to the engineering design process and to establish a framework for testing and analyzing product life so that imperative business decisions and design improvements could be made with regards to reliability. A detailed study and implementation of these process improvements to address reliability issues was conducted at New Valence Robotics Corporation (NVBOTS) in Boston, Massachusetts.

Systematic failure analysis was achieved through the creation and implementation of Failure Modes and Effects Analysis (FMEA) procedures. A single FMEA iteration was performed on the NVPro printer to identify the top risk component—linear ball bushings—for detailed life analysis. Following an in-depth investigation of potential failure modes of the linear bushings, an Accelerated Life Test (ALT) was designed using Design of Experiments (DOE) principles. An accompanying test apparatus with mechatronic control was also designed. The ALT was not actually executed but representative data was analyzed for illustrative purposes using the General Log-Linear (GLL) life-stress relationship and a 2-parameter Weibull distribution for the accelerating stresses of mechanical load and lubrication. The work performed provides NVBOTS and similar high-technology manufacturing startups a complete starting point for systematically analyzing their product's reliability and quantitatively evaluating its life in a resource efficient way.

Thesis Supervisor: David E. Hardt
Title: Ralph E. and Eloise F. Cross Professor of Mechanical Engineering

Acknowledgments

This thesis is the culmination of months of direct, and years of indirect, contribution from multiple people. I would like to express my sincerest gratitude and thank the following people:

Professor David Hardt, my thesis advisor, for your valuable guidance throughout the project and in writing this thesis, invaluable advice about life, and contagious passion for manufacturing.

Rahul Chawla and Derek Straub, my project teammates, MEngM classmates, and great friends for always being there in any capacity. This project and my thesis would not have been possible without you. The lasting memories created during our shared MEngM experience will always stay with me.

Mateo Peña Doll, VP Engineering at NVBOTS, for your continuous support of all project work and help propelling the project to successful completion.

NVBOTS, for sponsoring the project and supporting the MEngM program at MIT, and specifically AJ Perez, CEO, for your enthusiasm for manufacturing and entrepreneurship that has inspired me to someday pursue the same.

Jose Pacheco and others behind the scenes within the MEngM program, for managing this incredible program and making it an enriching experience.

My parents, for your unconditional love, unwavering support, and constant encouragement to be the best I can be. I would not be where I am today without you.

My brother Omar, for your support and admiration that motivates me to achieve my goals, one of which is to one day be as great of a person as you are.

My sister Sarah, for always putting a smile on my face and reminding me there is more to life than work.

"3PC" and "PHC", for keeping me sane with your friendship and brotherhood.

And most of all, Anaum, for always being there for me unconditionally, for encouraging me to pursue my ambitions, for being my reason to succeed, and for a few hundred other things that would take the rest of the thesis to cover.

Contents

List of Figures

List of Tables

Chapter 1

Introduction

There are two types of startup businesses in the world: those that scale-up and those that do not. The businesses that do not scale up either fail or settle into a truly small business with little or no growth potential.[1] These so-called lifestyle businesses have their place within the economy and among entrepreneurs who are perfectly at peace with running a small business. However, the businesses that do scale-up are the ones looking to change the world, impact customers lives in a profound way, and obviously, make significant financial gains along the way [1].

Scale-up in entrepreneurial business refers to the process of rapid growth and expansion of a company to adapt to a larger workload without compromising performance, revenues, and operational controls [2]. Scaling up can only occur once a startup has validated its business model through repeat revenue generation [2]. Once the foundation is in place, rapid growth in market access, employees, operations, and revenues can occur.

Scaling up is an absolute necessity for those startup businesses funded by external investors such as angel investors and venture capital (VC) firms. Venture capitalists (VCs) invest in early-stage startups when the risk is high, the technology is unproven, and the market is uncertain, but the potential upside is also very high. In return, they own equity in the company and demand a significant return on their investment within a short period of time, achieved through either sale to or merger with another company (merger and acquisition, or M&A) or less commonly, registering as a publicly traded company via an initial public offering (IPO). The significant investor pressure necessitates the need for scaling up the business as soon as feasible.

However, scale-up requirements significantly depend on the type of business. Software by nature is very scalable. The initial investment is spent on developing the back-end software and user experience. Once completed and released, subsequent iterations only cost a fraction of the initial development cost and time. Software also does not require significant capital investment, has almost instant global market reach via the Internet, and has a very rapid lifecycle of only a few years [3]. By far, software startups are the easiest to scale-up and thus have commanded the largest amount of VC attention and funding [4].

[1] According to data collected from the U.S. Department of Commerce, Bureau of the Census, and U.S. Department of Labor, 592,410 businesses closed and 28,322 declared bankruptcy in 2007 [1].

Startups involving a physical product, such as in consumer goods, manufacturing, and high-technology industries, or startups involving strict regulatory requirements such as in the biopharmaceuticals industry do not have the same luxuries as software or service-based startups. Significant up-front capital costs, a high burn-rate[2], and a longer horizon before a sizeable return on investment is realized are additional barriers to scale-up that causes VCs to shy away from funding startups in these industries and instead focus their funds on less risky soft startups, despite being less profitable in the long run [3].

Scale-up is absolutely critical even for companies without the added pressure from VCs. A company is only solvent and in business as long as it has sufficient liquid assets to meet current liabilities. Without a plan in place to rapidly increase company revenues, and the fortitude to execute the plan, the business will quickly be unable to meet its liabilities and become insolvent.

However, the financial risks discussed such as raising investor funding or generating revenues are only one type of risk faced by startups during scale-up. A risk by definition is any situation where there is a possibility of an outcome resulting in the loss of something of value [1]. Unforeseen circumstances and their negative consequences in startup businesses manifest themselves within the following types of risks, adapted from Hirai [1]:

Market the possibility of insufficient demand for the offering at the chosen price. True market demand is only realized once the company tries to sell; everything up until then is speculation.

Competitive the possibility of competitors having a better product, being first-to-market, deliberately underselling your offering, filing intellectual property disputes, poaching employees, et cetera.

Technology and operational any variety of risks associated with product design, functionality as intended, manufacturability, product quality and reliability, production and distribution logistics, supplier management, et cetera.

Financial aside from raising investor funding and generating revenues, there are risks associated with customer credit (defaulting on payments), commodity prices, currency exchange rates, interest rates, price of assets used as collateral, et cetera.

People any number of risks associated with employees of the company, their fit with corporate culture and vision, their productivity, the necessary combination of experience, contacts, and skill, et cetera.

Legal and regulatory any number of risks associated with corporate governance, taxation, intellectual property, liability claims, and regulatory approval.

Systemic risks that threaten the viability of entire market and not just one firm, such as fuel costs affecting the entire airline industry.

[2]Burn rate is the amount of cash a company spends per month.

All these risks can be systematically identified, monitored, and mitigated through appropriate risk management which begins with driving a culture of risk management throughout the organization. The technology and operational risks associated with a high-technology manufacturing startup are further explored in the subsequent section.

1.1 High-Technology Manufacturing Startups

Manufacturing is well regarded as the engine that drives innovation. The U.S. Bureau of Economic Analysis has determined that for every dollar spent on manufacturing, it generates $1.48 in economic activity [5]. Manufacturing only represents 12% of the U.S. Gross Domestic Product (GDP) and 9% of U.S. jobs, but two-thirds of all private research and development funding and employs one-third of all engineers [5].

Increasingly, the innovation behind manufacturing, whether it is new products or processes, is found in smaller startups rather than larger corporations [3]. Often these innovations come out of research laboratories at universities across the nation, or through companies founded by employees of larger corporations [3]. VC funding allows these startups to prove their technology, however when it comes time to scale-up, VCs prefer to exit via an M&A with a large corporation and let them scale-up in-house.[3]

High-technology manufacturing startups face a significant barrier to scale-up due to upfront capital investments required before production of their physical product can begin. This poses a financial risk well known within the entrepreneurial ecosystem of VCs and startups. However, there are significant risks associated with the technology and operational side of the business as well, specifically associated with manufacturing of the product that are further discussed in the following section.

1.1.1 Risks Associated with Manufacturing Scale-up

High-technology startups often mistake a successful prototype or the first iteration of the product as the scaling product, and the first customers as scaling users [6]. This is hardly ever the case. The first customers are typically lead users or early adopters that provide input for improvement. In fact these early sales should be thought of as market research input [6]. Early customers also are willing to put up product design and manufacturing quality shortfalls always present in the first product iteration; something that the mass market would reject. Startups often try to include as many features as possible in their initial offering in order to attract as many customers within their target market as possible. In doing so they lose focus of their most basic features, the competitive advantage that would win over their customers in the first place. The scaling customers prefer a simple, robust product with the basic differentiating feature [7].

[3] An example of this is DuPont's acquisition of Uniax in 2000, a start-up spun out University of California Santa Barbara. Uniax developed organic light-emitting diodes (OLEDs). It was only in late 2011, after 11 years of in-house development and scale-up that DuPoint announced the first commercialization project, under license to a major display manufacturer [3].

Quality and reliability are the most important features of any product. Marc Barros, serial entrepreneur and former CEO of Contour LLC, an action sports camera company, reflected on his experience with the following: "Shipping quality devices is by far the hardest part of building a hardware company. Customers don't care about how small you are or the difficulties you face. They expect you deliver on and surpass on your promise not just once, but multiple times, over thousands of units" [7].

Achieving this level of quality and reliability is a tremendous effort that involves the entire company to be focused on documenting and fixing problems during both initial product development and production scale-up. Having the right talent driving the manufacturing scale-up is critical. They must have a combination of skills, industry knowledge and experience, and network of contacts to ensure the product is manufactured at the highest level of quality [3]. Barros recommends also having at least one person solely dedicated to product testing, and quality and reliability improvement, and also working with an experienced production engineer from the beginning of the design phase to ensure a quality, manufacturable product with high yield rates. The company must always be willing to compromise of materials, methods, and location of production to ensure the highest level of quality and reliability is achieved at the lowest cost.

It is very common for a startup to outsource production to contract manufacturers and suppliers. Contract manufacturers, both domestic and foreign, are an invaluable source of in-depth volume manufacturing knowledge. However, it is critical to select suppliers that have the right specialized skills required for the startups product, prioritize speed and quality over cut-throat cost reduction, and are willing to work with company to improve the entire production process [3]. There is significant tactic knowledge during the initial pilot production runs that is very complex, and not easily reduced to simple instruction [8]. Therefore, face-to-face time with suppliers on-site is required during these stages to qualify their process and continuously improve, and more importantly, take the leanings back to the company.

Finally, scaling up production requires diligent effort in tracking the company's cash cycle. Payment for production is usually due upfront for a startup that is not well established in the industry yet, but revenues from sales are not expected for months [9]. Also there are large cash implications associated with sustaining and customer service if the product quality suffers and customers require repairs or replacements. This could leave the company in a cash-flow insolvency situation. Careful planning in terms of supply contracts, payment terms, and product sustaining must be executed from before the scale-up begins.

1.2 Research Motivation

New Valence Robotics Corporation (NVBOTS), founded in March 2013, is a Boston, Massachusetts-based robotics startup company that has developed the world's first fully automated cloud 3D printing management suite [10]. The 3D printing hardware, called the NVPro, is based on the material extrusion additive manufacturing process. NVBOTS is in the process of completing its in-house pilot production run and is

faced with the problem of scaling-up its production to meet customer demand. The scale-up project is the result of collaboration between the Massachusetts Institute of Technology (MIT) and NVBOTS. The project was a team effort conducted by the author, Rahul Chawla [11], and Derek Straub [12], all students in the Master of Engineering in Manufacturing (MEngM) program at MIT, between February and August of 2015.

1.2.1 Overall Problem Statement

The MEngM team consulted on the overall scale up project and specifically focused on integrating NVBOTS' business model into its operations. NVBOTS does not directly sell its printers to customers but rather leases them on 5-year terms, which includes a service package. This unique business model requires careful consideration by engineering and production as the company scales up.

Product reliability and quality were identified to be the most important factors to focus on during the scale-up process. As NVBOTS transitions from producing a few units per month entirely in-house to producing hundreds of units per month in partnership with contract manufacturers in the near future, a significant shift in current engineering and production operations would need to occur. The costs associated with unreliable or sub-par quality product are unsustainable with rapid growth.

Analyzing the complete product value chain–from design, to incoming supplier parts, assembly, and the complete product–identified opportunities for process improvement. These opportunities formed the basis of each MEngM team member's individual sub-project and thesis, further discussed in Section 1.2.2.

In addition to specific improvement opportunities, the research and work completed by the MEngM team also included:

- Establishing a framework and foundation of critical processes for future implementation;
- Inculcating discipline, structure, and industry best practises in engineering and production operations through learnings from industry experience; and
- Providing case studies of process improvement implementation at NVBOTS as reference for future use.

1.2.2 Overview of Sub-Projects

Analyzing the complete product value chain identified specific opportunities for process improvement with regards to product reliability and quality. The first subproject focused on early stages of the value chain by analyzing incoming part quality. As hardware startups initiate operation, their main focus is on product development efforts. When they scale up, they need to give more importance to suppliers, quality control and inspection procedures. This project focused on developing a framework for and

analyzing these attributes. Analyzing the outcomes of using this framework, key recommendations were made in this project for tolerancing techniques, data acquisition and inspection procedure. Also, suggestions were made to streamline strategy and operations and make full use of network effects. Chawla conducted this project and the reader is referred to his thesis for all details [11].

The second subproject focused on establishing a proper failure mitigation strategy at NVBOTS consisting of failure tracking, analysis, and failure resolution. The aim of this project was to create a foundation, framework, and methodology for NVBOTS to use in order to mitigate costly failures throughout the product life cycle. Failures, especially those that occur in the hands of the customer, can have devastating consequences to any company and even more so to a startup. This project details a structured plan to capture all failure data, how to analyze it statistically and objectively based on its cost to the company, and how to best resolve the failure for future units. As for profit companies exist to produce profits, the failure mitigation strategy is based on a least-cost model. The goal is to minimize the cost impact of failures by preventing them from occurring or by lessening their impact though multiple methods. This project details how to learn from failures and how use that knowledge to create a product with increased reliability, quality, and performance, while reducing manufacturing and service costs. This is critical for NVBOTS as the cost of failures will only increase as they begin to scale up production. Establishing a proper failure mitigation strategy will allow them to continually reduce the cost and impact of failures, allowing them to successfully scale up and providing them a commanding competitive advantage for the future. Straub conducted this project and the reader is referred to his thesis for all details [12].

The third subproject is the subject of this thesis. It focused on product reliability and life and was conducted by the author. A reliable product is absolutely critical to NVBOTS and their leasing business model. The costs associated with repeatedly servicing an unreliable product are unsustainable as the business scales up, and there is the potential to lose the customer entirely if unreliability is persistent. However, currently there is no estimate of the life of the NVPro product. Furthermore, there are no processes in-place to predict, analyze, and test potential in-service failures and mitigate these risks during product development or production. These oversights pose a significant financial risk if the future costs of service are unmanageable.

Therefore, this subproject focused on two key process improvements. The first was to implement Failure Modes and Effects Analysis (FMEA), a structured approach to predict future in-service failure modes and understand their impact. The second was to establish a methodology of actually testing the product to determine its reliability and predict its life. This was accomplished through Design of Experiments, accelerated life testing, and statistical analysis. A theoretical background on statistical reliability analysis was provided along with the experimental hardware design required to estimate the life of a product. Finally, the subproject served to establish a culture of reliability through systematic testing and analysis.

The opportunities identified and covered in detail between the three theses provide recommendations for near term implementation, as this would be of immediate benefit to NVBOTS. However, each subproject is also a process improvement that should be

adopted by operations to ensure long-term success during the entire scale up process.

1.3 Thesis Overview

As previously mentioned, the overall problem statement for the project was to scale-up production at NVBOTS as the company grows. This thesis specifically focuses on ensuring product reliability as the company grows and production scales up to match increased demand. This was imperative to NVBOTS as their business model is based on leasing the printer to customers, and any costs associated with servicing unreliable printers is the responsibility of the company.

1.3.1 Thesis Objective and Scope

The objective of this thesis was two-fold. The first was to introduce systematic failure analysis and Design for Reliability (DFR) to the engineering design process. This was achieved through the creation and implementation of Failure Modes and Effects Analysis (FMEA) procedures, and a single iteration was performed on the first generation of the NVPro printer. The second objective of the thesis was to establish a framework for testing and analyzing product life so that imperative business decisions and design improvements could be made with regards to reliability. The reliability study first identified the most significant failure modes for the machine. Product reliability was then estimated through Design of Experiments (DOE), accelerated life testing, and statistical analysis of a single high-failure-risk component. The outcome of the reliability study were the theoretical and hardware components necessary to execute a controlled accelerated life test.

The scope of the FMEA iteration was limited to the first generation of the NVPro printer, and the scope of the product life estimate was limited to the determining the reliability of the single most critical component in the printer as identified by FMEA: a 10mm linear ball bushing used to enable linear motion of the print head. However, a complete framework for future FMEA and accelerated life testing through DOE and statistical analysis was presented and strongly encouraged for adoption by the NVBOTS engineering.

1.3.2 Thesis Structure

The thesis is structured into multiple chapters that provide the necessary background information on the project and also follow the logical progression of the reliability study. Chapter 1 covered various risks involved in scaling up a manufacturing startup and provided motivation for the project. Chapter 2 presents an overview of the additive manufacturing industry written by Straub [12] and included here verbatim. Chapter 3 presents background on NVBOTS and an analysis of its competitive strategy written by Chawla [11] and included here verbatim. Chapter 4 presents the Failure Modes and Effects Analysis methodology, identification of the top risk

component, and literature review on failure modes of linear bushings. Chapter 5 covers accelerated life testing and associated statistical analysis background. Chapter 6 describes the experimental design and hardware design of a test appartus employed in accelerated life testing of the linear bushings. Chapter 7 presents representative results of the accelerated life test and illustrates the statistical analysis necessary to obtain reliability estimates. Finally, Chapter 8 summarizes the work performed and provides a roadmap for future work by NVBOTS and other researchers.

Chapter 2

Overview of the Additive Manufacturing Industry

2.1 Additive Manufacturing Overview

Additive Manufacturing (AM) is a field of manufacturing processes that create objects through successive addition of layers of material. Generally, the parts are built from digital three-dimensional (3D) computer aided design (CAD) data, but this need not always be the case. AM has been referred to by many different names, 3D Printing, Rapid Prototyping, and Freeform Fabrication, just to name a few; but the term Additive Manufacturing best differentiates this field of manufacturing processes from conventional manufacturing techniques, which usually involve subtraction, deformation, or formation of material as well as changes to material properties. AM has been around commercially since the late 1980s, but the industry really gained traction and momentum in the 2000s and it has continued to increase ever since, with an compound annual growth rate of 33.8% over the last three years [13]. In 1995, AM was only a $295 million industry; as of 2014 the AM industry has grown to $4.1 billion and is expected to exceed $12.7 billion by 2018 and $21.1 billion by 2020 [13].

AM has opened up the design space to engineers, designers, and artists allowing them to produce complex geometry that was once impossible or restricted by cost and/or time. Geometrical freedom is just one of the many benefits offered by AM. Speed[1], customization, increased part performance, flexibility, material and energy efficiency, in-house manufacturing, and reduction of the design cycle are some of the many benefits realized through use of AM. AM is a tool for part production, but it is not the solution to all manufacturing needs as there are some drawbacks. Cost, speed, and time are unfavorable compared to conventional manufacturing when dealing with parts of simple geometry. Surface finish, limited materials, material properties, and lack of standards are some of the other drawbacks to AM. The key for users is to

[1]Speed here is defined as the lead time from when a design is released for manufacture to when the first article is received. However, the actual manufacturing process time for complex geometries is usually faster than conventional subtractive methods. Therefore, speed can also refer to process time to convert raw material to finished good for complex geometries.

understand the capabilities and limitations and to know when it is best to use AM or rather chose a conventional manufacturing process instead.

Depending on the desired object(s) and machine to be used there is a certain work flow process to go from CAD data to having a physical part. This process can vary slightly for each job and machine but in general all AM processes follow the same seven generic steps adapted from Gibson. The seven steps, in order are: CAD, Conversion to STL, STL Slicing and Transfer to AM Machine, Machine Setup, Build, Removal, and Post Processing [14]. There are many factors such as geometry, material, intended use, cost, speed, etc. that factor into which AM machine to use for any given build. The American Society of Testing and Materials, now known as ASTM International, has categorized all of the current machines by their AM process. There are currently seven process methodology or technology categories defined by ASTM International: Binder Jetting, Directed Energy Deposition, Material Extrusion, Material Jetting, Powder Bed Fusion, Sheet Lamination, and Vat Photopolymerization [15]. The seven generic steps and seven AM technology categories will be described in more detail in the immediately following sections.

2.2 General AM Process Work Flow

The detailed AM process will vary slightly from machine to machine and from build to build but these seven generic steps cover the majority of all AM process work flows. Depending on the machine, part(s), orientation of part, material, build quality, support material required, etc. certain steps will be more extensive than others, while some may be skipped all together. Regardless, the following steps derived from Gibson portray the typical work flow required to transform CAD data into a physical object via AM [14]:

Step 1: CAD All AM parts must start from a software model that fully describes the geometry. This can involve the use of almost any CAD solid modeling software, but the output must be a 3D solid or surface representation. Reverse engineering equipment (e.g., laser and optical scanning) can also be used to create this representation.

Step 2: Conversion to STL Nearly every AM machine accepts the STL file format, which has become a de facto standard, and nowadays nearly every CAD system can output such a file format. This file describes the external closed surfaces of the original CAD model and forms the basis for calculation of the slices.

Step 3: STL File Manipulation/Slicing/Transfer to AM Machine The order of these three sub-steps may vary, but the STL file describing the part must be transferred to the AM machine. There may be some general manipulation of the file so that it is the correct size, position, and orientation for building. The STL file is sliced into build layers and support material and corresponding support layers are generated, if need be. These slices or layers represent the physical

build layers of material during the build. STL manipulation and slicing may occur on the AM machine or at a computer before transfer.

Step 4: Machine Setup The AM machine must be properly set up prior to the build process. Such settings would relate to the build parameters like the material constraints, energy source, layer thickness, timings, etc. Setup usually involves cleaning, clearing, and resetting of the build area altered from previous builds.

Step 5: Build The part is built out of the given material(s) layer by layer according to the slice data. Building the part is mainly an automated process and the machine can largely carry on without supervision. Only superficial monitoring of the machine needs to take place at this time to ensure no errors have taken place like running out of material, power or software glitches, etc. Newer and more industrial machines are beginning to monitor for errors and anomalies in order to notify the operator.

Step 6: Removal Once the AM machine has completed the build, the parts must be removed. This may require interaction with the part, raw material, and machine, which may have safety interlocks to ensure for example that the operating temperatures are sufficiently low or that there are no actively moving parts. Removal must be performed carefully and by experienced operators as many parts are damaged during this step.

Step 7: Post-processing Once removed from the machine, parts may require an amount of additional work before they are ready for use. Parts may be weak at this stage or they may have supporting features that must be removed. This therefore often requires time and careful, experienced manual manipulation. Post processing is usually the most laborious step and yet the most commonly unknown step for those outside of the industry.

2.3 Additive Manufacturing Technologies

In 2014 there were 49 industrial grade AM machine manufacturers, many selling multiple models. In the same year there were hundreds of mostly smaller companies selling desktop grade[2] machines as well [13]. All machine models are similar in that they build sequentially, layer by layer, defined by the slice data of the 3D CAD model. Yet all these AM machine models are different from one another in many ways, each with the technology and features the manufacturer believes their customers want. Still, they all fall into one of the seven AM process/technology categories defined by ASTM International. Below are the definitions of the seven standard AM process categories according to ASTM International [15]:

[2]Industrial grade and desktop grade machines are defined in Section 2.5

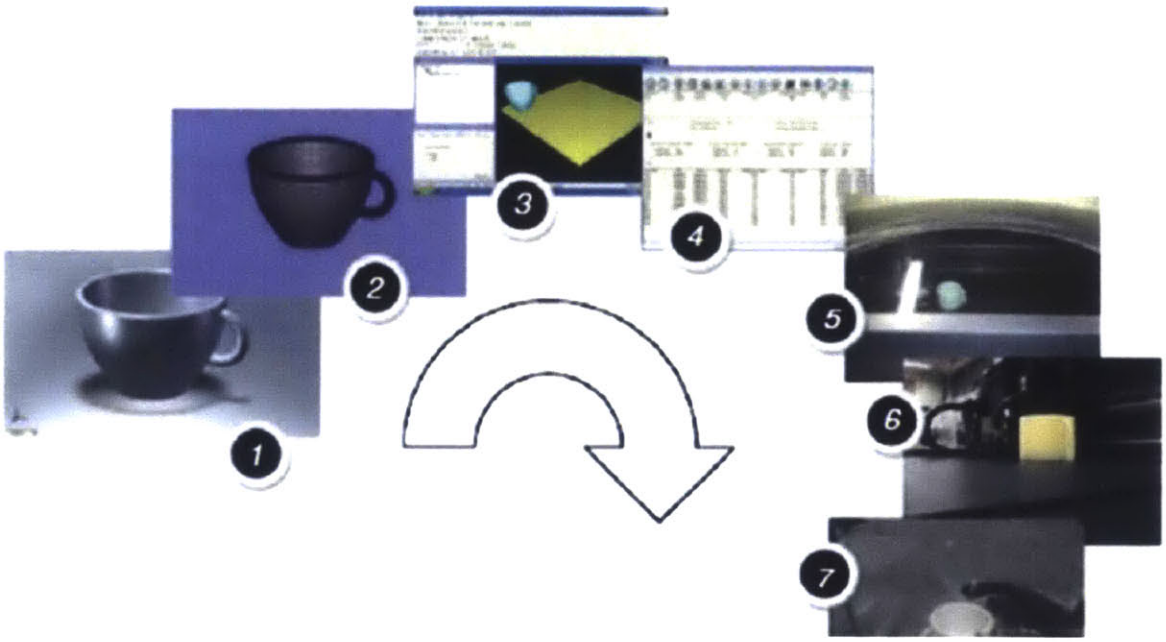

Figure 2-1: AM process work flow steps [14].

Binder Jetting An additive manufacturing process in which a liquid bonding agent is selectively deposited to join powder materials, visualized in Figure 2-2a.

Directed Energy Deposition An additive manufacturing process in which focused thermal energy is used to fuse materials by melting as they are being deposited, visualized in Figure 2-2b.

Material Extrusion An additive manufacturing process in which material is selectively dispensed through a nozzle or orifice, visualized in Figure 2-2c.

Material Jetting An additive manufacturing process in which droplets of build material are selectively deposited, visualized in Figure 2-2d.

Powder Bed Fusion An additive manufacturing process in which thermal energy selectively fuses regions of a powder bed, visualized in Figure 2-2e.

Sheet Lamination An additive manufacturing process in which sheets of material are bonded to form an object, visualized in Figure 2-2f.

Vat Photopolymerization An additive manufacturing process in which liquid photopolymer in a vat is selectively cured by light-activated polymerization, visualized in Figure 2-2g.

Within the seven categories there are many machine models employing multiple variants of the general process, yet they can all be summarized by the ASTM International categories. More advanced AM machines are beginning to incorporate conventional manufacturing processes in parallel to the additive processes. These

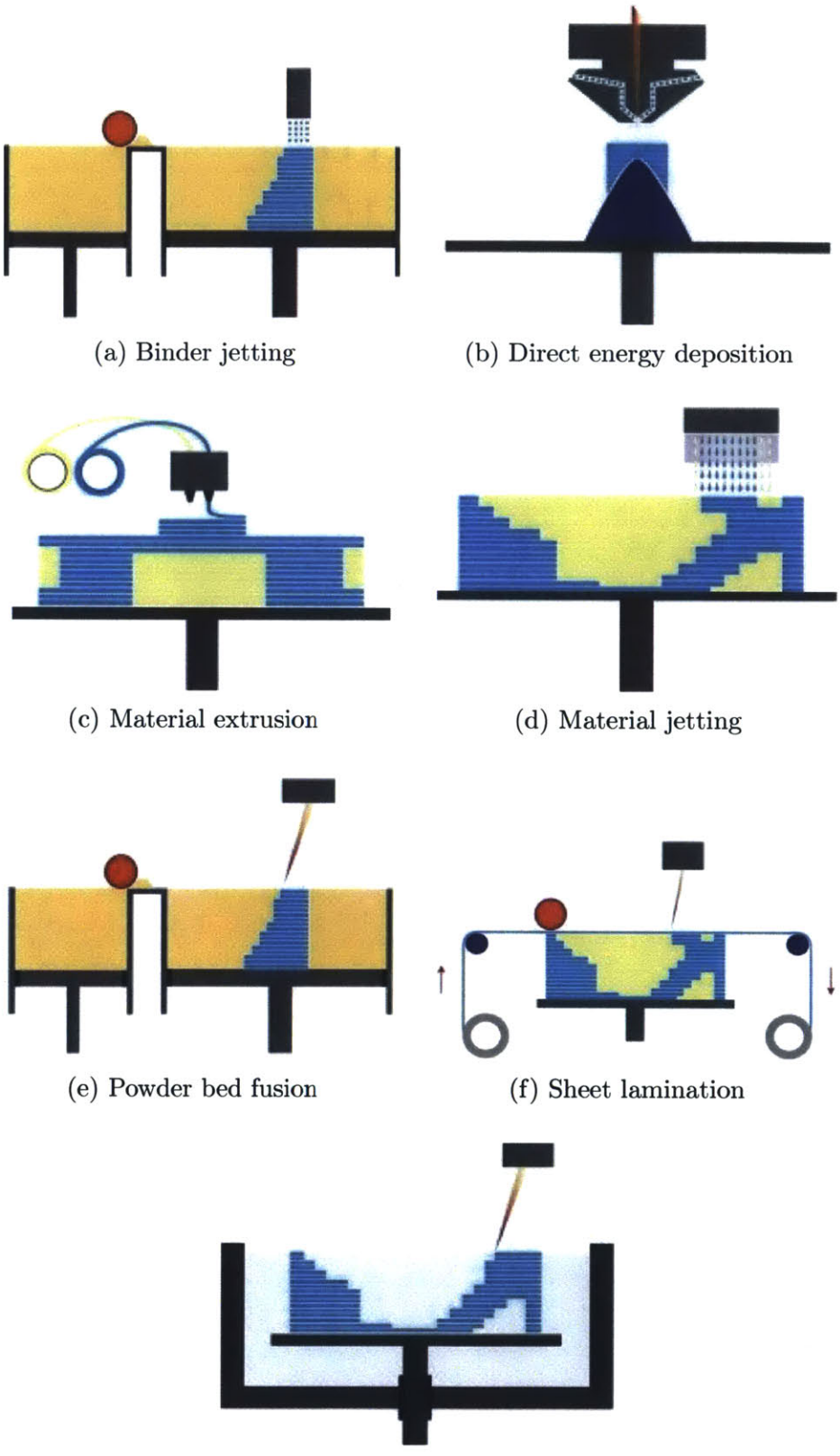

(a) Binder jetting

(b) Direct energy deposition

(c) Material extrusion

(d) Material jetting

(e) Powder bed fusion

(f) Sheet lamination

(g) Vat photopolymerization

Figure 2-2: Schematic representations of various additive manufacturing methods [16].

machines still fit into one of the seven categories, but are now being referred to as hybrid machines that are capable of both additive and subtractive processes. Some future AM machines currently in the research and design phase may not fit into one of these seven categories or actually blend two or more of the categories, but for now these seven categories will suffice.

2.4 Applications

Additive manufacturing has many applications and uses and more are being continuously thought of and put into use every year. As the machines and processes evolve and improve the application space continues to grow. Originally AM parts were used solely as visual models to better convey a conceptual design. Currently, AM part applications can fit into one or many of the following categories: visual models, fit check models, functional models, end use parts, tooling and molds, assembly guides and fixtures, education, and research. In recent years the percentage of parts built for end use has continued to climb and in 2014 end use parts accounted for 29% of all parts built, now the most popular application [13]. This can be attributed to the steady increase in performance and quality of the AM machines as well as the increased adoption and confidence from engineers, designers, and other users. Fit check models was the second most popular category in 2014 accounting for 17.8%, while the least popular use was that of tooling [13]. 2015 will see a rise in both end use parts and tooling as the AM machines are as capable as ever, there are increased material options, these two categories have the most untapped potential, and leading manufacturers have been heavily spotlighting these applications in their advertisements as well as at trade shows and conferences.

Many industries have realized the benefits of AM and its use has increasingly become more and more widespread in industries such as automotive, aerospace, industrial/business machines, consumer products and electronics, medical and dental, academic, government and military, architectural and others. The automotive and aerospace sectors were early adopters to AM and still represent a combined 30.9% of the total AM user-base , while consumer products and electronics are catching up with 16.6% [13]. The vast range of uses can be attributed to the widespread adoption throughout all the major sectors as they begin to truly realize the many benefits of AM. One of the most popular benefits that most sectors look to capture is that of reducing the development cycle time for new products. AM can speed up rounds of design, prototyping, and testing through quick or even parallel production of multiple iterations of a design. Typically after the development cycle there is a manufacturing cycle required to tailor the final development design to the manufacturing equipment, for quality and efficiency in mass production. When AM is used for production of end use parts the development cycle and manufacturing cycle are reduced even further, as the manufacturing cycle is no longer needed. The last iteration of parts that were built for the development cycle now become the manufacturing design and require no further work, as they are already being manufactured on the final manufacturing equipment. Because of this reduction in time and cost, among many other benefits,

many sectors are looking to increase their use of AM.

2.5 Industry and Market

The AM industry consists of two major classes of machines: desktop grade and industrial grade. For the intent of this publication any AM machine that retails for more than $5,000 USD is considered industrial grade. Any AM machine retailing for less than $5,000 USD is considered desktop grade. This provides a clear cut line between the two but their differences are quite obvious and extend well past their price tags.

Industrial grade machines are just that; they are built for industrial use and are intended to be operated in an industrial setting by trained operators. The machines range from $5,000 to over $2,000,000 USD and are very capable. Industrial machines can process the widest range of materials including, but not limited to, polymers, metals, ceramics, composites, and bio-matter. In general they have higher reliability, quality, resolution, layer thickness options, advanced build control, speed, efficiency, and robustness when compared to desktop models. Industrial grade machines are usually much more complex, yet easier to work with than desktop machines, due to better software and a more automated process. Typically they have larger build volumes and are able to build multiple parts in parallel. Industrial grade machines span all seven process categories and are starting to include hybrid machines that are capable of both additive and subtractive processes. Uses include all of the previously noted uses but in contrast to the desktop models, industrial grade machines offer a wider selection of selection and better build quality/resolution and thus are also used for end use parts, tooling, and fit checks. In 2014 Wohlers estimates that nearly 13,000 industrial grade machines were produced and sold. In total last year, industrial AM machine sales accounted for 86.6% of revenue from sales worldwide [13].

Desktop grade machines are designed for low cost and are able to fit on a desktop at work or at home. They range in price from about $400 to $5000 USD. These machines have not been around as long as their industrial counterparts, first breaking into the commercial market in 2007 and only truly being sold in large quantities beginning in 2011 [13]. Desktop models are notoriously known for being difficult to work with and lack in quality, resolution, and speed. The software, user interfaces, and calibration setting are weak points and cause most of the issues associated with this class of machines. Due mainly to their low cost, desktop grade machines have a very good price to performance ratio and are much less expensive to operate. They are limited to only a few simple material choices but usually have many build color options. These machines are more tailored to home, educational, artistic, and recreational uses. Currently desktop models are only available in one of two process/technology categories: extrusion and vat photopolymerization. Last year nearly 140,000 desktop machines were sold worldwide accounting for 13.4% of revenues from all AM machines, up from 9% the previous year [13].

The AM market is dominated by industrial and desktop machines but there is very little in-between. Recently hundreds of companies have started to produce thousands of desktop AM machines to satisfy the general publics craving for access to 3D

printing. There is truly an untapped market sitting directly between the two current machine grades. A very accurate analogy can be made to conventional printers: Industrial grade AM machines are similar to large printing presses and desktop grade AM machines resemble conventional desktop inkjet and laser printers, but there is currently nothing similar to that of the networked office printer. Xerox, Canon, HP, and others have truly excelled in the networked office printer market, yet not a single AM machine has been designed for a similar 3D market. NVBOTS aims to tackle this untapped market with their NVPro 3D printer. The NVPro is networked and designed for speed and autonomy. This should be a good fit for this open market but its safe to say that many of the existing industrial and desktop manufacturers are looking to fill this void as well. The classroom and office space may well be the next battleground for AM machine manufacturers.

Chapter 3

Company Background

New Valence Robotics, or NVBOTS, is a 3D Printer manufacturing startup founded in March 2013 by four MIT students. At present, NVBOTS has all of its operations in Boston, MA. The vision of NVBOTS is to build a globally distributed network of on-demand intelligent automated 3D printers in order to deliver high quality printed parts. The team here believes that the current additive manufacturing process is full of hassles and this acts as an encumbrance against increasing the user base of the technology. Theres a steep learning curve involved in designing for 3D printing, part removal is cumbersome and there is a lack of queuing which makes 3D printers difficult to share. To tackle these problems, NVBOTS has developed the worlds only 3D printer with automated part removal, which through their cloud-based interface can run continuously by itself and be controlled by any device [10].

Their current business model is to lease out printers for 5-year terms at different pricing and packages to their educational and industrial customers with full service offered as a part of every package [17]. The company recently closed a $2M seed round of funding.

3.1 The Product

The NVPro is a dual extrusion based printer with a resolution of 100 microns and an accuracy of 25.4 microns. The build volume is a cube of 8 inches and achievable printing speed is as high as 180 mm/s.

Other features of the NVPro include automated part removal which obviates manual presence to clear build area for subsequent prints, built-in camera that allows real time viewing of the printing process from any device. All the printer management is through the cloud so no extra software is required [18].

Figure 3-1: NVBOTS logo [10].

Figure 3-2: NVPro printer [10].

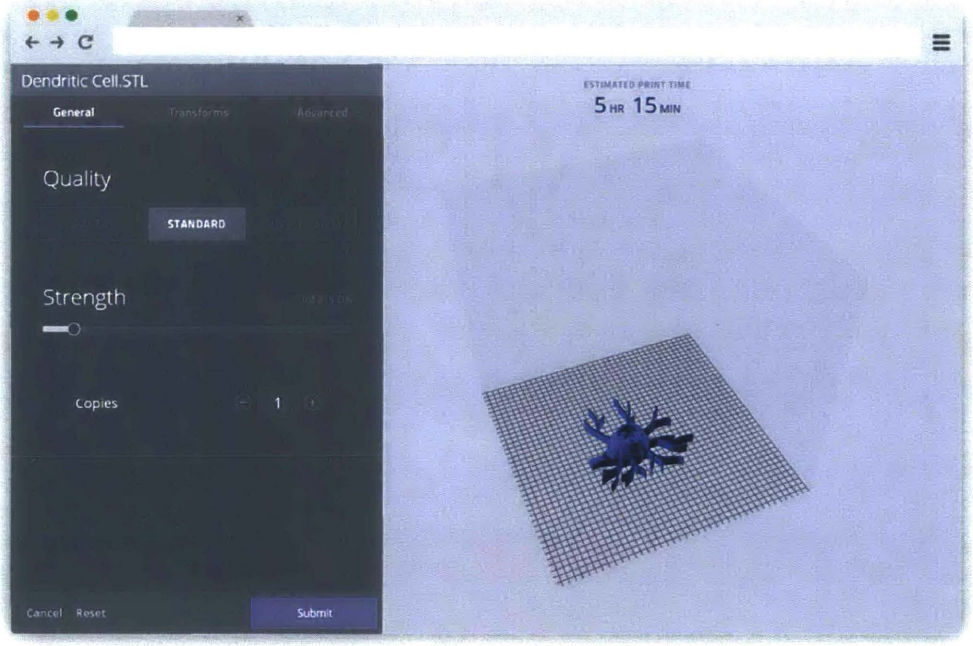

Figure 3-3: Print preview feature [19].

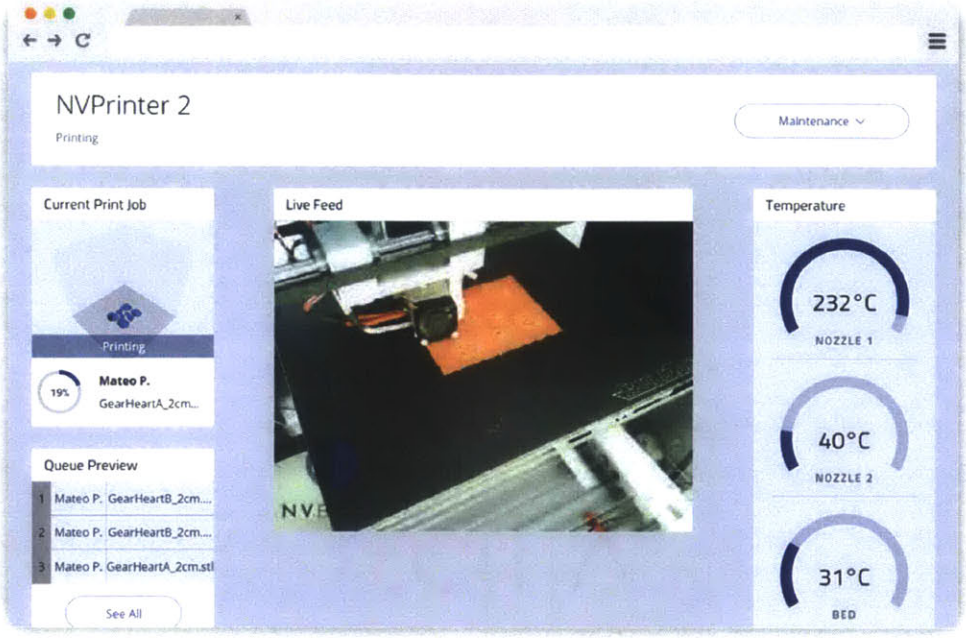

Figure 3-4: Printing dashboard [19].

The NVPro caters to the education market as their target audience. Additional offerings in the package include 3D printable curricula. These modules encourage project based and applicative learning and lessons include life sciences, earth or space sciences, engineering and many more [20]. The user interface is intuitive and easy to navigate. Its features include print preview with size, shape and quality adjustments, administrative control for queue management and a printer dashboard with a live video feed and other real time monitoring add-ons [19].

3.2 The Market

NVBOTS leases out printers on a yearly contract and ensures recurring consumables revenue (plastic filament) and cloud services fees. Their beachhead market is the education space in an attempt to capture the future designers and scientists early and also learn through their data what is desired from 3D printing. They currently have 16 printers rented by educational customers, 10 printers working internally and 12 printers currently on the assembly line. Once they successfully penetrate the education marketplace, they will approach the industrial marketplace with improved technology offerings in an attempt to make a stronghold there.

3.3 Company Analysis

Professor Michael Cusumano of the Sloan School of Management identifies eight key points of successful startup ventures [21]. The following section looks closely at how NVBOTS is currently positioned on the basis of these metrics.

1. Management team: The founding team of NVBOTS includes CEO AJ Perez, CTO Forrest Pieper, COO Chris Haid and VP of Engineering Mateo Peña Doll, all of them MIT mechanical or electrical engineers. NVBOTS also has an esteemed board of advisors in former experts of manufacturing and 3D printing industry and also esteemed professors at MIT. With new hires, including experienced people in key areas of supply chain, sales and production, this metric seems well cleared for NVBOTS.

2. Attractive market: The McKinsey Global Institute estimates the total economic impact of 3D printing by 2025 to be up to $0.6 trillion [22]. Hence, an attractive market certainly exists. With NVBOTS beachhead market being largely untapped and their value proposition being specifically advantageous to capture it, they are well on track. They are also targeting industrial markets with improved technologies.

3. Compelling new product: The NVPro is a compelling product in itself but it must be put in reference to the competition that they face. In terms of feature offerings such as 24/7 printing without human intervention, ease of sharing among consumers and use of data for future improvements, it is the only product that achieves it.

4. Strong evidence of customer interest: NVBOTS already has customers using the product and a high anticipated demand for FY15. Besides, NVBOTS is currently catering to its beachhead market and at the same time working on product innovations that will serve them well in the industrial marketplace. The true litmus test will come when they attempt to pitch to industrial customers and compete with other well-established players in that field.

5. Overcoming the"Credibility Gap": Professor Cusumano describes this as the fear among customers that the venture will fail, leaving the buyer without technical support or a future stream of product upgrades. In order to avoid this startups must use present customers as references for new customers [21]. This requires exceptional customer service and also a reliable product that does not face critical issues in the field. This is one concern area.

6. Demonstrating early growth and profit potential: NVBOTS has a well charted financial plan for growth and an existing customer base. Successful seed funding rounds are indicative of the companys merit.

7. Flexibility in strategy and technology: This metric cannot be assessed through plans made in advance but only after the company has been running for a certain

Table 3.1: NVBOTS evaluation

Evaluation Criteria	NVBOTS
Management Team	Strength
Attractive Market	Strength
Compelling New Product	Strength
Strong Evidence of Customer Interest	Opportunity
Overcoming the Credibility Gap	Threat
Demonstrating Early Growth and Profit Potential	Strength
Flexibility in Strategy and Technology	Opportunity
Potential for Large Investor Pay-off	Strength

period of time and proves to be responsive to market needs and technological changes in such disruption prone markets.

8. A startup that has established sources of funding beyond angel investors and family, friends etc. shows promise for large pay-off and looks better to potential investors [21]. This is an area of opportunity for NVBOTS..

In conclusion, the company has a bright future ahead with their strong performance in almost all of the above mentioned metrics. NVBOTS should have a strong focus on capitalising on opportunities by generating customer interest and also staying nimble and flexible in their strategy. By refining their product design and manufacturing process, they can eliminate the initial concerns that their product faces in the field and ward off their single potential problem.

Chapter 4

Failure Modes and Effects Analysis

Failure Modes and Effects Analysis (FMEA) is a systematic approach to failure analysis through a combination of inductive reasoning and deductive analysis. It involves a comprehensive review of potential failure modes of components, assemblies, and subsystems within a system or product and their underlying failure mechanisms. It is an essential reliability engineering tool that is used iteratively throughout the entire product development process from concept through production and sustaining.

A well-executed FMEA identifies potential failure modes, the effects of the failure on various system levels, and the mechanisms responsible for the failures. It results in a well-documented collection of design risks and mitigation strategies such as the development of system requirements, design changes, and testing to reduce or eliminate these risks permanently. The early identification and elimination of failure modes leads to a better engineered and more reliable product, improving company image and profitability.

Reliability of the NVPro is a primary concern for NVBOTS as its reputation as a professional grade consumer printer on the line. Moreover, the company's business model is based on 5-year NVPro rentals to customers. Ensuring reliable and failure free operation during the lifetime of the product is integral to the business' survival as any service costs are the company's responsibility. Thus a thorough understand of the failure modes of components was required in order to estimate printer reliability and life. A component level FMEA was conducted of the NVPro printer to identify the top risk item for subsequent accelerated life testing.

4.1 Methodology Overview

The FMEA study for the NVPro began with an analysis of the Bill of Materials (BOM) in order to identify which components to conduct the FMEA for. There are hundreds of unique parts in the printer and it was infeasible to conduct an FMEA for each. Therefore, the process of BOM filtering was employed to down-select to those components that were believed to have the greatest impact on the system if failed. These components can be broadly categorized as:

- Roller bearings;

- Linear bearings;
- Bushings;
- Gears;
- Machined components;
- 3D printed structural components; and
- Motors.

The slimmed down "Critical Parts BOM" was populated into a FMEA worksheet, adapted from MIL-STD-1629A.[1] Meticulous effort was made in ensuring the vertical relationships between each subsystem, subassembly, and component was captured both numerically through the "BOM Item Level Number" and visually through indentation.[2]

The FMEA worksheet was organized into five categories, some with further subsections to organize and document the analysis. These five categories are briefly highlighted below and are discussed in further detail in subsequent sections. A sample of the worksheet is found in Table 4.1 on page 33.[3]

Items an indentured list of the "Critical Parts BOM", including the NVBOTS part number, and NVBOTS subassembly and components name verbatim to ensure ease of tracking.

Potential Failure Modes the list of all potential failure modes of each critical component, along with its effects on the component itself and various system levels, and the impact severity of failure.

Potential Causes a deductive analysis to determine the root cause of failure and the physical mechanisms at work, along with an estimate of its probability of occurrence.

Risk The risk classification corresponding to the assigned severity index and probability of occurrence.

Recommended Actions a list of next steps to be taken to mitigate the risk, with assigned responsibility.

[1]MIL-STD-1629A is a United States Department of Defense document which describes in detail the procedure to perform a Failure Mode, Effects and Criticality (FMECA) Analysis, specifically to evaluate designs for aerospace applications [23].

[2]The NVPro BOM was created for the first time by NVBOTS as of May 2015 and this level of organization had not yet been conducted.

[3]The Recommended Actions section of the worksheet was not completed for the purpose of this thesis as a detailed set of recommendations could only be established after the necessary life testing and analysis. However, the FMEA worksheet should be updated continuously by NVBOTS and each iteration should include further recommendation actions to mitigate the identified risks.

Table 4.1: FMEA worksheet template

ITEMS				POTENTIAL FAILURE MODES						POTENTIAL CAUSES			Risk
BOM Item Level No.	Part No.	Subassembly / Component		Potential Failure Mode	Local Effect of Failure	Next Higher Level Effect	System Level End Effect	Severity(S) Score	Severity(S) Class	Potential Cause / Failure Mechanism	Probability (P) Score	Probability (P) Class	

4.1.1 Potential Failure Modes

Failure modes specify the manner by which an item fails to perform its designated function, and describes the failed end state of the item. For example, *seized bearing* or *motor burnout*. Failure modes are identified based on analogous products or an understanding of the physics involved during system operation. An intimate understanding of the system and experience with past failure modes provides a basis for the "brainstorming" of potential failure modes.

The effects of each failure mode describe the immediate consequence of failure and its propagation throughout the system. The *local effect* describes what happens to the component itself when failure occurs. The *next higher level effect* describes the effect of failure on the subassembly the component is a part of. Finally, the *system level end effect* describes what happens to the entire product.

Each failure mode is categorized by the severity of its impact on the system. This helps quantify the effects and is one of two factors considered when evaluating risk (see Section 4.1.3). A score between 1–6 is assigned, with 1 being the lowest in severity and 6 being the highest. Each score corresponds to a certain classification describing the severity in words. Table 4.2 presents the severity scoring and classification for the NVPro FMEA study, adapted from MIL-STD-882E [24].

Table 4.2: FMEA severity scores and classifications

Score	Class	Meaning
1	None	No relevant effect on reliability or safety
2	Very low	No or very minor damage, only results in a maintenance action, only noticed by discriminating customers
3	Low	Minor damage, affects very little of the system, noticed by average customer
4	Moderate	Moderate damage, mostly financial damage, most customers annoyed
5	Critical	Severe damage, causes loss of primary function
6	Catastrophic	Product becomes inoperative or completely unsafe operation

4.1.2 Potential Causes

As previously mentioned, potential causes involves deductive analysis to determine the root cause of failure and the physical failure mechanisms at work. This requires an in-depth knowledge of the system, its production process, and its various operating conditions and environments. The identification of failure mechanisms also requires

competent engineering skills developed through a firm grasp of fundamental concepts and experience.

Each failure mode and corresponding cause is categorized by the probability of occurrence during its lifetime. This helps quantify the effects and is the second factor considered when evaluating risk (see Section 4.1.3). A score between 1–6 is assigned, with 1 being the lowest in likelihood and 6 being the highest. Each score corresponds to a certain classification describing the likelihood in words. Table 4.3 presents the probability scoring and classification for the NVPro FMEA study, adapted from MIL-STD-882E [24].

Table 4.3: FMEA likelihood scores and classifications

Score	Class	Meaning
1	Extremely unlikely	Virtually impossible or no known occurrences on similar products with many running hours
2	Remote	Relatively few failures
3	Occasional	Occasional failures
4	Reasonably	Reasonably possible, repeated failures
5	Frequent	Frequent, failure is almost inevitable
6	Almost always	Almost guaranteed that every unit will fail, indicating a critical design flaw

4.1.3 Risk

Each failure mode represents a risk to operation of the product and thus should be addressed as soon as possible. However, in order to prioritize risks in order of significance, a risk index was assigned based on a combination of the failure mode's severity and probability of occurrence. Table 4.4 presents the risk matrix used for the NVPro FMEA study, adapted from MIL-STD-882E [24]. The risk matrix indicates that any failure modes that are either almost always likely to occur or are catastrophically severe are unacceptable and deserve immediate attention. For the purpose of the NVPro, only the risks identified as *Unacceptable* would be considered for accelerating life testing.

4.2 FMEA Results

FMEA was performed for approximately 70 unique components in the printer, with a fair amount of overlap in failure modes between some components, *e.g.* bearings. This process was partially completed in conjunction with engineering staff at NVBOTS.

Table 4.4: FMEA risk index

		Severity					
		1	2	3	4	5	6
Probability	1	Low	Low	Low	Low	Moderate	High
	2	Low	Low	Low	Moderate	High	Unacceptable
	3	Low	Low	Moderate	Moderate	High	Unacceptable
	4	Low	Moderate	Moderate	High	Unacceptable	Unacceptable
	5	Moderate	Moderate	High	Unacceptable	Unacceptable	Unacceptable
	6	Moderate	Unacceptable	Unacceptable	Unacceptable	Unacceptable	Unacceptable

Table 4.5: Unacceptable risk components in the NVPro

Part Name
Z Leadscrew
Gantry motor
0.4 mm Hot End Nozzle
Hot End Heat Break
Extruder Hob
5 mm Extruder Spur Gear
Extruder Motor
10 mm Linear Ball Bushing
8 mm Needle Bearing

Based on the risk priority index, the components in Table 4.5 had failure modes classified as *Unacceptable*. The complete FMEA is not included with this thesis to protect NVBOTS confidentiality.

The substantial number of components indicates an immediate need to investigate and mitigate all these failure modes before the product moves into the next development cycle, or at the very least, before finalized production release. Assuming independent failure distributions for each component, the reliability R of the entire system at time t is given by the multiplication of the each individual component reliability:

$$R_{system}(t) = \prod_{i=1}^{n} R_i(t) \tag{4.1}$$

where:

$R_i(t)$ = reliability of each individual component i at time t; $0 \leq R_i \leq 1$

However, only one component was selected for immediate investigation into determining its reliability function for the purpose of this thesis. The further prioritization was performed based on the impact to the customer of the failure mode if it were to occur in the field. This provided a method to quantify failures in relation to one of the most important aspects of the NVBOTS business: customer service and brand image.

A score between 1–6 was assigned, with 1 being the lowest in customer impact and 6 being the highest. Each score corresponds to a certain classification describing the customer impact in words. Table 4.6 presents the impact scoring and classification for the NVPro FMEA study.

Table 4.6: FMEA customer impact scores and classifications

Score	Class	Meaning
1	Almost negligible	No on-site service labor, no financial cost, minimal customer-end labor and downtime
2	Very low	No on-site service labor, very low financial cost, minimal customer-end labor and downtime
3	Low	No on-site service labor, low financial cost, moderate customer-end labor and downtime
4	Moderate	Some on-site service labor required, low to moderate financial cost, moderate customer-end labor and downtime
5	High	Significant on-site service labor required, moderate to high financial cost, significant customer-end downtime
6	Extremely high	Cost of repair is infeasible due to significant on-site service labor, very high financial cost, or need for complete re-build of machine

4.2.1 Top Priority Risk: Linear Bushings

Using the criteria in Table 4.6, the 10 mm Linear Ball Bushings (hereby referred to as "linear bushings" and "linear bearings" interchangeably) was identified as the top priority risk in the NVPro. The linear bushings are used in conjunction with precision shafts to enable precise X and Y linear movement of the extruder within the gantry system. If these bushings were to fail, it would have a catastrophic impact on the printer and would require an immediate swap at the customer site. This is because the XY gantry is one of the first assembly steps and replacing a failed bushing would require a complete teardown and rebuild at the NVBOTS facility.

X and Y movement in the NVPro printer occurs along a set of two parallel precision ground shafts in each direction. Linear bushings are found in sets of two on each shaft, housed within spaced apart yet concentric bores machined into custom designed aluminum blocks. The bearing is not axially constrained within the housing and is assembled with a sliding fit, and thus, the bearings only experience radial loads and bending moment loads at the extremities of travel. In total there are four linear bushings in X forming the X carriage and four in Y forming the Y carriage, as seen in Figure 4-1. The precision shafts and entire carriage system is visible and exposed to the print chamber environment, as seen in Figure 4-2. Note that this is an over-constrained bearing layout by design.

The linear bushing currently used in the NVPro is a fixed alignment, sealed, non-

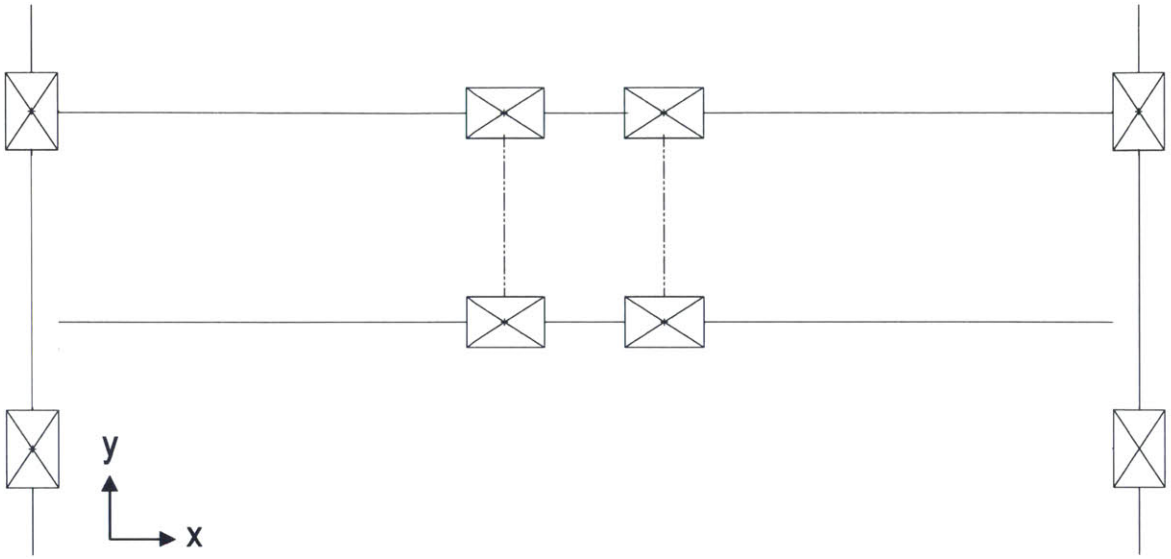

Figure 4-1: NVPro XY gantry linear bushing schematic.

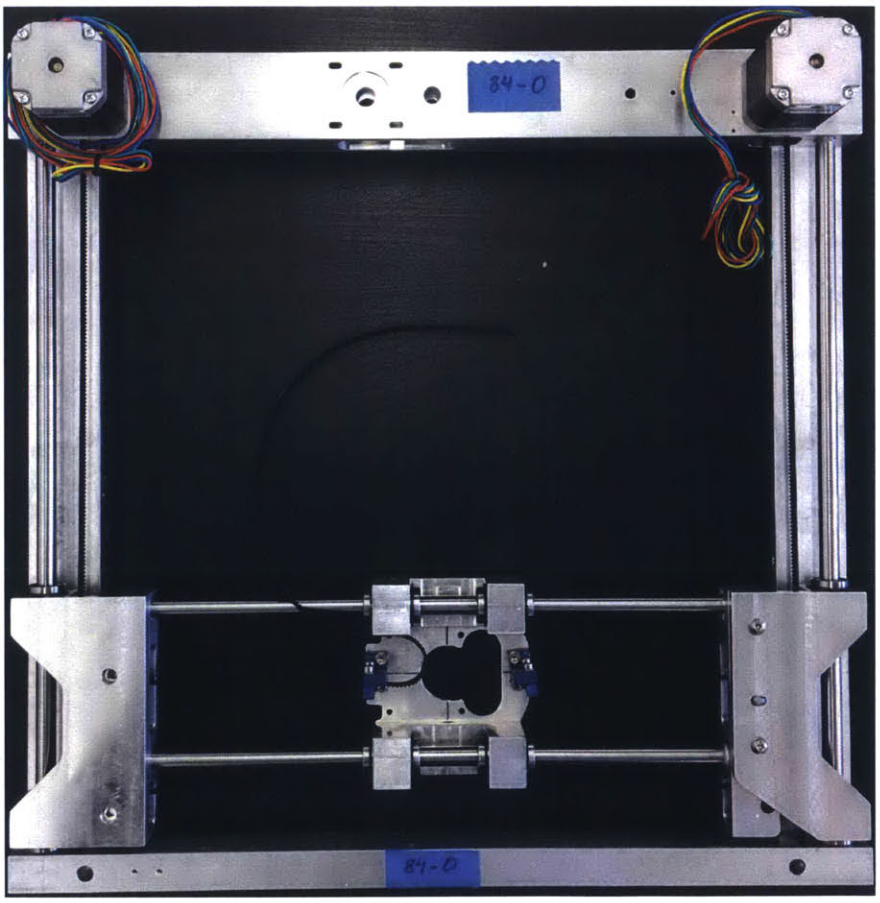

Figure 4-2: NVPro XY gantry.

greased linear bushing with a single track of recirculating 52100 steel bearing balls.[4]

The component-level FMEA of the linear bushing is included in Table 4.7 and each generalized failure mode is discussed in further detail in Section 4.3.

4.3 Failure Modes of Linear Bushings

This section presents literature review of the various failure modes of linear bushings identified in Table 4.7 and the underlying mechanisms. In general, bearing failures can be classified within four categories, which also apply to linear bushings despite the difference in operation—linear translation v. rotation [25]:

1. Inadequate lubrication: incorrect type or amount, degradation, et cetera;
2. Operating conditions: excessive loading, misalignment, et cetera;
3. Adverse environment: humidity, contaminants, vibrations, et cetera; and
4. Improper installation: incorrect fit design, careless handling, et cetera.

The specific failure modes discussed in the following sections all stem from these four primary categories. Some sample images will be drawn from radial ball bearing failure analysis, but the failure mode remains the same for linear bushings.

4.3.1 Adhesive Wear

Wear is damage to a solid surface characterized by progressive removal and deformation of material due to relative motion between itself and a directly contacting second surface [26]. The resisting force to the relative motion between the two surfaces is friction, which acts tangentially against the direction of motion at the contact interface [26]. As a surface wears, the material lost is transferred between surfaces leading to the formation of mechanical debris.

Adhesive wear, also known as galling, is a combination of friction and adhesion between two sliding surfaces. Every surface, no matter how clean, is characterized by asperities—tiny bumps and imperfections which create roughness. When the surfaces are pressed together with sufficient pressure to rupture any protective surface film (e.g. oxides), the microscopic asperities come into contact resulting in high localized stresses at over this true contact area [27]. The asperities elastically and plastically deform, resulting in plastic flow and "cold welding" [25]. These weldments increase in size with relative motion, which increases friction as the welds must be sheared to permit motion, resulting in wear particles [27]. The increased pressure combined with shearing leads to an energy density and heat increase within the contact zone, resulting in even greater adhesion between the two surfaces. Thus as the two surfaces slide relative to each other under compressive load, there is an accumulation of energy density as more asperities deform, weldments shear, and macrolevel plastic

[4]The exact make and model of the bearing is not disclosed to protect NVBOTS confidentiality.

Table 4.7: Linear bushing FMEA

POTENTIAL FAILURE MODES						POTENTIAL CAUSES			Risk
Potential Failure Mode	Local Effect of Failure	Next Higher Level Effect	System Level End Effect	Severity(S)		Potential Cause / Failure Mechanism	Probability (P)		
				Score	Class		Score	Class	
Adhesive wear	Polishing and then wearing of surface, eventual bearing seizure	High sliding friction of carriage, motor current draw spikes, possible loss of movement	Print quality suffers, possible failed prints due to lack of movement	5	Critical	Lubrication film breakdown due to insufficient amount or load carrying capacity; excessive heat	2	Remote	High
Abrasive wear	Polishing and then wearing of surface, eventual bearing seizure	High sliding friction of carriage, motor current draw spikes, possible loss of movement	Print quality suffers, possible failed prints due to lack of movement	6	Catastrophic	Abrasive wear due to debris/dirt collection on exposed rails, dirt ingress during assembly; loose shaft fit can lead to debris ingress	5	Frequent	Unacceptable
Spalling of bearing balls	Flaking of bearing balls, leading to eventual crack	Rough operation, excessive noise and vibration	Print quality suffers, possible failed prints due to lack of movement	6	Catastrophic	Bearing seating out of alignment or mounted skewed - increased contact stresses and fatigue failure	4	Reasonably	Unacceptable
Corrosion	Etching, streaking, and eventual pitting on surface	Rough operation, excessive noise and vibration	Print quality suffers, possible failed prints due to lack of movement	6	Catastrophic	Oxidation from moisture	4	Reasonably	Unacceptable
Fretting corrosion	Rough surface and pitting fromcorrosion leading to uneven load distribution	Rough operation, excessive noise and vibration	Print quality suffers, possible failed prints due to lack of movement	6	Catastrophic	Repeated relative motion between loaded bearing ring and shaft/housing due to loose fit create debris and eventual oxidization	2	Remote	Unacceptable
False brinelling	Surface depressions in raceway and wear produce cavities	Rough operation, excessive noise and vibration	Print quality suffers	4	Moderate	Vibration when stationary and lack of lubrication create debris from surface asperities	2	Remote	Moderate

deformation and material exchange occurs [27]. Material is visibly removed from one surface and stuck or friction welded onto the second surface. The result is localized patches of rough and gouged surfaces.

Galling in linear bushings occurs when there is inadequate lubrication within the bearing system, leading to metal on metal contact between the rolling elements and rails [28]. A properly lubricated bearing ensures smooth operation by creating a very thin film between the contact surfaces of the inner bearing race and the shaft [29]. This separation of the two solid surfaces with a fluid film reduces friction and ensures the microscopic asperities on each surface do not make contact.[5] As the lubricant degrades over time, is contaminated by moisture or debris, reduces in viscosity due to a sudden temperature rise, or the lubricant film breaks down to due excessive load, the two surfaces come in direct contact with each other [30]. The resulting galling causes a sharp increase in temperature, especially when under high loads, which further accelerates the adhesive wear process. The hardened bearing materials soften under the high temperatures, metal flow occurs, and eventually the bearing completely seizes [28].

Adhesive wear in linear bushings is characterized by damage of various levels of increasing severity. Initially, there only a slight discoloration of the bearing surface due to lubricant staining from metal-on-metal contact heat generation, as seen in Figure 4-3. The next level of damage results from a complete lack of lubrication and is characterized by scoring and galling of the bearing balls, shafts, or raceways. Finally, the last level of damage includes extremely high localized heat generation, resulting in large plastic flow and complete bearing seizure, as seen in Figure 4-4 [30].

4.3.2 Abrasive Wear

Abrasive wear occurs whenever a hard material slides against a softer one, damaging its surface by a plowing or gouging action [25,27]. This can occur via sliding, or "two-body" abrasion which occurs when hard particles are attached to one of the sliding bodies and move relative to the other triboelement. However, it is more common that abrasion occurs when free hard particles are interposed between the two sliding surfaces, described as rolling or "three-body" abrasion [26]. These wear particles create points of localized stress concentration that plastically deform and shear the underling bearing material, and also mark the onset of fatigue [27].

Abrasive particles can be the result of contamination or debris from adhesive wear. The ingress of foreign particles such as sand, metal powders, dirt, or even dust can occur with or without the presence of lubrication as the lubricant grease tends to attract dirt [28]. As abrasion occurs, material is worn off the bearing surfaces increasing the amount of debris in the system and increasing the surface roughness, thus accelerating both the abrasive and adhesive wear processes until the surface is rendered unfit for use. The stress concentration points can also lead to early fatigue failure by crack propagation.

[5]There is always an initial run-in period where the asperities penetrate the lubricant film and make direct contact. However, after these have been plastically deformed and sheared to the extent that the lubricant can fully support the load during relation motion, there very little direct contact [27].

(a) Initial discoloration (b) Galling

Figure 4-3: Sample images of adhesive wear in bearings provided by Barden Corp. [29]; (a) discoloration from lubricant staining due to excessive heat from direct metal-to-metal contact; (b) galling as indicated by gouging of the raceway.

Figure 4-4: Complete bearing seizure due to continuous lubricant-free operation. Excessive heat from galling caused plastic flow and bearing cage deformation [30].

Abrasive wear in linear bearings is characterized by dull, worn surfaces and small indentations in raceways, balls, and shaft, as well as the presence of foreign particles in the grease or embedded in the raceways. Figure 4-5 depicts samples of abrasive wear in roller bearings.

4.3.3 Corrosion

Etching occurs on the steel surfaces of the bearing in the presence of water or other corrosive agents [28]. It is most often caused by a humid environment and condensate collecting in the bearing housing from temperature changes, and subsequent deterioration of lubricant due to moisture [30]. As the surface corrodes, iron oxide particles initiate abrasive wear. The loss of material also leads to increased radial clearance, loss of preload, and increased vibration [29]. The patches of etching also lead to deep seated rust as oxidation penetrates deeper into the material which can initiate early fatigue failure and spalling [28].

Corrosive wear in linear bushings is characterized by the common signs of corrosion on the bearing balls: red/brown stains or deposits of rust, surface etching, pitting, and flaking. Figure 4-6 provides an example of corrosion damage in bearings.

4.3.4 Fretting Corrosion

Fretting is defined by the ASM Handbook of Fatigue and Fracture as, "A special wear process that occurs at the contact area between two materials under load and subject to minute relative motion by vibration or some other force" [31]. This vibration can be the result of a loose fit between the bearing and shaft or housing, allowing for relative movement [28]. The small amplitude vibrations result in thorough cleaning action, disallowing relubrication of the contact area between the two surfaces. Thus as asperities are damaged during adhesive wear from oscillation, fine particles are released which are subsequently oxidized [25].

Fretting corrosion in linear bushings is characterized by deteriorated surface quality as a result of rust, micropitting, and heavy markings from uneven load distribution in the bearing [28]. Figure 4-7 depicts an example of fretting corrosion damage.

4.3.5 False Brinelling

True brinelling occurs when a static overload or impact exceeds the elastic limit of the ring materials, causing indentation marks from the bearing balls [29]. Examples include using a hammer during installation or dropping a bearing.

False brinelling is a type of fretting corrosion that occurs when the bearing system is stationary. External vibrations under static loading cause the rolling elements to move relative to the raceway, forming a groove into the raceway via adhesive wear as an oil film cannot be formed when stationary to separate the two surfaces [29,30]. Wear debris is formed which oxidizes and leads to further corrosive and abrasive wear.

False brinelling in linear bearings is characterized by elliptical grooves in the raceway or shaft. The depressions can be distinguished from true brinelling as the surface

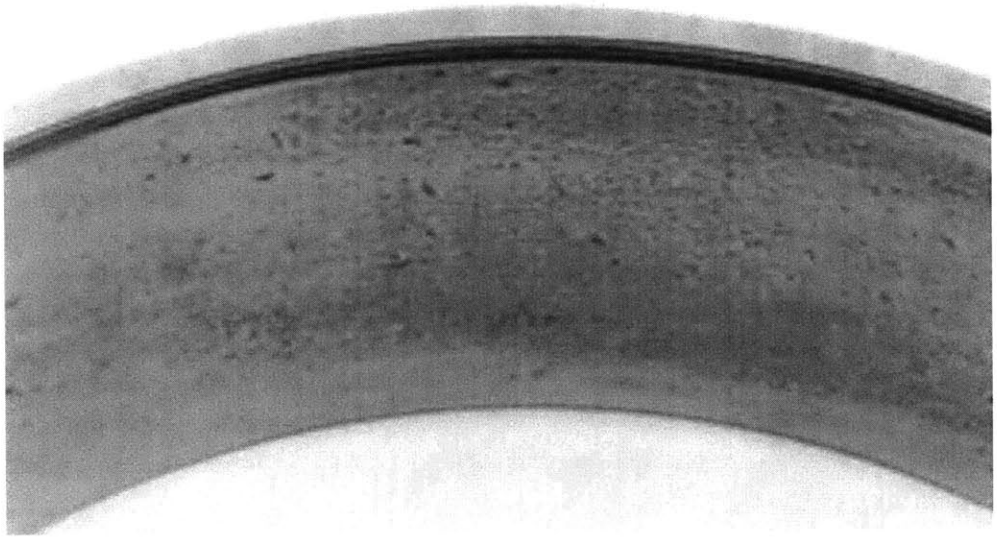

(a) Indentations

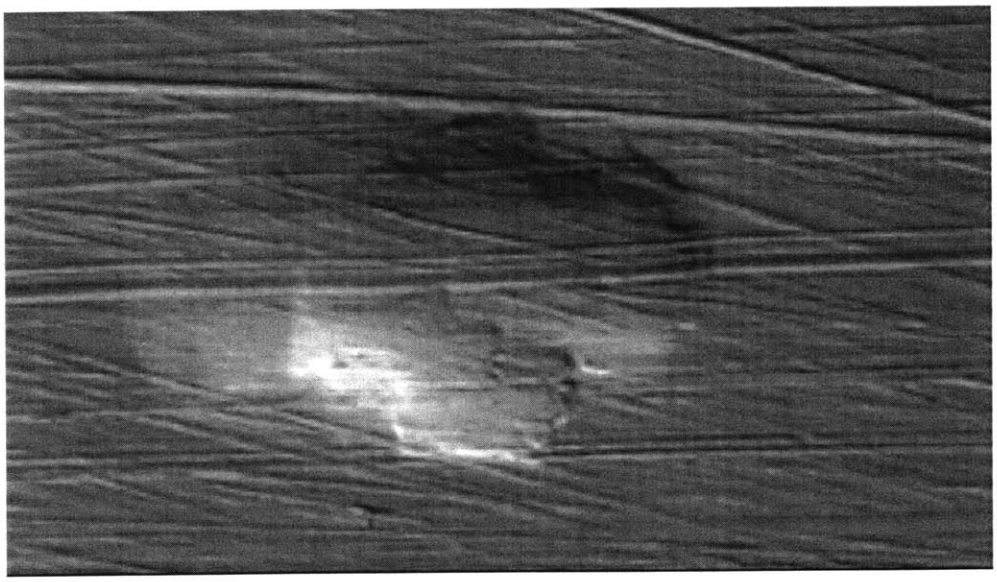

(b) Indentation at 50x

Figure 4-5: Abrasive wear in bearings; (a) indentations caused by metallic debris on tapered roller bearing race; (b) indentation at 50x magnification [30].

Figure 4-6: Corrosion on roller bearing raceways and balls as a result of moisture, as indicated by reddish-brown stains, flaking, and pitting [29].

Figure 4-7: Extensive fretting corrosion in the bore of a self-aligning ball bearing [28].

of the depression itself will be worn away in false brinelling but the original surface texture will remain in the depression of a true brinell [30]. Figure 4-8 presents examples of false brinelling.

4.3.6 Spalling

Spalling is localized pitting or flaking of bearing material due to surface fatigue failure after a large number of cycles [30]. Spalling can occur as a primary failure mode as a result of normal fatigue, however it likely a secondary damage mode accelerated by another factor [28]. The fatigue life is extremely sensitive to contact stresses; if contact stresses increase due to any variety of reasons listed below, the fatigue life is significantly reduced and spalling occurs as secondary damage:

- Heavy external loading;
- Excessive preload from incorrect fits or misalignment;
- Oval distortion due to shaft or housing out-of-roundness;
- Axial compression from thermal expansion;
- Indentations from abrasion or brinelling;
- Surface roughness from galling; and
- Corrosion—both deep-seated rust and fretting corrosion.

Spalling in linear bushings is characterized by an increase in noise and vibration during operation and the flaking of the ball bearings. Figure 4-9 provides examples of bearings with spalling damage from a variety of primary reasons.

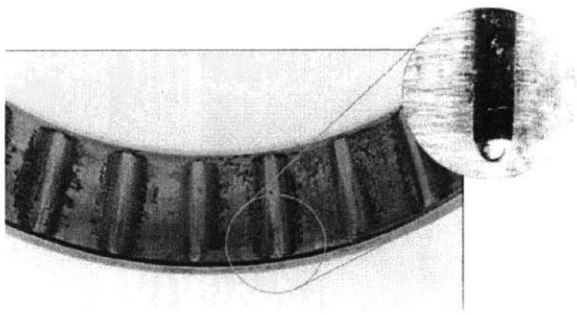

Figure 4-8: Wear caused by false brinelling in a tapered roller bearing outer ring, resulting from relative axial movement between rollers and races when stationary [30].

(a) Spalling due to abrasion

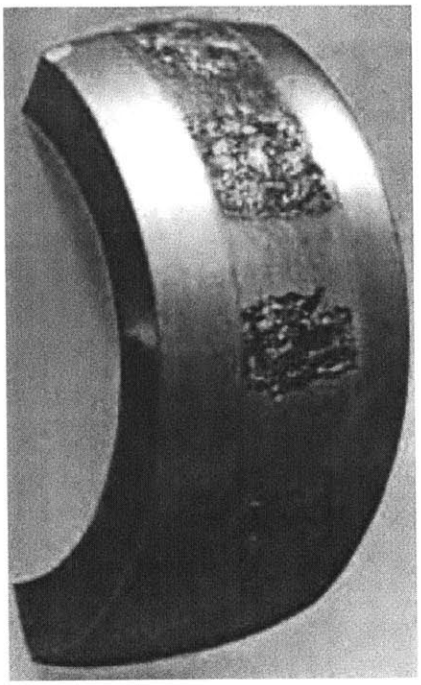

(b) Spalling due to galling

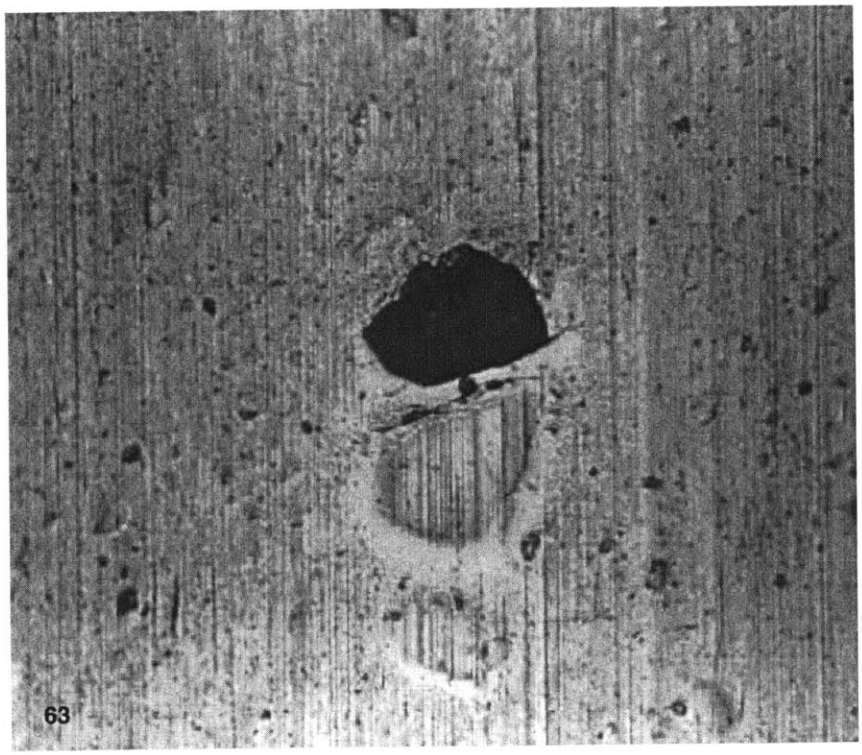

(c) Flaking and indentations (100x)

Figure 4-9: Spalling in bearings as a result of (a) abrasive wear, (b) indentations on raceway from abrasive wear (100x magnification), and (c) galling on the inner ring of a cylindrical roller bearing [28].

4.4 Summary

This chapter presented Failure Modes and Effects Analysis (FMEA) as a systematic approach to analyzing failures with the NVPro printer. FMEA could be used to analyze system levels failure modes or failure modes for individual components. A methodology was presented to organize critical components from the product into a Bill of Materials (BOM) within a custom-made FMEA worksheet. The FMEA worksheet categorized failures by BOM level, potential failure mode, and potential causes of failure.

Failure modes for each component were determined based on an intimate understanding of the system and past failures. Its effects on various system levels were analyzed, and the overall severity of each failure mode based on its impact on the system was assessed. A severity score between 1–6 was assigned, with 1 being the lowest severity and 6 being the catastrophically severe.

The potential causes of each failure mode was investigated through deductive analysis to determine the root cause of failure and the physical failure mechanism at work. Each failure mode and corresponding cause was categorized by probability of occurrence during component lifetime by assigning a score between 1–6; 1 meant the failure mode and root cause was extremely unlikely to occur, and 6 meant the failure mode would almost guaranteed to occur by the indicated root cause.

An overall risk priority index was assigned based on a combination of the severity and probability score, and risks deemed *Unacceptable* were candidates for immediate further investigation. The top priority risk was selected by analyzing the customer impact of the *Unacceptable* component failures, and scoring on a scale of 1–6 similar to severity and probability scores. Through this systematic approach, the 10mm Linear Ball Bushings (or just "linear bushings") in the XY gantry of the NVPro printer were identified as the top priority risk and would be further investigated to mitigate the risk of failure.

Finally, a literature review of linear bushing failure modes was presented to provide insight into root cause failure mechanisms. The various failure modes covered included:

- Section 4.3.1: Adhesive wear;
- Section 4.3.2: Abrasive wear;
- Section 4.3.3: Corrosion;
- Section 4.3.4: Fretting corrosion;
- Section 4.3.5: False brinelling; and
- Section 4.3.6: Spalling.

Chapter 5

Accelerated Life Testing Literature Review

5.1 Overview

Product life is defined as total operational time under typical or use conditions before complete failure, *i.e.* complete loss of performance [32]. The two sources of life data are field data collected from actual units used by customers, and laboratory data collected through specifically designed experiments. Collecting field data is usually a very expensive process where the data is not available for years, and therefore not usually an option except for warranty analysis. Life testing can also be a very time consuming and costly process for highly reliable components. Therefore, special experiments specifically designed to cause failure in a shorter period of time are used, referred to as accelerated life tests (ALT) [32].

An accelerated life test can serve many purposes, such as identifying design failure modes, burn-in, measuring or demonstrating reliability, acceptance sampling, and qualification [33]. The purpose of the test must be well-defined prior to proceeding with experiment design and execution. Statistical analysis of life data only yields a numerical result and it up to the design engineer and manager to interpret the result for an engineering purpose [33].

5.1.1 Accelerating Stresses

The actual acceleration of the test can be accomplished through various means such as a higher usage rate, overstress testing, or degradation [33]. A higher usage rate involves operating a moving object either at a higher speed than usual or at close to 100% duty cycle for products that typically operate in intervals. These methods compress the testing time but also make the assumption that the number of cycles to failure at a high usage rates is the same at normal usage rates [33]

Overstress testing involves operating the product at higher than normal levels of stress to shorten its life. These accelerating stresses can include temperature, voltage, mechanical load, thermal cycling, humidity, chemical exposure, radiation, and vibration [32, 33]. The selection of accelerating stress levels is the subject of

significant academic and industrial research. Statistical models are available to select stress levels as discussed by Nelson [33], Rinne [32], and Reliasoft Corporation [34]. However in practise the selection of the which accelerating stress to use and which level to set it at is based on process physics and engineering judgement. The accelerating stress and its corresponding level should be selected such that it only induces the same failure mode as at the design stress level and does not introduce new failure modes that would not regularly occur [35]. Typically this stress value lies between the design stress and the destruction stress limit.

Degradation is a special case of overstressing in which the decline in product performance over time is observed and measured rather than the product's life [33]. A model is subsequently fit to the the performance degradation data and the failure time is extrapolated. Failure is assumed once the performance degrades below a threshold value set by customer specifications or engineering analysis.

5.1.2 Various Stress Loadings

The stress loading can be applied in the ways described below and pictured in Figure 5-1 [32, 33]:

Constant stress the specimen is subjected to an increased constant stress level until failure or test termination. This is the most common stress loading method.

Step stress the specimen is subjected to progressively higher levels of constant stress. It is first subjected to a specified constant stress for a given amount of time. If it does not fail, the stress level is increased in a step-wise manner until failure occurs.

Progressive stress the specimen is subjected to a continuously increasing stress. The stress ramp is usually linear.

Cyclic stress the specimen is subjected to a repeatedly alternating stress.

Random stress the specimen is subjected to uncontrolled and changing levels of stress, such as wind loading on airplane structural components.

5.1.3 Types of Data

The stress loading can be applied in the ways described below and pictured in Figure 5-1 [32, 33]:

Complete data consists of the *exact* life (failure time) of each sample.

Right censored (suspension) data consists of units that did not fail by the end of test, which could be a predetermined run time or cumulative number of failures. The failure would occur if the test were allowed to continue running, hence the failure event would occur to the right.

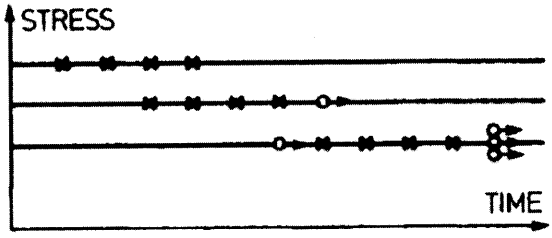

(a) Constant stress test

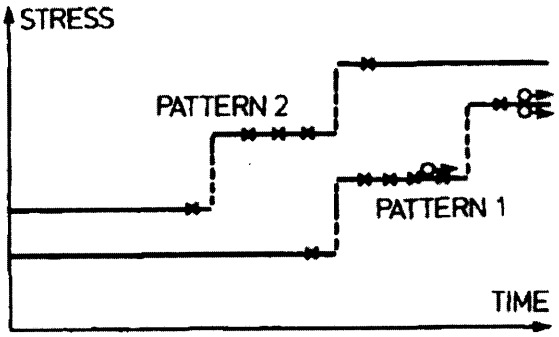

(b) Step stress test

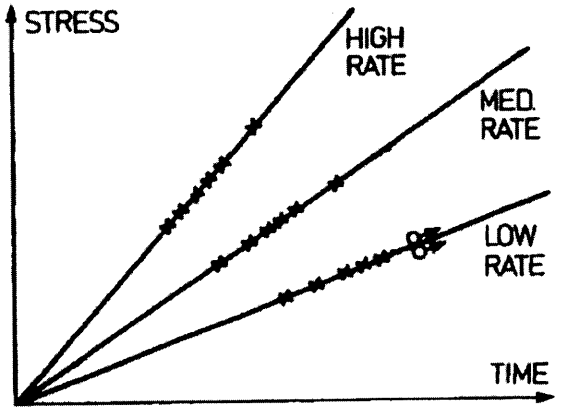

(c) Progressive stress test

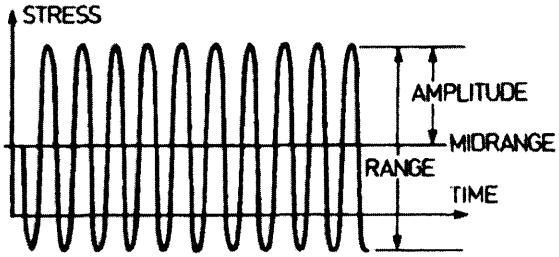

(d) Cyclic stress test

(e) Random stress test

Figure 5-1: Various stress loading tests ($\times$ failure, $\bigcirc \rightarrow$ runout) [33].

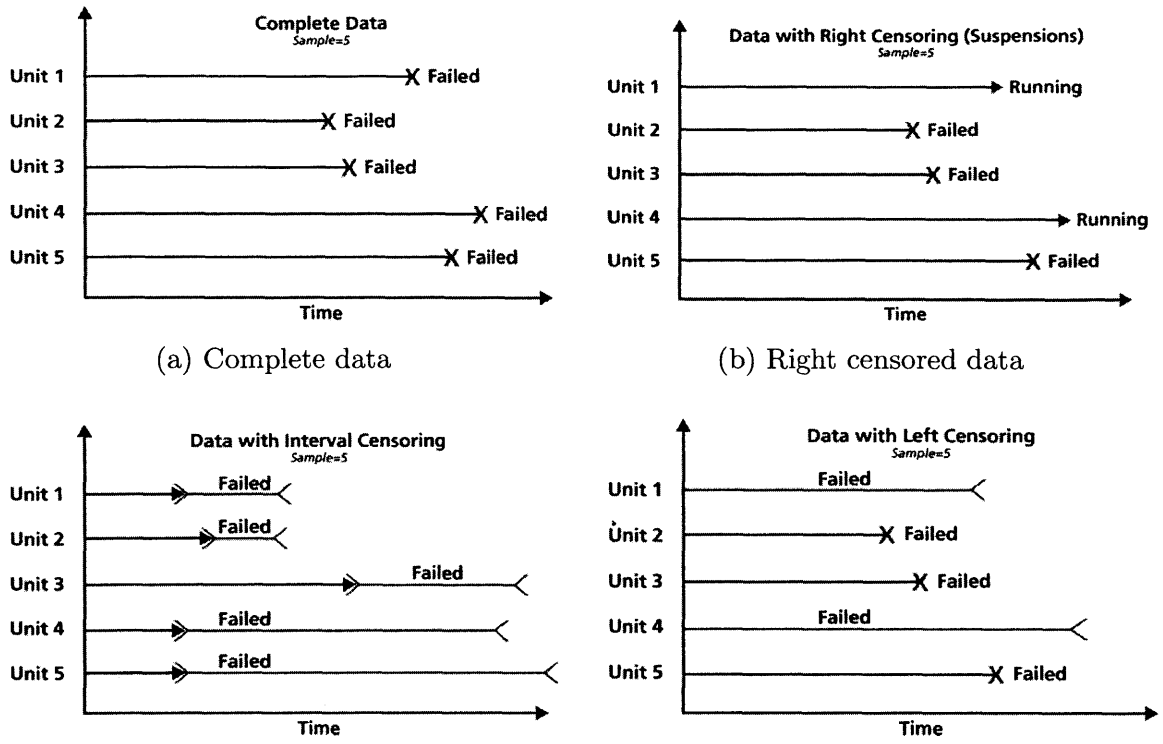

(a) Complete data

(b) Right censored data

(c) Interval censored data

(d) Left censored data

Figure 5-2: Various types of data [35].

Interval censored data consists of units that failed between predetermined inspection times. Therefore, there is uncertainty about the exact failure time as it could be anywhere between the previous and current inspection.

Left censored data consists of data where failure is only known to occur before a certain time. It is identical to interval censored data where the starting time for the interval is zero.

5.1.4 Test Design

The test specimens themselves must be carefully selected. The specimens must be representative of the actual component or product being tested. Ideally, the product itself is tested however this may not always be feasible. Therefore, a test specimen that models actual geometry, materials, loading characteristics, et cetera should be selected [33]. These specimens should also be from a representative sample—ideally a random sample the entire population [33].

Finally, the statistical design of the ALT and allocation of test specimens to various stress levels is also the subject academic and industrial research. Many "optimal" plans exist for the allocation of test units such that variance in life data collected is minimized, and these can be found in Nelson [33], Rinne [32], and by Reliasoft Corporation [34]. However, a simple two-factor factorial design could also be used

as an ALT with life as the response variable [36]. This was the approach taken by the author for this project, and details on the experimental design can be found in Chapter 6.

5.2 Statistical Models of Accelerated Life Tests

This section presents three statistical models for accelerated life tests at a constant stress level. Statistical models for ALT consist of: (1) a probability distribution which represents the scatter in product life, and (2) a life-stress relationship which provides a mathematical relationship between life at the accelerated stress level and the design or use level. This life-stress relationship is required to extrapolate life data at the accelerated stress level to determine reliability parameters, such as mean life or % of units failed at a given time t, at the use or design stress level.

5.2.1 Basic Concepts

The basic probability theory concepts presented in this section are adapted from Nelson [33] and Montgomery [36].

Cumulative distribution function

The cumulative distribution function, or *CDF* represents the fraction of the population failing by age t. The CDF $F(t)$ has the following properties:

1. is continuous for all t;
2. $F(t) \leq F(t')$ for all $t < t'$;
3. $\lim_{t \to -\infty} F(t) = 0$ and $\lim_{t \to \infty} F(t) = 1$

Reliability function

The reliability function $R(t)$ is defined as the probability of survival beyond any age t given a life distribution $F(t)$.

$$R(t) \equiv 1 - F(t) \tag{5.1}$$

Probability density function

The probability density function, or *PDF* describes the relative likelihood of the random variable life to take on a particular value [36]. It corresponds to a histogram of population life times with an infinitesimally small bin size. It is defined as the derivative of the CDF

$$f(t) \equiv \frac{\mathrm{d}F(t)}{\mathrm{d}t} \tag{5.2}$$

Thus, the area under the PDF curve is the population fraction failing by age t, *i.e.* the CDF

$$F(t) = \int_{-\infty}^{t} f(t)\,\mathrm{d}t \tag{5.3}$$

Mean, median, mode

The mean of a distribution is the expected value of the random variable across the entire range of possible values [36]. It is the average or expected life of the product or component, also referred to as the *Mean Time to Failure* or *MTTF*, given by

$$\mathrm{E}[T] = \int_{-\infty}^{\infty} tf(t)\,\mathrm{d}t \tag{5.4}$$

The median of a distribution is defined as the value T at which exactly half the population has a value less than T and half is greater, *i.e.* half the area under the PDF curve lies to the left of T and half to the right.

$$\int_{-\infty}^{T} tf(t)\,\mathrm{d}t = \frac{1}{2} \tag{5.5}$$

The mode of a distribution is the value T that has the highest probability of occurrence. Therefore, T is the value at which the PDF is at a maximum, or the derivative of the PDF is zero. The mode is the most likely life of the product.

$$f'(T) = 0 = \frac{\mathrm{d}f(t)}{\mathrm{d}t} \tag{5.6}$$

Variance and standard deviation

The variance is a measure of the spread of the distribution, given by the formula:

$$\mathrm{Var}[T] \equiv \int_{-\infty}^{\infty} (t - \mathrm{E}[T])^2 f(t)\,\mathrm{d}t = \int_{-\infty}^{\infty} t^2 f(t)\,\mathrm{d}t - (\mathrm{E}[T])^2 \tag{5.7}$$

The standard deviation is also a measure of distribution spread and is simply the square root of the variance. It is the preferred measure of spread because it has the same dimensional units as life, *e.g.* hours, days, et cetera.

$$\sigma(T) = (\mathrm{Var}[T])^{1/2} \tag{5.8}$$

The MTTF, median, mode, and standard deviation are important characteristics in reliability engineering as they provide the basis for preventative maintenance scheduling and servicing cost analysis.

Hazard function

The hazard function of a distribution describes its instantaneous failure rate at age t [33]. It is defined as

$$\lambda(t) \equiv \frac{f(t)}{1 - F(t)} = \frac{f(t)}{R(t)} \tag{5.9}$$

The hazard function indicates whether the failure rate increases or decreases with age and can be used to plan maintenance and replacement intervals. *Infant mortality* is characterized by a decreasing hazard function during early product life. This often indicates design flaws or manufacturing defects in the product [33]. *Wear out* is characterized by a hazard function that increases unbounded during late product life, indicating that failures are the result of wear [33].

5.2.2 Probability Distributions

The life of a product or component is not a deterministic value, but is rather a random variable subject to natural variation [33]. The stochastic behavior of failure time is described by either a discrete or continuous probability distribution. For mechanical components where the degradation mechanism is fatigue, fracture, or wear, the Weibull distribution or the lognormal distribution are frequently used; both these distributions are continuous [33]. Further details of both these distributions are presented below as either distribution could be used to model the reliability of the NVPro printer components.

Weibull

The Weibull distribution is one of the most versatile and widely used probability distributions in reliability engineering. It models increasing or decreasing failure rates simply and can take on characteristics of other distributions through different shape parameter values [33, 34]. Common applications include modelling mechanical material properties such as strength, electrical properties such as resistance, and life of bearings, ceramics, electronics, et cetera.

The 3-parameter Weibull CDF, also referred to as *unreliability*, is given by

$$F(t) = 1 - \exp\left(-\left(\frac{t-\gamma}{\eta}\right)^{\beta}\right), \quad t \geq 0, \gamma \tag{5.10}$$

where:

t = time to failure
β = shape parameter or slope, a unitless pure number estimated from a Weibull plot; $\beta > 0$
η = scale parameter or characteristic life[1], always equal to the 63.2th percentile life and has the same units as t; $\eta > 0$
γ = location parameter or failure free life; $-\infty < \gamma < \infty$

[1]Life is the total operational time under use conditions before complete failure.

Table 5.1: Effect of β on the Weibull distribution

β Value	Interpretation	Effect on PDF $f(t)$	Potential Cause
< 1	Early life failure (infant mortality)	Decreases monotonically, convex	Production/QC problems, inadequate burn-in
1	Random failures (independent of age)	Exponential distribution	Human error, or natural causes
1–4	Early wear out failures	Positively skewed (right tail)	Low cycle fatigue, corrosion
> 4	Old age (rapid) failures	Approximately normal, then negatively skewed (left tail)	Stress corrosion, brittle failures

The 3-parameter Weibull PDF is given by

$$f(t) = \frac{\beta}{\eta}\left(\frac{t-\gamma}{\eta}\right)^{\beta-1} \cdot \exp\left(-\left(\frac{t-\gamma}{\eta}\right)^{\beta}\right), \quad t \geq 0, \gamma \tag{5.11}$$

As seen in Figure 5-3, β determines the shape of the PDF which can vary greatly depending on the value of β. The possible β values and their effect on the distribution shape and subsequent analysis is summarized in Table 5.1, adapted from Rinne's *The Weibull Distribution: A Handbook* [32].

The location parameter γ describes the shift of the distribution from the origin along the abscissa, as seen in Figure 5-4. The failure free life is the period of time $0 \leq t \leq \gamma$. In this interval, the Weibull CDF and PDF equal zero indicating zero probability of failure and hence the name "failure free life".

On a logarithmic scale, β determines the spread of log life, with high β corresponding to small spread *i.e.* a steep slope, and vice versa. This logarithmic plot, called the *Weibull plot*, is a powerful tool used in reliability engineering. It provides visual assessment of the fit of the data to the Weibull distribution and can be used to infer reliability and life characteristics such as B_x life. A sample Weibull plot is seen in Figure 5-5. The linearized CDF is as follows

$$\begin{aligned} F(t) &= 1 - \exp\left(-\left(\frac{t-\gamma}{\eta}\right)^{\beta}\right) \\ -\ln\left(1 - F(t)\right) &= \left(\frac{t-\gamma}{\eta}\right)^{\beta} \\ \underbrace{\ln\left(-\ln\left(1-F(t)\right)\right)}_{\text{“}y\text{”}} &= \underbrace{\beta \ln\left(t-\gamma\right)}_{\text{“}mx\text{”}} - \underbrace{\beta \ln \eta}_{\text{“}b\text{”}} \end{aligned} \tag{5.12}$$

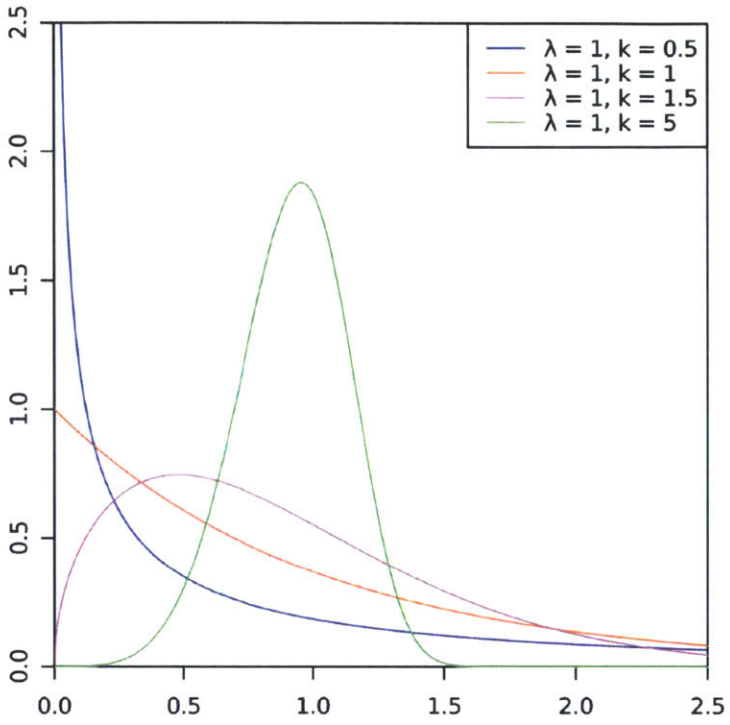

(a) PDF

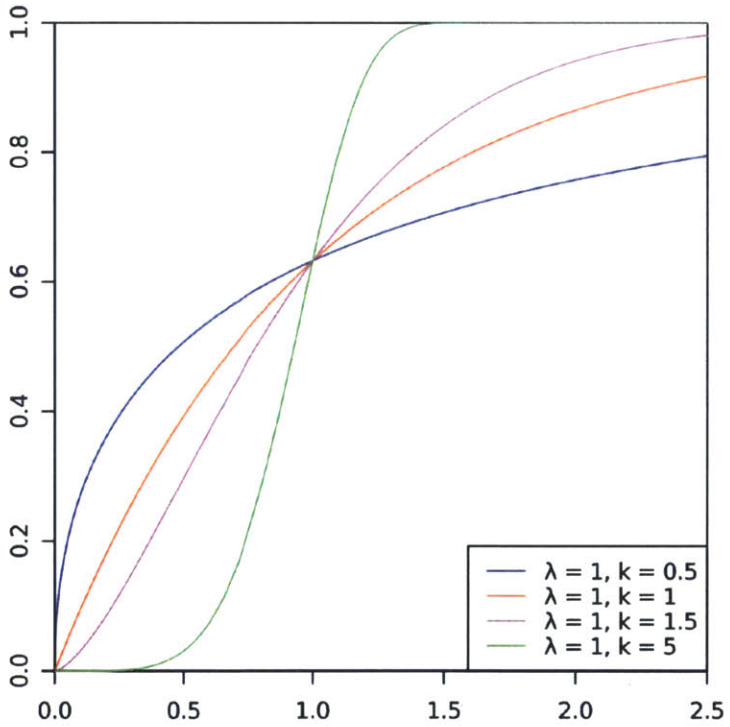

(b) CDF

Figure 5-3: The effect of the shape parameter β on (a) the Weibull PDF, and (b) on the Weibull CDF. Note: λ refers to η and k refers to β [37].

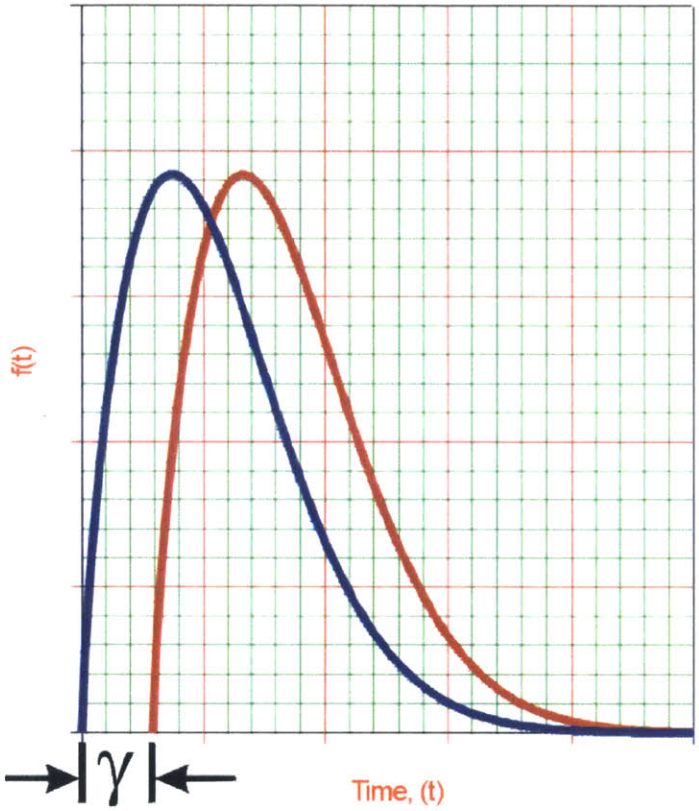

Figure 5-4: Effect of location parameter γ on Weibull PDF [34].

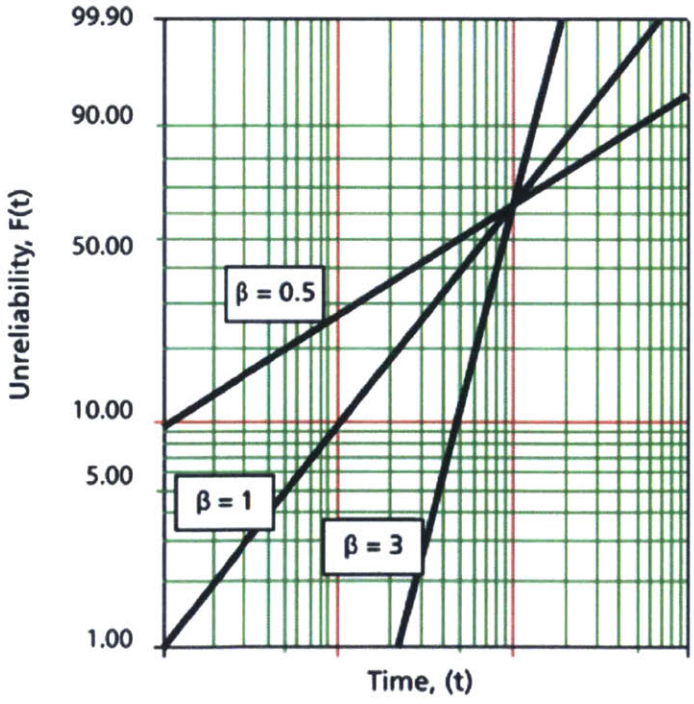

Figure 5-5: Sample Weibull plot with different values of β [35].

The 2-parameter Weibull distribution, obtained by setting $\gamma = 0$, is more common in ALT analysis. The use of the 3-parameter model would require physical justification for the presence of a failure free operating period for positive γ or failures before test or field use for negative γ, *i.e.* failures during production, storage, or transit [35]. If there is a downward curvature in the Weibull plot after data collection, a shift to the right (positive γ) may be used, resulting in a deterministic offset and a failure free operating period. However the cause of the shift should investigated and understood.

The remainder of this section will continue present results derived from the 3-parameter model for the sake of completeness. 2-parameter models are identical except with $\gamma = 0$, as seen in the 2-parameter CDF and PDF presented below.

$$F(t) = 1 - \exp\left(-\left(\frac{t}{\eta}\right)^{\beta}\right), \quad t \geq 0 \tag{5.13}$$

$$f(t) = \frac{\beta}{\eta}\left(\frac{t}{\eta}\right)^{\beta-1} \cdot \exp\left(-\left(\frac{t}{\eta}\right)^{\beta}\right), \quad t \geq 0 \tag{5.14}$$

Furthermore, if the shape parameter β is known *a priori* from past experimentation with identical or similar products, then the Weibull distribution can be further reduced to the 1-parameter model by assuming $\beta = C$ were C is an assumed constant value. The 1-parameter CDF and PDF are given by

$$F(t) = 1 - \exp\left(-\left(\frac{t}{\eta}\right)^{C}\right), \quad t \geq 0 \tag{5.15}$$

$$f(t) = \frac{C}{\eta}\left(\frac{t}{\eta}\right)^{C-1} \cdot \exp\left(-\left(\frac{t}{\eta}\right)^{C}\right), \quad t \geq 0 \tag{5.16}$$

Note that if $\beta = 1$, the 2-parameter Weibull reduces to the exponential distribution, which is simply another probability distribution used to model life.

$$F(t) = 1 - \exp\left(-\frac{t}{\eta}\right), \quad t \geq 0 \tag{5.17}$$

$$f(t) = \frac{1}{\eta}\exp\left(-\frac{t}{\eta}\right), \quad t \geq 0 \tag{5.18}$$

The Weibull reliability function, representing the population fraction surviving at age t is

$$R(t) = \exp\left(-\left(\frac{t-\gamma}{\eta}\right)^{\beta}\right), \quad t \geq 0, \gamma \tag{5.19}$$

The Weibull reliable life, τ_R is the life at which the product will be functioning without failure with for a given reliability R [34], *i.e.* the $100R$th percentile of the Weibull distribution [33]. This is also referred to as the B_x life, an extensively used reliability parameter in industry. B_x life represents the the time t at which $x\%$ of units have failed, where $0 < x < 1$. It is found by substituting $R = 1 - x$ into (5.19)

and solving for t. Note that by definition, $\tau_{0.632} \approx \eta$ for any 2-parameter Weibull distribution ($\gamma = 0$).

$$\tau_R = B_x = \gamma + \eta\,(-\ln R)^{1/\beta}, \quad 0 < R < 1 \tag{5.20}$$

The median life $T_{0.5}$ is given by the reliable life at $R = 0.5$

$$T_{0.5} = \gamma + \eta\,(\ln 2)^{1/\beta} \tag{5.21}$$

The median life represents the time at which 50% of all units have failed, *i.e.* the B_{50} life. It is a parameter sometimes used in warranty analysis.

The mean life $\overline{T}$ or MTTF is given by

$$\overline{T} = \gamma + \eta \cdot \Gamma\left(\frac{1}{\beta} + 1\right) \tag{5.22}$$

where Γ is the gamma function defined as

$$\Gamma(n) = \int_0^\infty e^{-x} x^{n-1}\,\mathrm{d}x \tag{5.23}$$

Gamma function values are typically tabulated and readily available in many statistics textbooks [36].

The mode is given by

$$T_{mode} = \gamma + \eta\left(1 - \frac{1}{\beta}\right)^{1/\beta} \tag{5.24}$$

The standard deviation is given by

$$\sigma_T = \eta \cdot \sqrt{\Gamma\left(\frac{2}{\beta} + 1\right) - \left(\Gamma\left(\frac{1}{\beta} + 1\right)\right)^2} \tag{5.25}$$

The MTTF, mode, and standard deviation are important characteristics in reliability engineering as they provide the basis for preventative maintenance scheduling and servicing cost analysis.

The hazard function, or instantaneous failure rate, is given by

$$\lambda(t) = \frac{\beta}{\eta}\left(\frac{t - \gamma}{\eta}\right)^{\beta - 1} \tag{5.26}$$

An increasing failure rate with time (product life) is indicated by $\beta > 1$, a decreasing failure is given by $\beta < 1$, and a constant failure rate is given by $\beta = 1$ (the exponential distribution). A firm understanding of product failure rates with time is required when planning product warranties and performing service cost analysis.

Lognormal

The lognormal distribution is frequently used to model metallic fatigue failures and thus is often considered alongside the Weibull distribution when modelling mechanical failures [33, 34]. A random variable is lognormally distributed if the logarithm of the random variable is normally distributed [34]. Common applications include modelling failure times of mechanical fatigue, solid state components such as semiconductors and diodes, and electrical insulation.

The lognormal CDF, also referred to as *unreliability*, is given by

$$F(t') = \Phi\left(\frac{t' - \mu'}{\sigma'}\right), \quad t \geq 0 \tag{5.27}$$

where $\Phi()$ is the standard normal cumulative distribution function defined as

$$F(x) = \Phi\left(\frac{x-\mu}{\sigma}\right) = \int_{-\infty}^{x} \frac{1}{\sigma\sqrt{2\pi}} \exp\left(-\frac{1}{2}\left(\frac{x-\mu}{\sigma}\right)^2\right) \mathrm{d}x, \quad -\infty < x < \infty \tag{5.28}$$

and where:

$t' = \ln t$, the natural logarithm of the time to failure
$\mu' =$ the mean of the log of life random variables; $-\infty < \mu' < \infty$
$\sigma' =$ the log standard deviation; $\sigma' > 0$

The lognormal PDF is given by

$$f(t) = \frac{1}{t\sigma'\sqrt{2\pi}} \exp\left(-\frac{1}{2}\left(\frac{\ln t - \mu'}{\sigma'}\right)^2\right), \quad t > 0 \tag{5.29}$$

As seen in Figure 5-6, σ' determines the shape of the PDF which can vary greatly depending on the value of σ', and μ' is the scale parameter which determines the spread of the PDF [34]. For a given μ', the degree of skewness increases as σ' increases, and for a given σ', the skewness increases as μ' increases. For $\sigma' > 1$, there is a sharp rise for small values of t, and followed by a sharp decrease.

The lognormal reliability function, representing the population fraction surviving at age t is

$$R(t) = \Phi\left(\frac{\ln t - \mu'}{\sigma'}\right) = \int_{\ln t}^{\infty} \frac{1}{\sigma'\sqrt{2\pi}} \exp\left(-\frac{1}{2}\left(\frac{x-\mu'}{\sigma'}\right)^2\right) \mathrm{d}x, \quad t > 0 \tag{5.30}$$

The lognormal reliable life, τ_R is the life at which the product will be functioning without failure with for a given reliability R [34], *i.e.* the $100R$th percentile of the lognormal distribution [33]. This is also referred to as the B_x life, an extensively used reliability parameter in industry. B_x life represents the the time t at which $x\%$ of units have failed, where $0 < x < 1$. It is found by substituting $R = 1 - x$ into (5.30)

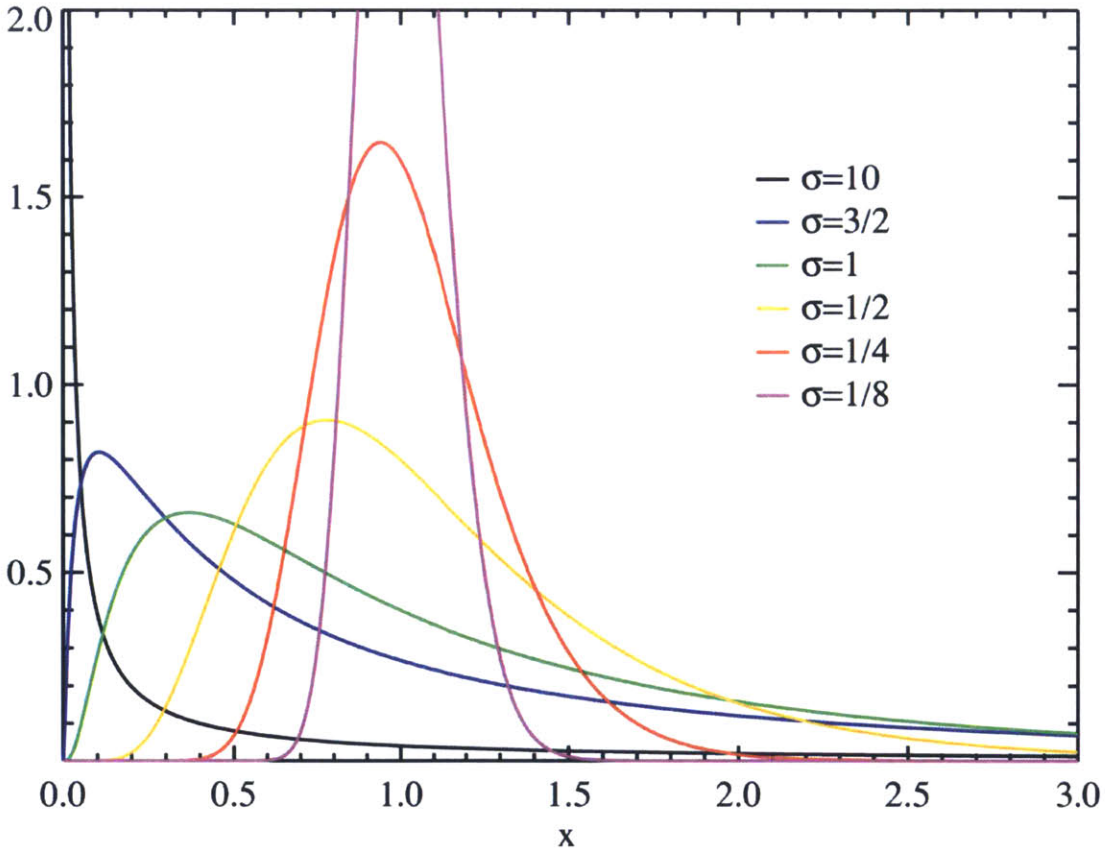

Figure 5-6: The effect of the shape parameter σ on the lognormal PDF [38].

and solving for t.

$$\tau_R = B_x = \Phi\left(\frac{\ln t - \mu'}{\sigma'}\right) = \exp\left(\mu' + z_R\sigma'\right) \tag{5.31}$$

where z_R is the $100R$th standard normal percentile, typically tabulated and readily available in many statistics textbooks [36].

The median life $T_{0.5}$ is given by the reliable life at $R = 0.5$

$$T_{0.5} = \exp\left(\mu'\right) \tag{5.32}$$

The mean life $\overline{T}$ or MTTF is given by

$$\overline{T} = \exp\left(\mu' + \frac{1}{2}\sigma'^2\right) \tag{5.33}$$

The mode is given by

$$T_{mode} = \exp\left(\mu' - \sigma'^2\right) \tag{5.34}$$

The standard deviation is given by

$$\sigma_T = \exp\left(\mu' + \frac{1}{2}\sigma'^2\right)\sqrt{\exp\left(\sigma'^2\right) - 1} \tag{5.35}$$

The MTTF, median, mode, and standard deviation are important characteristics in reliability engineering as they provide the basis for preventative maintenance scheduling and servicing cost analysis.

5.2.3 Life-Stress Relationships

As previously mentioned, a life-stress relationship provides a mathematical relationship between life at the accelerated stress level and the design or use level. This life-stress relationship is required to extrapolate life data at the accelerated stress level to determine reliability parameters at the use or design stress level. It transforms the statistical distribution which describes the stress at the accelerated levels to a distribution at the use stress levels, as seen in Figure 5-7, by equating the characteristic life or mean life in the distribution to the life-stress relationship. Two common life-stress relationships used for *constant, single stress* tests are the *Inverse Power Law* and the *Arrhenius* relationship. For multiple accelerating stresses, the *General Log-Linear* relationship is used. All three of these relationships are discussed in further detail in subsequent sections.

Inverse Power Law

The inverse power law (IPL or simply, power law) relationship is commonly used for non-thermal accelerating stresses, such as mechanical fatigue or voltage [33]. It is

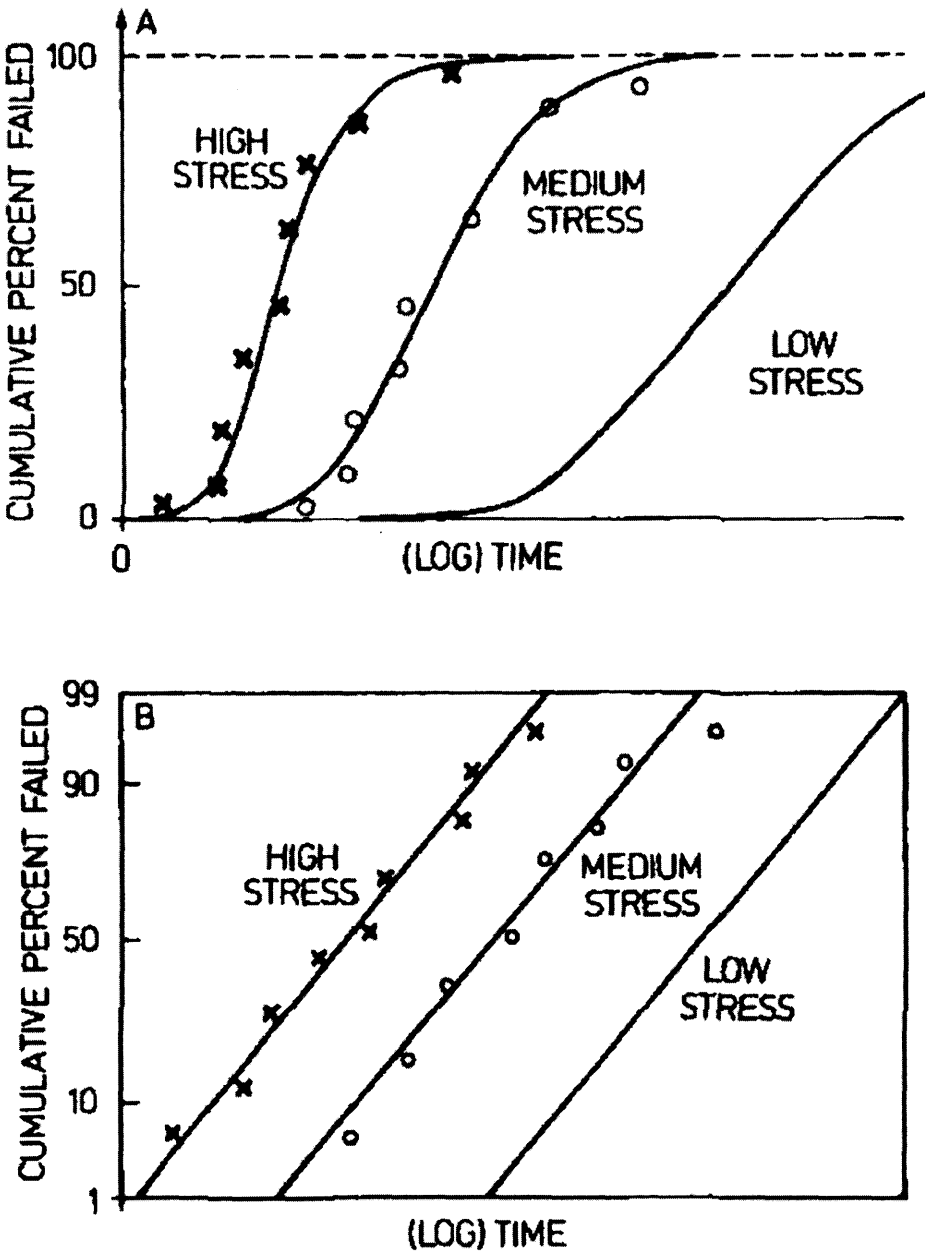

Figure 5-7: Statistical life distributions at various stress levels [33].

given by

$$L(V) = \frac{1}{KV^n} \tag{5.36}$$

where:

L = a quantifiable life measure or reliability parameter, such as mean life, median life, B_x life, et cetera
V = the stress level
K, n = model parameters characteristic of the product, specimen geometry and fabrication, and the test method; $K > 0$

Linearized, the power law is given by

$$\ln L = -\ln K - n \ln V \tag{5.37}$$

Acceleration factor for a given life-stress relationship is the ratio of use-stress-level life to accelerated-stress-level life. It is an indication of how much longer the product is expected to last in the field than in the test. The metric should neither be too high, resulting in potentially unreliable extrapolation of data, or too low, resulting in long test times. Thus, industry practitioners typically use a pre-selected acceleration factor as a guide for selecting stress levels for the test when other model parameters are known *a priori* [35].

The acceleration factor for this model is given by

$$A_F = \frac{L_{use}}{L_{accelerated}} = \left(\frac{V_A}{V_u}\right)^n \tag{5.38}$$

Arrhenius

The Arrhenius relationship is commonly used when temperature is the accelerating stress. It is based on the Arrhenius rate law which describes the rate of a simple first-order chemical reaction dependent on temperature. It assumes failure occurs when a critical amount of chemical has reacted. The relationship is given by

$$L(\vartheta) = C \exp\left(\frac{E_a}{k\vartheta}\right) \tag{5.39}$$

where:

L = a quantifiable life measure or reliability parameter, such as mean life, median life, B_x life, et cetera
ϑ = the temperature in absolute units, degrees Kelvin or Rankine
E_a = the activation energy of the reaction, in units of eV
k = $8.6171 \times 10^{-5}\,\mathrm{eV\,K^{-1}}$, Boltzmann's constant
C = a model parameter characteristic of the product failure mechanism and test condition

The linearized Arrhenius relationship is given by

$$\ln L = \ln C + \frac{E_a}{k\vartheta} \tag{5.40}$$

The acceleration factor for this model is given by

$$A_F = \frac{L_{use}}{L_{accelerated}} = \exp\left(\frac{E_a}{k}\left(\frac{1}{\vartheta_u} - \frac{1}{\vartheta_A}\right)\right) \tag{5.41}$$

General Log-Linear

The general log-linear (GLL) relationship is used when the life of the product is a function of two or more accelerating stresses [35]. The multivariable relationship is given by

$$L(X) = \exp\left(\alpha_0 + \sum_{j=1}^{n} \alpha_j X_j\right) \tag{5.42}$$

where:

L = a quantifiable life measure or reliability parameter, such as mean life, median life, B_x life, et cetera
X_j = the stress or transformed stress level
α_0, α_j = model parameters to be estimated using best-fit methods such as Maximum Likelihood Estimation (MLE), discussed in section 5.2.6

The power of the GLL relationship arises from the use of stress transformations such that $X = f(V)$, where V is the actual stress level, which allows for reduction of the GLL model to the previously discussed relationships (Arrhenius, power law, and exponential). Each X_j can have a different transformation applied to it based on the desired life-stress relationship for the stress V_j. The three most common transformations are summarized in Table 5.2

The acceleration factor for this model is given by

$$A_F = \frac{L_{use}}{L_{accelerated}} = \exp\left(\sum_{j=1}^{n} \alpha_j (X_{j,u} - X_{j,A})\right) \tag{5.43}$$

5.2.4 Power-Weibull Model

A commonly used statistical model for accelerated life tests is the Power-Weibull model, where the life of the product is described with a Weibull life distribution and reliability parameters and characteristic life is a power function of stress [33]. Applications include tests where voltage and mechanical load or stress are accelerating variables. This model is very commonly used for bearings. Model assumptions include:

1. Product life has a Weibull distribution at stress level V;

Table 5.2: GLL stress transformations

Transformation	$X = f(V)$	Resulting Life-Stress Relationship
None	$X = V$	Exponential
Reciprocal	$X = 1/X$	Arrhenius
Logarithmic	$X = \ln V$	Power

2. The Weibull shape parameter β is constant (independent of V);

3. The characteristic life L is an inverse power function of V.

The power-Weibull model is derived by modelling the Weibull characteristic life parameter with the inverse power law, *i.e.* setting $\eta = L(V) = (KV^n)^{-1}$ in the 2-parameter Weibull distribution. This yields the power-Weibull CDF and PDF as follows

$$F(t,V) = 1 - \exp\Big(-(KV^n t)^\beta\Big), \quad t \geq 0 \tag{5.44}$$

$$f(t,V) = \beta K V^n (KV^n t)^{\beta-1} \cdot \exp\Big(-(KV^n t)^\beta\Big), \quad t \geq 0 \tag{5.45}$$

The power-Weibull reliability function, representing the population fraction surviving at age t is

$$R(t,V) = \exp\Big(-(KV^n t)^\beta\Big), \quad t \geq 0, \gamma \tag{5.46}$$

The Weibull reliable life, τ_R is the life at which the product will be functioning without failure with for a given reliability R and stress level V [35], *i.e.* the $100R$th percentile of the Weibull distribution [33]. This is also referred to as the B_x life, an extensively used reliability parameter in industry. B_x life represents the the time t at which $x\%$ of units have failed, where $0 < x < 1$.

$$\tau_R = B_x = \frac{(-\ln R_V)^{1/\beta}}{KV^n}, \quad 0 < R < 1 \tag{5.47}$$

The median life $T_{0.5}$ is given by the reliable life at $R = 0.5$

$$T_{0.5} = \frac{(\ln 2)^{1/\beta}}{KV^n} \tag{5.48}$$

The mean life $\overline{T}$ or MTTF is given by

$$\overline{T} = \frac{1}{KV^n} \cdot \Gamma\left(\frac{1}{\beta} + 1\right) \tag{5.49}$$

The mode is given by

$$T_{mode} = \frac{1}{KV^n}\left(1 - \frac{1}{\beta}\right)^{1/\beta} \tag{5.50}$$

The standard deviation is given by

$$\sigma_T = \frac{1}{KV^n} \cdot \sqrt{\Gamma\left(\frac{2}{\beta}+1\right) - \left(\Gamma\left(\frac{1}{\beta}+1\right)\right)^2} \tag{5.51}$$

The hazard function, or instantaneous failure rate, is given by

$$\lambda(t, V) = \beta K V^n \left(K V^n t\right)^{\beta-1} \tag{5.52}$$

5.2.5 GLL-Weibull Model

A commonly used statistical model for accelerated life tests with multiple accelerating stresses is the GLL-Weibull model, where the life of the product is described with a Weibull life distribution and reliability parameters and characteristic life are given by the GLL relationship [35]. Applications include tests where a combination of engineering stresses, thermal stresses, and indicator (binary) variables are accelerating stresses. Model assumptions include:

1. Product life has a Weibull distribution at stress level V;
2. The Weibull shape parameter β is constant (independent of V);
3. The characteristic life L is described the the GLL relationship, with stress transformations of $X = f(V)$.

The GLL-Weibull model derived by modelling the Weibull characteristic life parameter with the GLL relationship, *i.e.* setting $\eta = L(X)$ in the 2-parameter Weibull distribution, yielding the GLL-Weibull CDF

$$F(t, X) = 1 - \exp\left(-\left(\frac{t}{\exp\left(\alpha_0 + \sum_{j=1}^{n} \alpha_j X_j\right)}\right)^{\beta}\right) \tag{5.53}$$

The power-Weibull reliability function, representing the population fraction surviving at age t is

$$R(t, X) = \exp\left(-\left(\frac{t}{\exp\left(\alpha_0 + \sum_{j=1}^{n} \alpha_j X_j\right)}\right)^{\beta}\right) \tag{5.54}$$

The Weibull reliable life, τ_R is the life at which the product will be functioning without failure with for a given reliability R and stress level V [35], *i.e.* the $100R$th

percentile of the Weibull distribution [33]. This is also referred to as the B_x life, an extensively used reliability parameter in industry. B_x life represents the the time t at which $x\%$ of units have failed, where $0 < x < 1$.

$$\tau_R = B_x = \exp\left(\alpha_0 + \sum_{j=1}^{n} \alpha_j X_j\right) \cdot (-\ln R)^{1/\beta}, \quad R > 0 \tag{5.55}$$

The median life $T_{0.5}$ is given by the reliable life at $R = 0.5$

$$T_{0.5} = \exp\left(\alpha_0 + \sum_{j=1}^{n} \alpha_j X_j\right) \cdot (\ln 2)^{1/\beta} \tag{5.56}$$

The mean life $\overline{T}$ or MTTF is given by

$$\overline{T} = \exp\left(\alpha_0 + \sum_{j=1}^{n} \alpha_j X_j\right) \cdot \Gamma\left(\frac{1}{\beta} + 1\right) \tag{5.57}$$

The mode is given by

$$T_{mode} = \exp\left(\alpha_0 + \sum_{j=1}^{n} \alpha_j X_j\right) \cdot \left(1 - \frac{1}{\beta}\right)^{1/\beta} \tag{5.58}$$

The standard deviation is given by

$$\sigma_T = \exp\left(\alpha_0 + \sum_{j=1}^{n} \alpha_j X_j\right) \cdot \sqrt{\Gamma\left(\frac{2}{\beta} + 1\right) - \left(\Gamma\left(\frac{1}{\beta} + 1\right)\right)^2} \tag{5.59}$$

The hazard function, or instantaneous failure rate, is given by

$$\lambda(t) = \frac{\beta}{\exp\left(\alpha_0 + \sum_{j=1}^{n} \alpha_j X_j\right)} \left(\frac{t}{\exp\left(\alpha_0 + \sum_{j=1}^{n} \alpha_j X_j\right)}\right)^{\beta - 1} \tag{5.60}$$

An increasing failure rate with time (product life) is indicated by $\beta > 1$, a decreasing failure is given by $\beta < 1$, and a constant failure rate is given by $\beta = 1$ (the exponential distribution).

5.2.6 Parameter Estimation for ALT Data by Maximum Likelihood Estimation

There are many methods of estimating the various statistical model parameters from a given set of data. These include graphically through probability plotting, least squares or rank regression, and maximum likelihood estimation (MLE) [33,34]. MLE is considered the most robust of the three methods, and is versatile enough to be

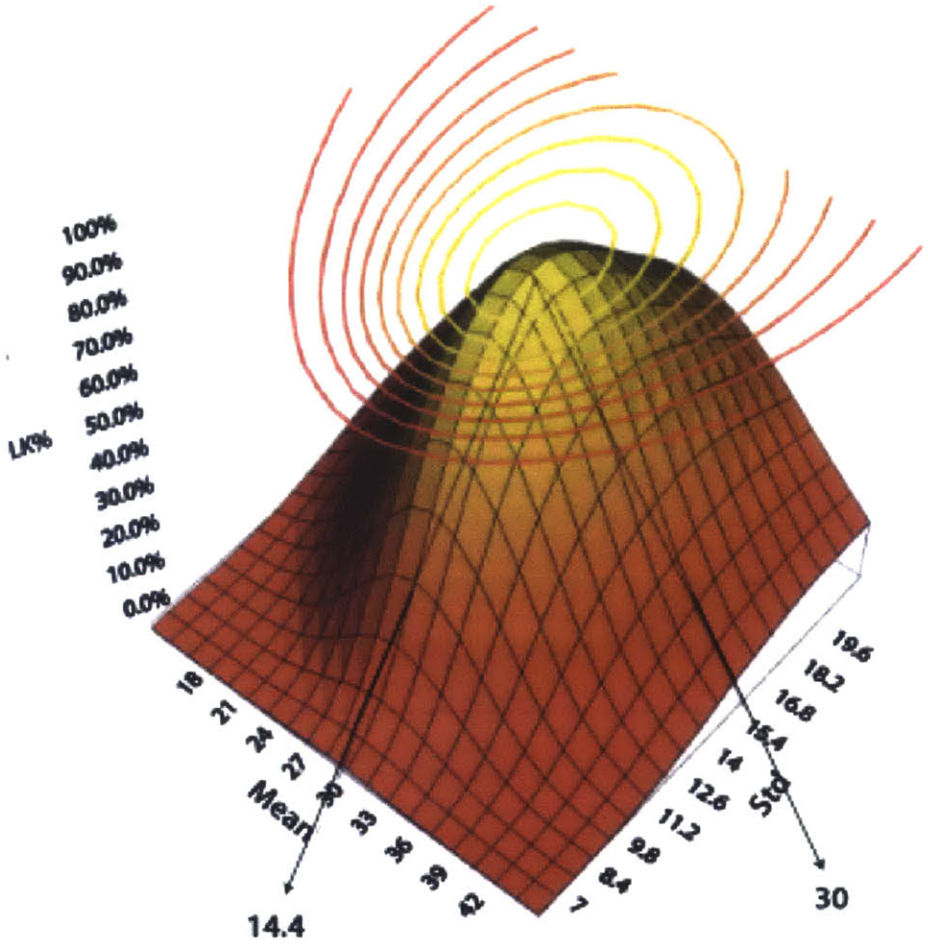

Figure 5-8: Maximum likelihood function surface for a normal distribution [35].

applied to many different models and types of data (complete or censored) [35].

The basic principle behind MLE is to develop a likelihood function from the collected data and determine the values of parameters that maximize the likelihood function. This can be time consuming, therefore the simpler method is to take the natural logarithm of the likelihood function, take partial derivatives with respect to the parameters, set the resulting equations equal to zero and solve simultaneously to determine parameter estimate values which maximize the likelihood function [34]. The general mathematical formulation is covered in detail below and then equations specific to the power-Weibull model parameter estimation are presented. Figure 5-8 provides a visual representation of the MLE process.

General Formulation

This section is presented almost verbatim from Reliasoft's Accelerated Life Testing Reference Guide [35] and Life Data Analysis Reference Guide [34].

Consider a continuous random variable $x(v)$, where v is the stress, with PDF

$$f(x, v; \theta_1, \theta_2, \ldots, \theta_k) \tag{5.61}$$

where $\theta_1, \theta_2, \ldots, \theta_k$ are unknown constant parameters which need to be estimated. After an experiment is conducted and N independent observations $x_1, x_2, \ldots, x_N$ which correspond to failure times each at a corresponding stress $v_1, v_2, \ldots, v_N$. The likelihood function for *complete data* is given by

$$L\left((x_1, v_1), \ldots, (x_N, v_N) | \theta_1, \theta_2, \ldots, \theta_k\right) = \prod_{\substack{i=1 \\ i = 1, 2, \ldots, N}}^{N} f(x_i, v_i; \theta_1, \theta_2, \ldots, \theta_k) \tag{5.62}$$

The logarithmic likelihood function is given by

$$\Lambda = \ln L = \sum_{i=1}^{N} f(x_i, v_i; \theta_1, \theta_2, \ldots, \theta_k), \quad i = 1, 2, \ldots, N \tag{5.63}$$

The maximum likelihood estimators of $\theta_1, \theta_2, \ldots, \theta_k$ are obtained by maximizing Λ. The estimators of $\theta_1, \theta_2, \ldots, \theta_k$ are the simultaneous solutions of k equations such that

$$\frac{\partial \Lambda}{\partial \theta_j} = 0, \quad j = 1, 2, \ldots, k \tag{5.64}$$

Power-Weibull MLE Parameter Estimates

The Weibull log-likelihood function for the power-Weibull model, for complete, right censored, and interval censored data is given by

$$\Lambda = \overbrace{-\sum_{i=1}^{F_e} N_i \left(KV_i^n T_i\right)^{\beta} \cdot \ln\left(\beta K V_i^n \left(KV_i^n T_i\right)^{\beta - 1}\right)}^{\text{complete data}} \underbrace{-\sum_{i=1}^{S} N_i' \left(KV_i^n T_i'\right)^{\beta}}_{\text{right censored data}} + \underbrace{\sum_{i=1}^{F_{int}} N_i'' \ln\left(R_{Li}'' - R_{Ri}''\right)}_{\text{interval censored data}} \tag{5.65}$$

where:

$$R_{Li}'' = \exp\left(-\left(KV_i^n T_{Li}''\right)^{\beta}\right) \tag{5.66}$$

$$R_{Ri}'' = \exp\left(-\left(KV_i^n T_{Ri}''\right)^{\beta}\right) \tag{5.67}$$

and where:

F_e = number of groups of exact times-to-failure data points
N_i = number of times-to-failure data points in the i^{th} time-to-failure data group
β = Weibull shape parameter unknown—first of three parameters to be estimated
K = power law parameter—unknown, second and third of three parameters to be estimated
n = power law parameter—unknown, third and third of three parameters to be estimated
V_i = stress level of the i^{th} group
T_i = exact failure time of the i^{th} group
S = number of groups of suspension data points
N_i' = number of suspensions in the i^{th} group of suspension data points
T_i' = running time of the i^{th} suspension data group
F_{int} = number of interval data groups
N_i'' = number of intervals in the i^{th} group of data intervals
T_{Li}'' = the beginning of the i^{th} interval
T_{Ri}'' = the end of the i^{th} interval

The parameter estimates $\hat{\beta}$, $\hat{K}$, and $\hat{\eta}$ are found by setting the respective partial derivatives $\partial\Lambda/\partial\beta$, $\partial\Lambda/\partial K$, and $\partial\Lambda/\partial\eta$ to zero and solving the equations simultaneously using software and numerical techniques.

5.3 Summary

This chapter presented an overview of accelerated life testing (ALT), covering topics such as purpose, accelerating stresses, stress loadings, types of data, and test design. The chapter then covered various aspects of statistical models of ALT such as probability distributions, life-stress relationships, reliability characteristics, and model parameter estimation techniques. The purpose of this chapter was to present the theoretical component of accelerated life testing, whereas the next chapter presents the experimental design and hardware components.

An accelerated life test is a special experiment designed specifically to collect life data, such as time until a failure mode appears, in a significantly shorter period of time than collecting the same data from the field. The acceleration is typically accomplished through overstressing, whereby stresses such as temperature, voltage, mechanical load, thermal cycling, humidity, chemical exposure, radiation, and vibration are at increased levels from design or use levels. The higher stress levels lead to accelerated degradation in product performance and life. However, care must be taken to ensure the higher stress levels do not induce new failure modes not seen at lower design stress levels.

The failure data collected from ALT is subsequently analyzed using a statistical model consisting of: (1) a probability distribution which represents the scatter in product life, and (2) a life-stress relationship which provides a mathematical relationship between life at the accelerated stress level and the design or use level.

Two commonly used probability distributions for mechanical failures due to fatigue, fracture, or wear are the Weibull distribution and the lognormal distribution. The Arrhenius life-stress relationship is typically used when temperature is the accelerating stress, and the inverse power law life-stress relationship is typically used where mechanical load or stress is the accelerating stress.

A common statistical model for ALT of bearings is the power-Weibull model. The details of this model were presented along with the maximum likelihood estimation (MLE) method to determine model parameters from a set of sample data. Finally, the details to the general log-linear-Weibull model, a common multivariable model which allows the inclusion of two or more accelerating stresses, was presented.

Chapter 7 presents an example of ALT data analysis where the application of all theory presented in this chapter is illustrated.

Chapter 6

Design of Experiment for Accelerated Life Test

Reliability analysis is typically performed using one of two methods: (1) a statistically optimal accelerated life test where stress levels and the number of units are calculated such that variance in the results is minimized, or (2) using a test designed based on engineering judgement and experience [33]. However, these methods are less suitable when the exact stresses that actually affect life are unknown, *i.e.* mechanical load, voltage, temperature, humidity, etc. Such is usually the case with a new system or design with which the engineering team has no prior experience and numerous factors are suspected to affect life. A statistically optimal design of ALT with more than two accelerating stress is mathematically complex and therefore, it is in the engineer's best interest to determine with confidence which factors actually affect life.

In situations like this, a third method that can be used for ALT analysis is Reliability Design of Experiments (R-DOE). The primary purpose of R-DOE is to identify which factors affect product life with statistical significance [39]. This is done by investigating whether changing input factor levels leads to a statistically significant change in the response, *i.e* life of the product. Once the significant stresses have been identified, ALT statistical analysis can be carried out on the data collected to determine life characteristics, or the R-DOE results can be used to plan a follow-up ALT that is very efficient as it does not include insignificant factors.

DOE was the approach taken to accelerated life testing of the linear bearings for the NVPro because many factors were suspected of affecting bearing life, but it was not known which were significant. This chapter details the R-DOE approach and all considerations taken when designing the experiment and associated hardware components.

6.1 DOE Literature Review

This section provides a very brief overview of relevant DOE concepts required for understanding the ALT experimental design. For more details, the reader the referred to Montgomery [36] or DeVor *et al.* [40].

6.1.1 DOE Overview

DOE is a systematic method to establish a cause-and-effect relationship between a number of independent variables and a dependent variable of interest in the most efficient way possible [41]. The dependent variable is the *response* and the independent variables are *factors*. *Control factors* are those inputs that could be modified in the experiment and *noise factors* are those inputs that cannot be controlled.

An experiment is run at various factor values called *levels*, determined using knowledge of the system, physics, and engineering judgement. A combination of levels across all factors is called a run or *treatment*. The measurement taken at a treatment is called an *observation*, and repeated observations at a treatment are called *replicates*.

The number of treatments is based on the number of factor levels being investigated. If all possible combinations of factor levels are run, then the DOE is a *full factorial* design. If only some of the treatment combinations are run, then the DOE is a *fractional factorial* design. In a full factorial design, the significance of all factors and their interactions can be determined, whereas in a fractional factorial, the significance of certain or all interactions may not be possible depending on the experiment design.

The basic principle behind a DOE is to vary the factor levels for each run and observe whether there is a change in the response [36]. The aggregate change in response for each factor is referred to as the *contrast* of the control factor. To determine whether a factor is statistically significant, a statistical quantity derived from the contrast is compared against the overall variation and sampling error in the sample data. A factor is statistically significant if the change in response is greater than the variation in the system, as determined by the *p-value* of a test statistic being less than some significance level α, where $0 < \alpha < 1$ [36]. The p-value represents the probability that random chance could explain the result. If $p < \alpha$, then change in response due to a change in the factor of interest falls outside the probability distribution limits set by α.

Through this systematic approach, each factor and interaction term is tested for statistical significance. If found significant, it is included in the system's mathematical response model, otherwise it is left out as its effect could not be distinguished from random variation.

6.1.2 R-DOE Considerations

In a R-DOE, the response variable is life and the control factors are the accelerating stresses under consideration for ALT. However, two key differences between R-DOE analysis and traditional DOE analysis are as follows:

1. In traditional DOE analysis, the response is assumed to follow a normal distribution and therefore, the error terms can be assumed to be normally and independently distributed. This is not valid for R-DOE analysis as life data is typically modelled by a Weibull or lognormal distribution.

2. The life data from a R-DOE may be complete or censored, which does not allow standard regression analysis techniques employed in DOE analysis to be used in a R-DOE analysis.

   This limitation is overcome with using parameter estimation techniques such as maximum likelihood estimation (MLE) instead of regression analysis. The significance of factors and interaction terms is tested using likelihood ratio tests, where a ratio of the likelihood function without the factor under consideration, A, and the likelihood function value with the factor A is compared to the chi-squared (χ^2) distribution [39]. Further details of this method of significance testing can be found in Reliasoft's Experiment Design and Analysis Reference [39].

6.2 Factors Affecting Bearing Life

The factors that affect the life of the linear bushings are derived from the various failure modes described in Section 4.3. Any of these factors could be significant in regards to bearing life.

Excessive radial load excessive loading results in premature fatigue failure of the bearing balls. It can be the result of excessive mass supported by the bearings, moment loading due to eccentricity between the carried load center of gravity and bearing set center of stiffness, pre-load from an excessively tight fit, or misalignment of the shaft and bearing. Misalignment can be the result of a radial offset between bearing bores, an angular offset, or due to shaft deflection from excessive loading, as pictured in Figure 6-1.

Axial load linear bushings are not designed to support axial loads, therefore any significant axial loading could compromise the integrity of the bearing and lead to failure.

Contact hardness hardness is a measure of a material's resistance to plastic deformation by penetration under an applied compressive force [43]. The hardness of the two contacting surfaces–bearing balls and shaft–is critical to smooth operation and long bushing life. If one of the two contacting materials is significantly harder than the other, it will deform the other surface under applied load, leading to rough operation, increased vibration, and eventual failure.

Lubrication lubrication creates a thin fluid film between the contact surfaces of the bearing balls and the shaft, reducing friction and creating separation between the microscopic asperities on each surface. In the absence of lubrication, galling occurs between the surfaces, leading to a sharp increase in temperature, a decrease in contact hardness, metal flow, and eventually complete bearing seizure. Therefore, the correct amount and type of lubrication is required for bearing longevity.

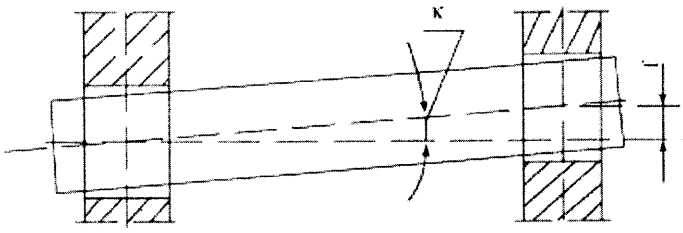

(a) Radial and angular misalignment

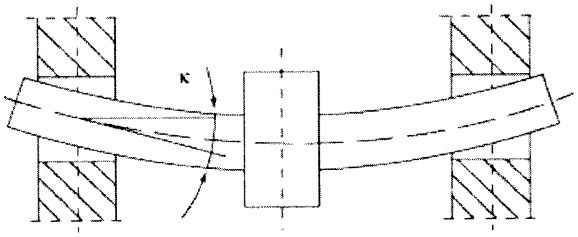

(b) Shaft deflection

Figure 6-1: Various types of bearing–shaft misalignment resulting in uneven loading of the bearing balls and pre-mature fatigue failure [42].

Temperature the contact temperature between the two surfaces is controlled by lubrication. In the absence of lubrication, adhesive wear leads to excessive temperature rise, a decrease in contact hardness, metal flow, and bearing seizure. The ambient operating temperature also affects the bearing system. High ambient temperatures cause the components to expand, potentially leading to excessive thermo-mechanical stresses. High ambient temperatures also can cause the lubrication to break down.

Moisture the presence of moisture in the bearing system, likely due to humidity in the operating environment, reduces lubrication effectiveness and can cause lubrication breakdown. Moisture can also lead to corrosion of the bearing, shaft, or housing components.

Debris various forms of contamination, such as dirt, dust, metal shavings or powders, and wear particles, can lead to the initiation and subsequent acceleration of abrasive wear.

Vibration excessive radial clearance of the linear bushings causes chatter during operation, leading to failure by fretting corrosion.

Brinelling the surface of the bearing or shaft could be damaged during assembly of the printer due to improper handling.

6.2.1 Selected Accelerating Stresses

It would be impractical to design an experiment to test all nine of the potentially significant factors identified. A full factorial 2^9 experiment would consistent of 512

treatments. A 2^{9-5}_{III} fractional factorial design would only consist of 16 treatments and still allow for estimation of the main effects, however even this would be impractical. Factors such as temperature (contact or ambient), moisture, debris, and vibration would be difficult to accurately control and maintain at a prescribed level for the accelerated life test given the resources available for the test.[1]

Using engineering judgement, axial load was eliminated as a potential design factor. The design of the NVPro ensured the linear bearings were not axially loaded, *i.e.* they did not butt up against a housing lip, and there was no operating condition in which the linear bearings would be axially loaded. Contact hardness was set by the design and selection of components used in the current production revision of the NVPro and thus was eliminated as a design factor. Brinelling was eliminated as a design factor as careful inspection and handling of the linear bushings is part of the current assembly process and would also be during the experiment.

Therefore, through process of elimination, the following stresses were left: radial load and lubrication. Radial load was further discretized into *system mass* and *misalignment*. These accelerated stresses are discussed in further detail below.

System mass

The radial load on the bearings is primarily the weight of the carriage mass being supported by the bearings. Radial load is known to affect the life of the bearings with absolute certainty as increased cyclic contact stresses accelerate fatigue damage of the ball bearings. The American Bearing Manufacturers Association (ABMA) defines bearing *rating life*, or L_{10}, or B_{10} as the number of revolutions that 90 percent of a group of identical bearings will achieve before a predetermined failure criterion develops, typically spalling of load carrying surfaces exceeding an area of $0.01\,\text{in}^2$ [44]. In other words, the rating life is the 10th percentile location of the bearing group's failure distribution. This is typically taken as 1,000,000 revolutions. It then follows that the *Basic Dynamic Load Rating*, or C_{10} is the load at which 10 percent of a group of bearings would fail at the L_{10} life [44]. The C_{10} load is unrealistically high to cause failure at only 10^6 revolutions, and thus should only be viewed as a reference value and not an actual load to be achieved by the bearing [44].

Applied to linear ball bushings, the L_{10} life is taken as 50 km of travel and the C_{10} rated load is the load at which 90 percent of ball bushings would achieve the rated life [45]. The relationship between bearing life and load is given by Palmgrens equation [46]:

$$L_{10} = \left(\frac{C_{10}}{F}\right)^{\alpha} \cdot 50 \tag{6.1}$$

where:

[1]Controlling these factors with accuracy would require specialized equipment, which there was neither the budget nor the time for at the time this thesis project was conducted. However, it is recommended that future tests be conducted using these factors as accelerating stresses.

L_{10} = bushing life in kilometres
F = applied radial load
α = 3 for ball bearings, or 10/3 for roller bearings

The inverse cubic relationship between life and radial load suggests that system mass has a significant effect on bearing life, and thus should definitely be used as an accelerating stress in the experiment.

Lubrication

The type of lubrication would not be changed during the experiment. White lithium grease is currently used on the NVPro in production and would also be used in the DOE. However, the amount of lubrication would be varied and entirely eliminated to greatly accelerate the bearing wear.

Misalignment

Though it is true that bearing-shaft misalignment leads to an increase in radial load, it is difficult to precisely measure and predict the increase in load. Therefore, misalignment itself was selected as a design factor. The DOE results would indicate whether misalignment of the shaft during assembly does affect bearing life in a statistically significant manner.

6.2.2 Noise Factors and Mitigation Strategies

Some of the stresses previously eliminated from consideration in the DOE were now potential noise factors in the experiment. Their mitigation strategies are discussed below.

Contact hardness the bearing balls and shaft were both made of 52100 bearing steel, with a hardness value of approximately 58 HRC. Assuming no manufacturing defects and significant variation in hardness in the batch of components in stock, there would be no impact of contact hardness on the results.

Temperature the ambient temperature in the NVBOTS office is controlled to within $\pm 3\,^{\circ}\mathrm{C}$. The open-to-air encasements would ensure sufficient natural convection of components during test operation. The contact temperature itself would likely increase in treatments involving little to no lubrication. However this leads to the desired failure mode and therefore, is not a problem.

Moisture the relative humidity in the NVBOTS office is controlled to within $\pm 10\%$, and the test would be conducted away from any windows and other sources of moisture. The test units would not be exposed to moisture at any stage during assembly or operation.

Debris great care would be taken during handling, assembly, and operation of the test units to ensure no external debris contamination. Debris in the form of wear particles was desirable as this would lead to a predicted failure mode.

Vibration as the linear bearings wear, there would be noticeable chatter and vibration due to increased radial clearance, eventually leading to a predicted failure mode. External vibrations were not present in the test environment.

Brinelling great care would be taken during handling, assembly, and operation of the test units to ensure bearing and shafts surfaces are not damaged.

6.3 Response Variable Definition

The response variable in the accelerated bearing life test is the life of the bearing itself. Life can be defined in a few different ways:

- The number of hours before failure;
- The number of cycles before failure, if continuously traversing the same pattern; and
- The total distance travelled before failure.

The most robust of the three methods is total distance travelled as involves the least number of assumptions to extrapolate accelerated life data to regular operating condition life. Linear bearings are also life rated by distance. Therefore, the life of the bearing would be measured in total distance travelled, given by the equation

$$L = t_{fail} V_{avg} = N_{fail} d \tag{6.2}$$

Where:

t_{fail} = time elapsed continuously operating until failure
V_{avg} = d/t_{avg}
N_{fail} = number of cycles to failure
d = total travel per bearing in one cycle
t_{avg} = average time to complete one cycle

The criterion describing a failure event must also be specified. The Timken Corporation specifies failure as spalling or pitting of load carrying surfaces exceeding an area of $0.01\,\text{in}^2$ [44]. However, since the contact surface would not be actively or periodically monitored during the test, this criterion could not be used. Instead, failure was specified as the occurrence of one of the following events:

- Bearing seizure and lockup resulting in the inability to move the carriage;
- Visible spalling or pitting of shaft surface;
- Cracking of bearing balls;
- Excessive noise and vibration indicating complete loss of bearing efficacy;
- Motor over-current situation due to excessive resistance to motion.

6.3.1 Degradation Analysis: Wear Measurement

In the event there were insufficient bearing failures recorded within the allotted testing time, wear was could also be selected as a secondary response variable for degradation analysis. Degradation analysis would specify the failure criterion as a certain level or amount of wear deemed unacceptable, based on a maximum performance degradation, and then subsequent analysis and extrapolation of measured wear rates to predict bearing life.

Wear could be defined in the following ways:

- The depth of wear, measured as the change in a linear dimension such as the inner radius of the ball bushing;
- The amount of material lost from the bearing during the wear process, measured as change in volume or mass;
- The change in shaft surface profile, measured using a profilometer;
- Increase in vibrations due to increased radial clearance, as measured by an accelerometer; or
- Increase in average motor current draw due to increased resistance to motion as the bearing wears.

Each method presents its advantages and disadvantages, however the selected methods of wear measurement were the change in mass of the ball bushing and the change in the inner radius of the ball bushing. These were the simplest to measure—the mass lost would be measured using a precision mass scale, and the increase in inner radius would be measured using an optical microscope—and provided accurate data for subsequent degradation analysis.

6.4 Test Apparatus Design

6.4.1 Overview

In order to perform the accelerated life test of the linear bushings, they must accumulate as much travel as possible in order to initiate any of the failure modes discussed in Section 4.3. The failures must also occur in the shortest amount of time to ensure that test resources are not efficiently utilized. This acceleration of linear bushing travel can be accomplished by two means: testing each bushing individually with reciprocating motion on a separate shaft, or moving the actual printer's XY gantry system and thus testing the four linear bushings in the X direction and four linear bushings in Y at once.

After investigating both options and careful consideration, the actual XY gantry, pictured in Figure 6-2, was selected for the following reasons:

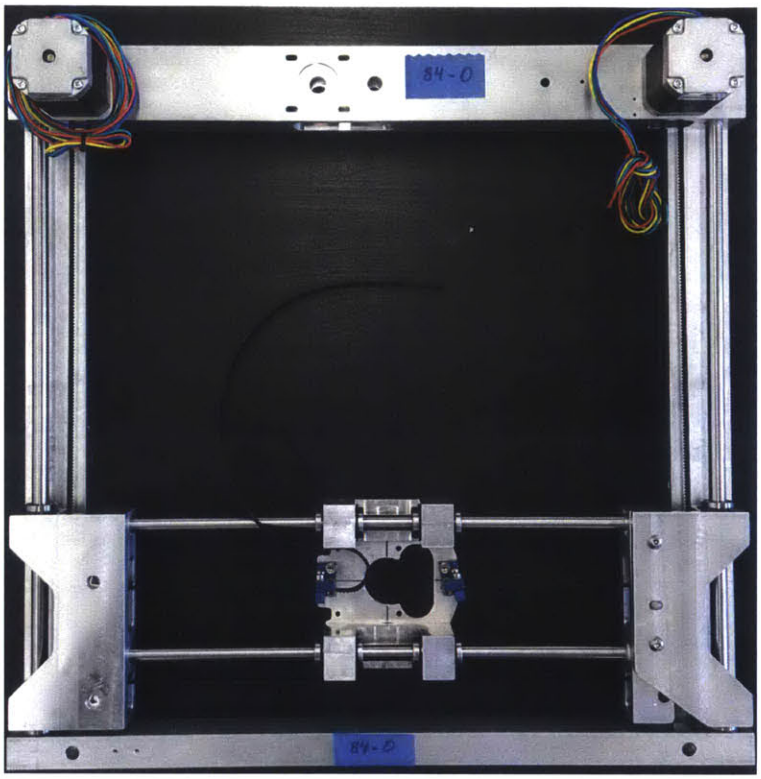

Figure 6-2: NVPro XY gantry used in ALT apparatus.

- All components for a test bench were already available as they were standard production parts from the actual printer. A entirely new test bench would have to be designed to test each linear bushing separately. The cost, design effort, and procurement lead time associated with this option was not worth the potential benefit of isolated bearing life results.

- The entire linear bearing system found in the printer was being tested as opposed to a single bearing model representing a bearing in the system. Though this led to potential noise factors such as assembly and fit effects, the benefit of a more accurate representation of the entire overall system outweighed this.

- The XY gantries would physically occupy less space within the NVBOTS office than a test bench designed to test individual bearings.

In the production NVPro, each XY gantry includes a Z axis which controls the movement of the build plate through the use of a leadscrew and precision shafts. The entire XY gantry with Z components is secured in a sheet metal encasement with screws, and then subsequently secured in the cosmetic outer shell of the NVPro. The Z axis and outer shell were not included as part of the XY gantry accelerated testing as they were external to the linear bushing operation and did not affect it in any way. This opened up space within the encasement below the XY gantry and thus, a second XY gantry was secured within the encasement approximately 10 inches below

Figure 6-3: XY gantries double stacked within encasement.

the first, pictured in Figure 6-3. Doing so was economical both in terms of space occupied by the all the test apparatuses and production stock of encasements.

6.4.2 Additional Loading

One of the accelerating stresses selected in Section 6.2.1 was bearing load. In order to increase the load on each bearing, additional mass was added to the entire gantry system in the form of standard strength training barbell plates. 5 lb and 10 lb barbell plates, pictured in Figure 6-4, were added to the system by mounting the desired quantity of barbell plates to the extruder mounting plate which was secured to the X-bearing blocks via screws. Thus the X bearings were directly loaded as the additional mass was added it its carriage, and the Y bearings were also directly loaded as Y movement entailed movement of the entire X carriage.

The mounting accomplished through the use of the 1–1/8" holes in the center of the barbell plates. The extruder plate was modified by drilling a 1–1/8" clearance hole in its center, and then a 1"–8 UNC bolt with a corresponding hex nut and washers were used to secure the plates to the extruder plate. An aluminum tube with a 1–1/8" inner diameter was cut to length and used as a spacer so that the X-bearing blocks did not get loaded. The entire assembly can be found in Figure 6-5.

As seen in Figure 6-5b, barbell plates were in exactly the center of the X carriage (*i.e.* in the center of stiffness of the X bearings). This ensured that there was no roll or pitch moment loading on the X bearings. Dynamic moment loading on the Y

(a) 5 lb (b) 10 lb

Figure 6-4: Standard 5 lb and 10 lb barbell plates used for additional system loading.

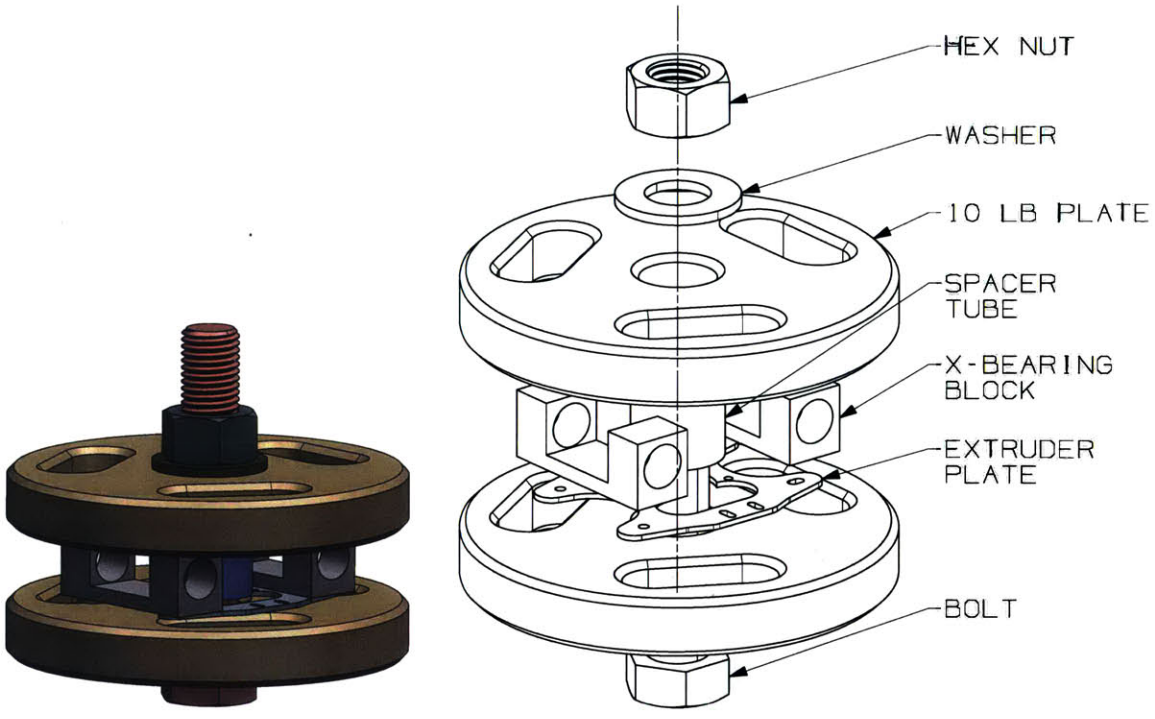

(a) Isometric (b) Exploded

Figure 6-5: CAD layout of mounting configuration for additional system loading.

bearings is further discussed and analyzed in Section 6.5.3.

Pitching Moment

However a pitching moment could also be generated if the center of gravity of the loaded carriage in the Z axis was not on the line of action of the belt tension force, as depicted in Figure 6-6. In the NVPro, the belt was used in a H–gantry setup to drive the extruder in both X and Y. The same setup was used in testing to drive the load in X and Y.

The effect of center of gravity eccentricity, e was very significant. It acted as a moment arm for the belt tension force, F_T, resulting in a moment, M_T about the system center of gravity. The reaction force couple, given by F_R and L, on the bearings would result in abnormal loading that does not model actual operation and possibly cause the system to bind.

The equations of motion for the pitching moment situation depicted in Figure 6-6b are

$$\begin{aligned} \sum F_x &= ma_x \\ F_T &= ma \end{aligned} \tag{6.3}$$

$$\begin{aligned} \sum F_y &= ma_y = 0 \\ F_g &= 4F_N \end{aligned} \tag{6.3a}$$

$$\begin{aligned} \sum M_{CG} &= I\alpha = 0 \\ 0 &= M_T - 4F_R\left(\frac{L}{2}\right) \\ 0 &= F_T e - 2F_R L \\ F_R &= \left(\frac{e}{2L}\right) F_T = \left(\frac{e}{2L}\right) ma \end{aligned} \tag{6.3b}$$

The result from (6.3b) shows that the force on the bearing is linearly proportional to the eccentricity of the center of gravity from the tension force's line of action, where the tension force is given as ma. The distance in x between the bearing centers is $L = 58.8\,\text{mm}$. The maximum possible linear acceleration is $10\,000\,\text{mm/s}^2$ in regular operation when moving just the 1.8 kg extruder. Assuming the acceleration is $500\,\text{mm/s}^2$ when the system is loaded to 18 kg using barbell plates, the pitching moment reaction force on each bearing for just 1 mm eccentricity is:

$$F_R = \left(\frac{e}{2L}\right) ma = \left(\frac{1}{117.6}\right)(18)(500) = 76.5\,\text{N} = 7.8\,\text{kgf} \tag{6.4}$$

The dynamic load capacity of the linear bushing was 372 N, and the additional mass loading would be on the order of the 7.8 kgf moment reaction force. Therefore it is absolutely critical to minimize center of gravity eccentricity. In order to mitigate

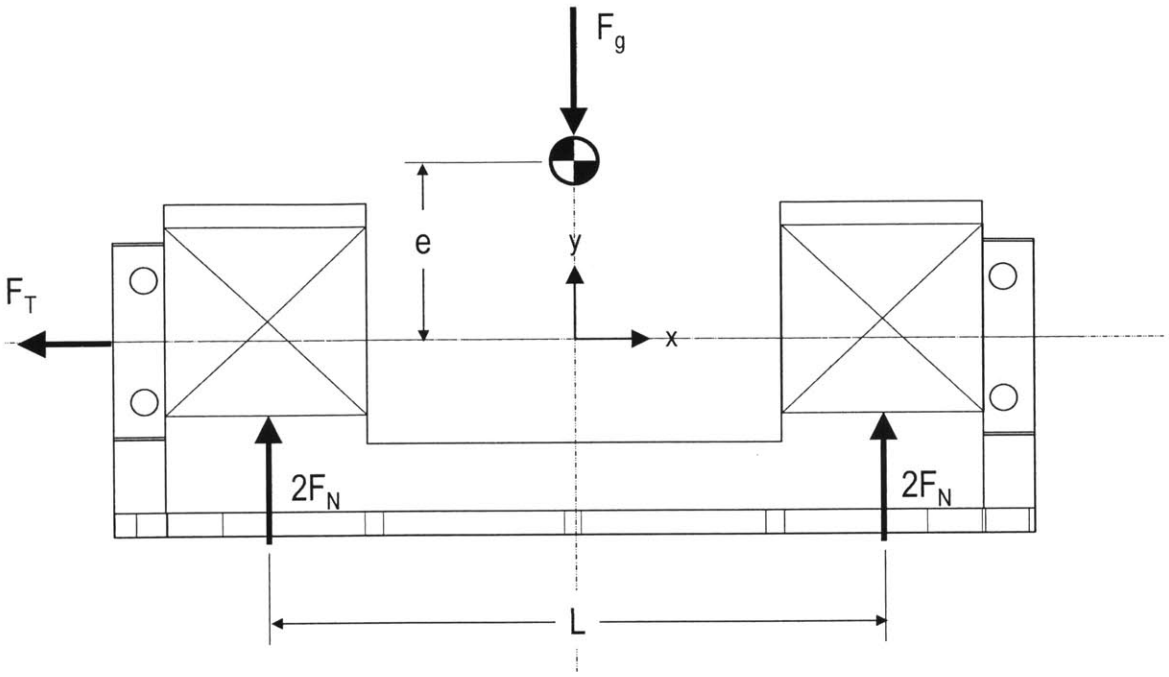

(a) Eccentric loading

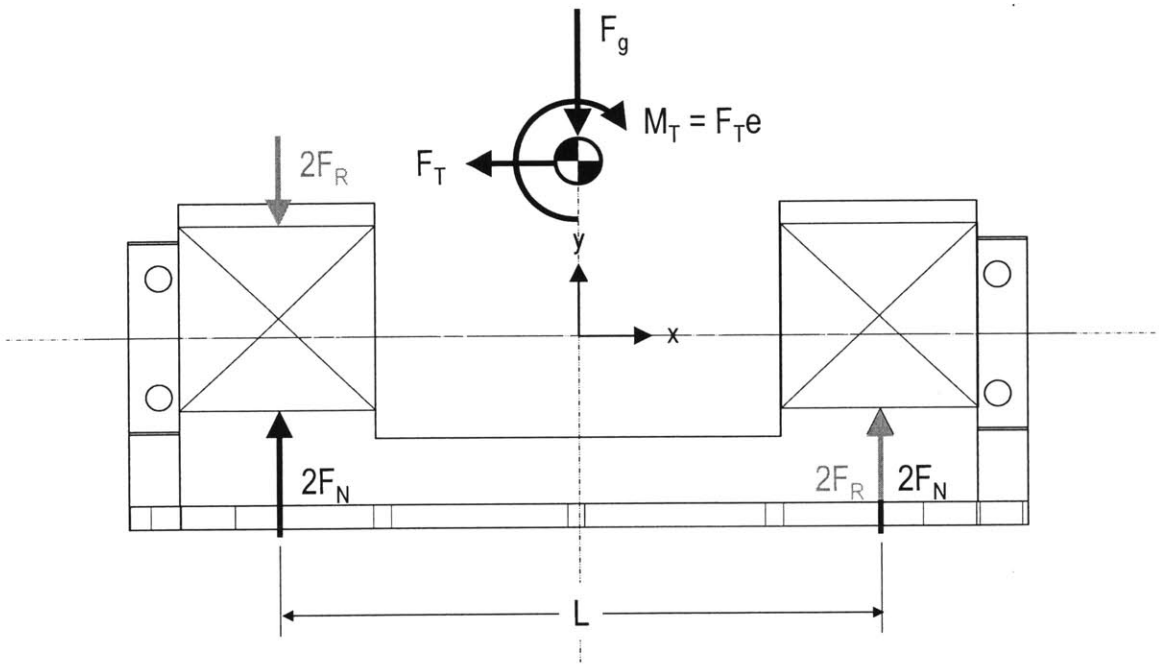

(b) Equivalent loading

Figure 6-6: Actual and equivalent loading scenarios on the X carriage with center of gravity eccentricity, resulting in a pitching moment and additional force on each bearing. Note that there are 4 bearings total in the X carriage, however only 2 are seen in the side view, hence the "2" multiplier for all bearing forces.

this risk, the barbell plates were added from both underneath and above the extruder plate, as seen in Figure 6-5b, to ensure that the center of gravity of the system was as close to the belt tension force's line of action thus reducing the size of the moment arm. At all levels of loading discussed in Section 6.5.1, a CAD model was used with correct material density inputs for each component to verify that the eccentricity was $< 0.1\,\text{mm}$.

6.4.3 Mechatronic Control

As mentioned earlier, the NVPro uses an H-frame-type XY positioning system, or simply an H-gantry, to achieve accurate positioning of the extruder head within the XY plane. An excellent overview of H-gantry systems and dynamic modelling by Jouaneh *et al.* in [47]. The primary takeaways are that a system of six idler pulleys, two motors with sprockets, and one long belt continuous belt are required to position in X and Y.

The NVPro accomplishes motion through the use of two NEMA 17 stepper motors.[2] These motors are driven by a motor driver and the logic is supplied by the on-board Raspberry Pi computer. To simplify the electronic control and achieve the most cost-effective solution, a breadboard based system was designed by the author and Forrest Pieper, co-founder and CTO of NVBOTS, pictured in Figure 6-7. A single motor driver per motor was used and one Teensy 3.1 Arduino-based microcomputer per four motors, or two complete gantries. The system was programmed to continuously travel in a reciprocating diagonal path, thus ensuring both the X bearings and Y bearings accumulate travel per cycle. Each cycle consisted of the forward and backward diagonal stroke, which consisted of 137 mm of travel in X and 203 mm of travel in Y per stroke. The reduced travel as compared to the $8\,\text{in} \times 8\,\text{in}$ printer build area was due interference between the large diameter barbell plates and the gantry structure if operated full stroke. The system would be operated at the maximum possible speed and acceleration before the motors skipped to ensure the bearings accumulated as much travel as possible with the given test time of 7 days, or 168 hours. One complete cycle provided 0.274 m of travel in X and 0.406 m in Y simultaneously, and took approximately 3.86 s to complete. Therefore, in 7 days, each bearing would be cycled 156,684 times, resulting in 42.9312 km of travel for X bearings and 63.6135 km of travel for Y bearings.

A total of four limit switches, two on each end of X travel and two on each end of Y travel, were mounted on each frame. In the event of a bearing failure, the carriage would no longer be able to move in a diagonal and the motor would skip. This would cause the system to move in only the direction orthogonal to the failed bearing direction, *e.g.* if a bearing in X fails, the carriage will only move in Y. A limit switch will subsequently be hit and this would signal the motor driver to disable the motor.

[2]The make and model of the motor is not revealed to protect NVBOTS confidentiality.

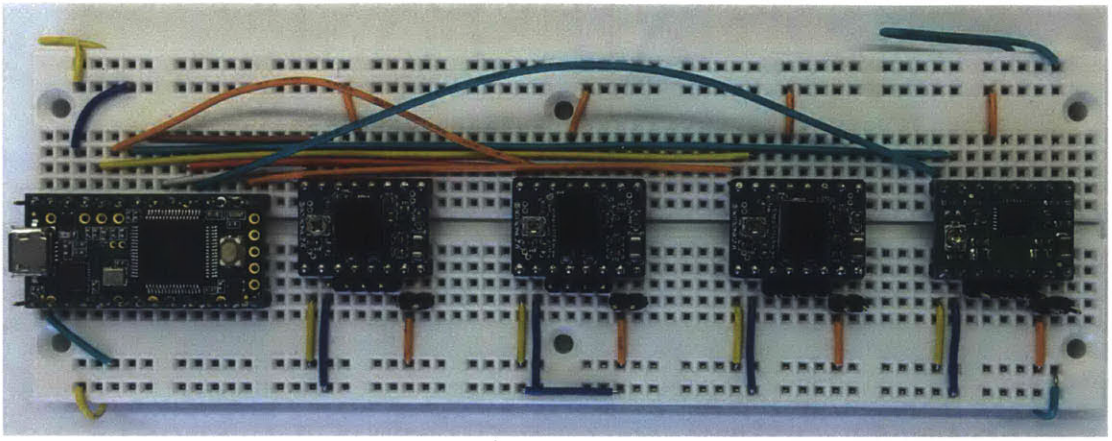

Figure 6-7: Breadboard based control system used in accelerated life test.

6.5 Accelerated Life Test

6.5.1 Experimental Design

A full factorial 2^3 experiment with a center point and eight replicates for each treatment was selected. Eight replicates were the result of the XY gantry design. Only one XY gantry was tested per treatment, but there were eight linear bearings in total per gantry and thus all eight bushings were exposed to the treatment level. A full factorial design meant that all main effects, two-way interactions, and the three-way interaction between factors could be determined.

Design Factor Levels

Table 6.1 summarizes the coded design factor levels for the experiment.

Table 6.1: Design factor levels

Design Factor			Low (-1)	Center (0)	High (+1)
A	Additional System Load	kg	5.27	12.28	19.08
B	Amount of Lubricant	mg	~ 300	~ 100	0
C	Misalignment (X & Y)	°	$< 0.01°$	$0.05° - 0.08°$	$\sim 0.115°$

The loading levels for *Factor A: Additional System Load* were based on the addition of barbell plates and mounting hardware to the extruder plate. The full list of mounting hardware and associated mass is found in Table 6.2. A precision mass balance was used to determine the mass of the each hardware item in the entire batch ordered, and then the average mass of each item was calculated for any further analysis. Note, for the center and high load levels, a 6 in long bolt was used, and a 4 in

long bolt was used for the low load level due to partial threading on the bolt and the thickness of the barbell plates.

The low level represented the standard loading case where the filament extruder was the only additional mass moved by the gantry. The extruder weighed approximately 1.8 kg or 3.97 lb, however a low loading level of 5.27 kg was selected for two reasons:

1. Two 5 lb barbell plates had to be loaded on the extruder plate, one from above and one from below, to ensure the center of gravity remained as close to the line of action of the belt tension force as possible; and

2. The author hypothesized that the true extruder mass of 1.8 kg was far too low to cause failure within the allotted test time of 168 hours, as bearing life is proportional to

$$L \propto \left(\frac{C}{F}\right)^3 \tag{6.5}$$

   Where F is the load per bearing and C is the bearing's rated dynamic equivalent load. Therefore increasing the system load even slightly has an inverse cubic effect on bearing life.

The high level of additional system load was based on the addition of four 10 lb plates and associated mounting hardware mass. The center point load level was set to correspond to an additional 25 lb in barbell plates plus additional mounting hardware mass.

The low level for *Factor B: Amount of Lubrication* referred to a well-lubricated state, *i.e.* the standard amount of lubrication used in production assembly. This was approximately 300 mg per bearing. The high level represented a case where accelerated wear would occur, such as when all lubrication in the system had been used up and was in need of replacement. Thus the high level was set to "no lubrication". The center point level represented a case of minimum lubrication—one-third the standard amount, approximately 100 mg.

The low level for *Factor C: Angle of Misalignment* referred to the Y axis, and meant to represent a "perfect" frame with nearly zero misalignment between parallel shafts. The high level represented the maximum possible misalignment by design, calculated using the designed slot width (800 µm) and length of shaft (400 mm) for one shaft in each axes:

$$\theta_{max} = \arcsin\left(\frac{0.8}{400}\right) = 0.115° \tag{6.6}$$

The center point level was an approximate middle range of misalignment levels. Misalignment levels were achieved using shims during the assembly process of the test frames.

Table 6.2: Additional System Load Breakdown

		Low (-1)		Center (0)		High (+1)	
Component	Unit Mass [g]	Qty	Item Mass [g]	Qty	Item Mass [g]	Qty	Item Mass [g]
1"–8 UNC, 4" long bolt	509.03	1	509.03	0	0	0	0
1"–8 UNC, 6" long bolt	707.08	0	0	1	707.08	1	707.08
1"–8 UNC hex nut	124.31	1	124.31	1	124.31	1	124.31
1" washer	37.73	2	75.46	2	75.46	2	75.46
Spacer tube	29.87	1	29.87	1	29.87	1	29.87
5 lb barbell plate	2,667.96	2	4,535.92	1	2,667.96	0	0
10 lb barbell plate	4,535.92	0	0	2	9,071.84	4	18,143.68
Total			5.27 kg		12.28 kg		19.08 kg

Table 6.3: Experimental run order

Treatment	Frame No.	A	B	C
(1)	35	−1	−1	−1
a	64	+1	−1	−1
b	88	−1	+1	−1
ab	82	+1	+1	−1
c	87	−1	−1	+1
ac	89	+1	−1	+1
bc	85	−1	+1	+1
abc	81	+1	+1	+1
0	84	0	0	0

Run Order

All treatments would run simultaneously on different frames. Table 6.3 summarizes the treatment levels by frame and the coded values of each design factor.

6.5.2 Standard Operating Procedure

As previously mentioned in Section 6.4.3, the accelerated life test would be conducted through continuous, reciprocating diagonal motion of the carriage. The diagonal motion ensured an equal number of cycles per direction, however given that the stroke length was the not the same in each direction, the X and Y bearings accumulated unequal travel.

The maximum possible acceleration for 19.08 kg additional loading, *i.e* when design factor A was +1, was empirically determined to be 1000 mm/s^2 before the stepper motor skipped. Therefore, all units were operated at this maximum acceleration. At this acceleration, the maximum achievable feed speed was 12 000 mm/s for the high loading case, therefore the speed for all treatments was also limited to 12 000 mm/s

The test would be run 24 hours a day for 7 days straight, resulting in approximately 42.9 km travel per X bearing and 63.6 km travel per Y bearing, at which point the test would be suspended. If a bearing failed within the 7 days, the test for that particular frame was stopped and the failure time of the bearing was recorded. The remaining 7 bearings in the system would be recorded as suspended at the failure time, known as right-censored data [33]. If a bearing failed while the author was physically present at the NVBOTS office, the exact failure time was known. Otherwise, if a bearing failed while the author was away from the office, the only information known was that it failed within the away interval. This was referred to as interval censored

Table 6.4: Total loads by direction and design factor level

		Low (−1)	Center (0)	High (+1)
X carriage mass	kg	0.285	0.285	0.285
Y carriage mass	kg	1.304	1.304	1.304
Additional mass	kg	5.27	12.28	19.08
Total weight supported by X bearings	N	54.55	123.23	189.98
Total weight supported by Y bearings	N	64.54	133.23	199.98

data as the failure time was known to lie somewhere on the interval between when the author last left the office and returned [33]. Units that did not have any failed bearings after seven days were recorded as right-censored data at the suspension time of 168 hours, referred to as Type I censoring [33]. The failure or suspension time in hours would subsequently be converted back to distance travelled in kilometres for further analysis.

If a bearing failed, the mechatronic control system ensured that the motor would stop running and no further travel would occur, which could result in catastrophic failure modes not seen during regular operation. When the failure would eventually be noticed, the testing for the other frame double stacked in the same enclosure would also momentarily stopped so the failed bearing frame could be removed from the encasement. After removal from the encasement, the entire frame should be taken apart to extract the linear bearings. The bearings would then be analyzed under an optical microscope at 20x zoom and a digital image saved. The image would be used to determine the wear depth in µm by measuring maximum inner bearing radius position. The difference from the standard inner radius of 5 mm was the wear depth, and subsequently the increase in radial clearance. The bearing mass would also be measured using a precision mass balance to record the change in mass, corresponding to the mass lost as wear debris.

6.5.3 Bearing Load Calculations and Test Justification

The total mass supported by the X bearings includes the mass of the X carriage components and the additional mass added at each treatment level. The total mass supported by the Y bearings includes the entire mass of the X carriage and the additional system mass, and the Y carriage components. This is because when the system moves in Y, the entire X axis moves with it as dictated by H-gantry dynamics. The mass and equivalent system load at each of the three design factor levels (high, center, low) are summarized in Table 6.4.

The load on the linear bearings during reciprocating diagonal motion is different for the X and Y bearings. As seen in Figure 6-8a, the center of gravity of the system

is always in the center of stiffness of the four X bearings regardless of the position of the carriage. Therefore, the load supported by each bearing is simply

$$F_{xi} = F_g/4 \qquad i = 1, \ldots, 4 \tag{6.7}$$

However, the loading on each individual Y bearing fluctuates with carriage position due to eccentricity of the center of mass from the geometric center of stiffness of the Y bearings. As seen in Figure 6-8b, the center of gravity is always a distance e_y from the Y bearing center by design, and a distance of e_x as the carriage travels in a diagonal. The eccentricity e_x ranges between $-l_x/2 \leq e_x \leq l_x/2$, where l_x is the X stroke length, representing the far ends of diagonal travel. Taking the sum of forces and moments, the following bearing equivalent loads are determined

$$F_{y1} = F_g \left(\frac{1}{4} + \frac{e_x}{2x_0} + \frac{e_y}{2y_0} \right) \tag{6.7a}$$

$$F_{y2} = F_g \left(\frac{1}{4} - \frac{e_x}{2x_0} + \frac{e_y}{2y_0} \right) \tag{6.7b}$$

$$F_{y3} = F_g \left(\frac{1}{4} + \frac{e_x}{2x_0} - \frac{e_y}{2y_0} \right) \tag{6.7c}$$

$$F_{y4} = F_g \left(\frac{1}{4} - \frac{e_x}{2x_0} - \frac{e_y}{2y_0} \right) \tag{6.7d}$$

Figure 6-9 includes plots of the Y bearing loads as a function of e_x at the high system loading level, where $F_g = 199.98\,\text{N}$, thus representing the change in load as the carriage moves along its diagonal path. The Y eccentricity was as designed at $e_y = 15.43\,\text{mm}$, and the X stroke length was $l_x = 2e_x = 137\,\text{mm}$. The X distance between the rails was a designed at $x_0 = 407.22\,\text{mm}$ and the Y distance between the bearing centers was designed as $y_0 = 107.4\,\text{mm}$. The maximum peak loads are seen in bearings Y_1 and Y_2 in the high loading treatments. These bearings fluctuate between $F_{y1} = F_{y2} = 81.18\,\text{N}$ and $F_{y1} = F_{y2} = 47.54\,\text{N}$ and the load during diagonal motion is described by (6.8).

$$\begin{aligned} F_{y1,2}(x) &= \frac{F_a}{e_x} x + F_m \\ &= \frac{(|F_{y1} - F_{y2}|/2)}{e_x} x + \left(\frac{F_{y1} + F_{y2}}{2} \right) \\ &= \frac{16.82}{e_x} x + 64.36 \end{aligned} \tag{6.8}$$

The average load on bearings Y_1 and Y_2 can be determined using the following formula, adapted from the manufacturers discrete fluctuating loads formula to evaluate

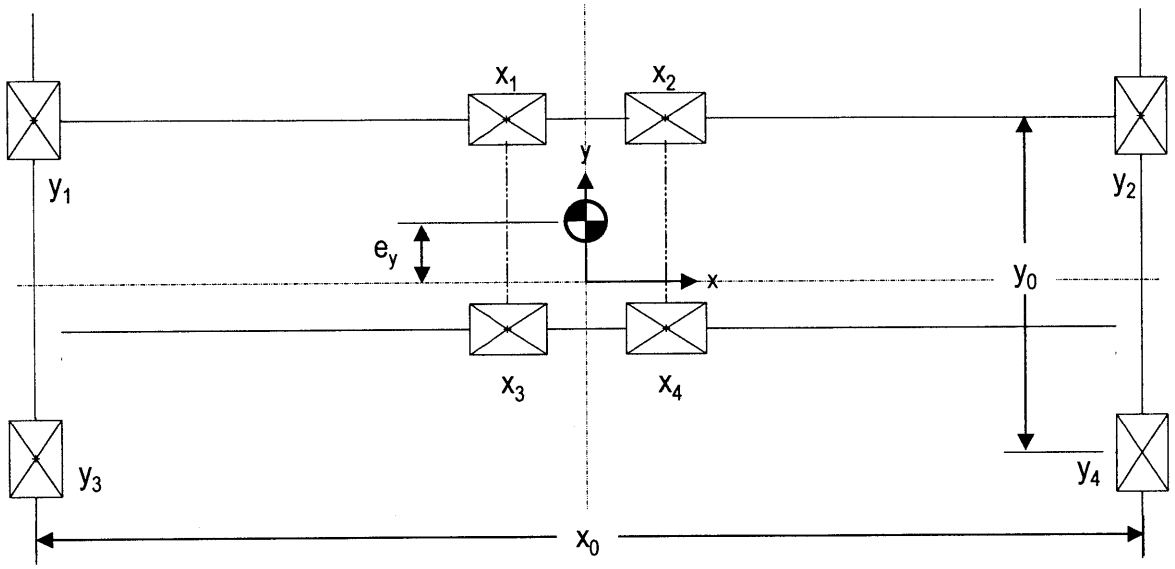

(a) Center position

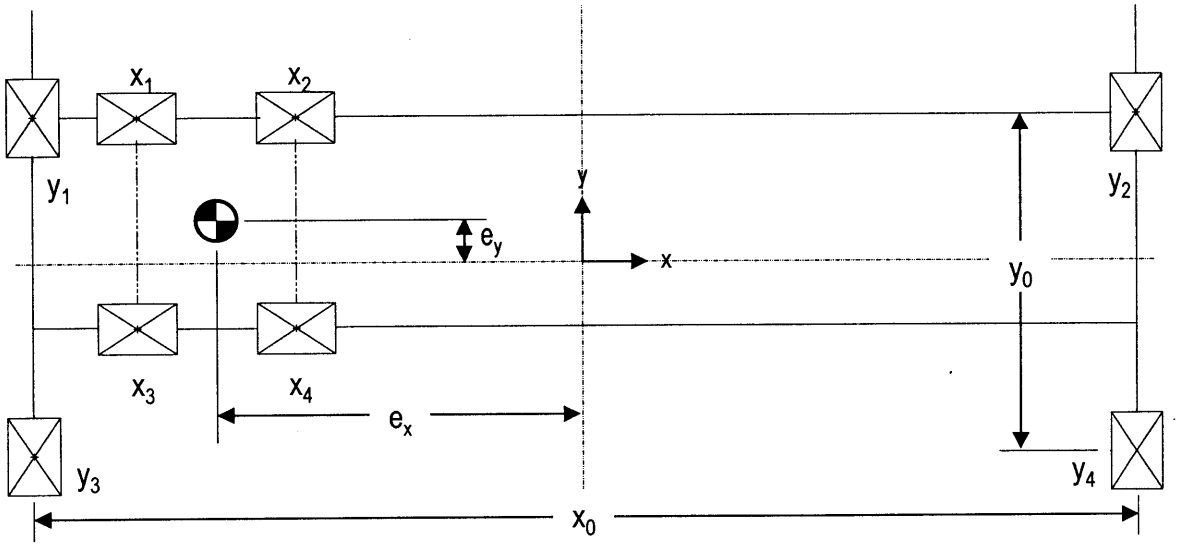

(b) Diagonal end position

Figure 6-8: Center of gravity position with respect to Y carriage and bearings during various stages of diagonal travel. The eccentricity results in a moment and thus additional force on each bearing.

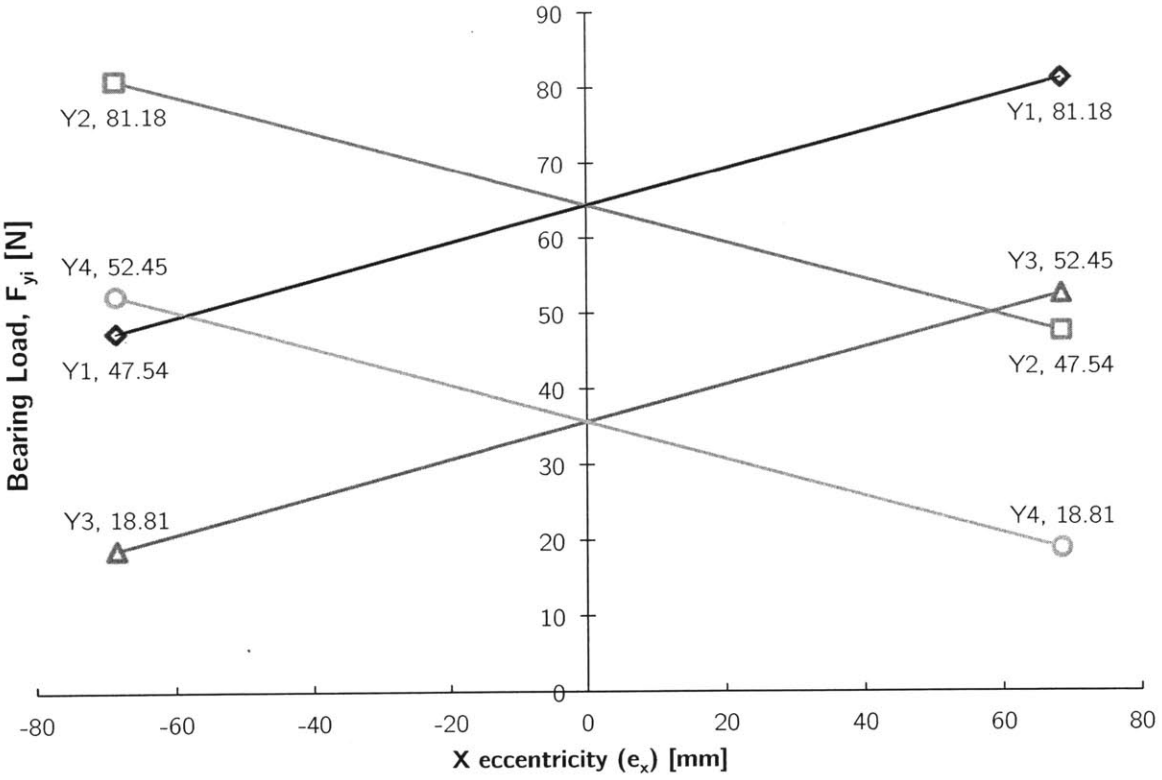

Figure 6-9: Y bearing loads as a function of X eccentricity of system center of gravity as carriage travels in diagonal path.

the average from a continuous function [45]:

$$\overline{F}_{y1,2} = \left(\frac{1}{l_x} \int_{-e_x}^{e_x} F_{y1,2}^3(x)\,\mathrm{d}x \right)^{1/3} \tag{6.9}$$

Using (6.9), the average load on the bearings Y_1 and Y_2 is found to be 65.79 N. Using the bearing life equation provided by the manufacturer, the total travel each of these bushings could endure without fatigue failure of the ball bearings in 10% of the bushings is

$$\begin{aligned} L_{10} &= \left(\frac{f_H f_T f_C}{f_W} \cdot \frac{C}{F} \right)^3 \cdot 50 \\ &= \left(\frac{1 \cdot 1 \cdot 0.81}{1.25} \cdot \frac{372}{65.79} \right)^3 \cdot 50 \\ &= 2459\,\mathrm{km} \end{aligned} \tag{6.10}$$

Where:

f_H = hardness coefficient, taken from Fig. 1 in [45]
f_T = temperature coefficient, taken from Fig. 2 in [45]
f_C = contact coefficient, taken from Table 3 in [45]
f_W = load coefficient, taken from Table 4 in [45]

If each cycle takes 3.86 s and covers 0.406 m of travel (average speed of 0.105 18 m/s), then the L_{10} life of 2459 km translates to 6494 hours or 270 of continuous loaded operation!

This result is highly suspect for a few reasons.

- It only considers one possible failure mode: flaking or spalling due to fatigue of the bearing balls;
- It predicts an astronomically high bearing life even for the highest possible loading scenario in the DOE—the highest additional system mass combined with the highest loaded bearings due to eccentricity; and
- The manufacturers equation assumes well lubricated bearings. Therefore, it does not account for the effect, if any, of lack of lubrication and of bearing-shaft misalignment, both of which are design factors in the DOE.

Therefore, these calculations serve as justification for conducting the accelerated life test and using the DOE results to estimate actual linear bushing reliability with accuracy. The results and subsequent analysis are presented in the next chapter.

6.6 Summary

This chapter presented the systematic approach taken in designing the accelerated life test for the NVPro linear bushings and designing the required testing hardware.

Factors affecting bearing life, response variable definition, test apparatus design, experimental design, and bearing load calculations were described in detail.

The various factors affecting bearing life, based on the failure modes presented in Section 4.3 were investigated. The three factors selected as accelerating stresses were system mass, amount of lubrication, and shaft-bearing misalignment. Increasing system mass and misalignment would increase the imposed load on the bearings, which has an inverse cubic relationship to bearing life. The absence of lubrication accelerates adhesive wear in the bearings.

The two response variables selected for the experiment were the bearing life, measured in distance travelled, and the amount wear, measured as the mass lost from the bearings using a precision mass scale, and change in inner bearing radius determined using an optical microscope.

The testing would be conducted using the production NVPro XY gantries which consisted of four linear bushings in the X axis and four linear bushings in the Y axis. Therefore, each frame tested eight bearings simultaneously. The system mass was increased by loading the X carriage with 5 lb and 10 lb barbell weights. Careful attention was paid to ensure the center of gravity of the loaded system was as close to the line of action of the belt tension force to mitigate the risk of pitching moment loads which could be significant and lead to binding.

A full factorial 2^3 experiment with a center point and eight replicates, a result of eight bearings per XY gantry, for each treatment was selected. Design factor levels set based on current design values, engineering judgement, and practical considerations. The additional system mass was varied between 5.27 kg and 19.08 kg, the amount of lubrication was either the standard amount used in production (300 mg) or no lubrication, and the misalignment was varied between near perfect ($< 0.01°$) and the maximum allowable misalignment given the designed slot width ($0.115°$)

Finally, the testing consisted of continuously moving the loaded carriage in a reciprocating diagonal path until either a bearing failed or the test duration of 7 days (168 hours) was completed. If a bearing failed, its failure time in hours would be recorded and converted to distance travelled. All bearings would have the amount of wear measured after testing was complete to perform degradation analysis.

Chapter 7

Accelerated Life Test Sample Results

The actual accelerated life test of the linear ball bushings was not executed due to resource constraints. However the experiment was completely designed, as explained in Chapter 6, and was ready for execution by NVBOTS at the end of the project. Therefore, the data presented in this section is fictitious and was generated based on the author's engineering judgement and basic bearing life calculations to estimate potential failure times. The purpose of using the representative data is to demonstrate the ALT analysis techniques presented in Chapter 5 and provide guidance for analysis NVBOTS would perform with actual test data.

7.1 Life Analysis

The first step before any life analysis should be a thorough qualitative failure analysis of the failed linear bushings to determine the active failure mode and verify that it was the cause of failure for all failed bearings. This is necessary because any subsequent life analysis assumes a single failure mode. The qualitative failure analysis could be performed by taking pictures of the bearing surfaces using a microscope and comparing to images and descriptions of failure modes covered in Chapter 4.

The following assumptions were made for life analysis of the representative data:

1. Load and lubrication were found to be statistically significant control factors. Misalignment was not significant;
2. The failure mode was a combination of both adhesive and abrasive wear;
3. Each treatment had a single bearing failure, and the remaining seven bearings were suspended data points;
4. The test was run continuously, *i.e.* 24 hours/day, for 7 days straight without any unexpected interruptions;
5. The exact failure time, rounded to the nearest hour, was known for each data point;

6. The life data was described by a 2-parameter Weibull distribution; and

7. The general log-linear (GLL) relationship was used to as the life-stress relationship for the multiple accelerating stresses. The load was transformed logarithmically to characterize its inverse power law relationship, and the lubrication was treated as an indicator variable, *i.e.* binary, and thus not transformed at all.

7.1.1 Results

The data presented in Tables 7.1 and 7.2 and is not actual data collected through ALT of the linear bushings, but is characteristic of the type of data to expect. The subsequent analysis is meant to illustrate one approach to interpreting life data. Note that the travel data in Table 7.2 is simply the failure or suspension times from Table 7.1 multiplied by the average X and Y speeds:

$$\overline{V}_x = \frac{l_x}{t_{stroke}} = \frac{137\,\text{mm}}{1.93\,\text{s}} = 70.98\,\text{mm/s} = 0.255\,544\,\text{km/h} \tag{7.1}$$

$$\overline{V}_y = \frac{l_y}{t_{stroke}} = \frac{203\,\text{mm}}{1.93\,\text{s}} = 105.18\,\text{mm/s} = 0.378\,653\,\text{km/h} \tag{7.2}$$

7.1.2 Statistical Model

The general log-linear life-stress relationship was used in conjunction with the Weibull distribution to analyze the data. The GLL likelihood function is given by

$$L(X) = \exp\left(\alpha_0 + \sum_{j=1}^{n} \alpha_j X_j\right) \tag{7.3}$$

A logarithmic stress transformation was applied to the load (control factor A or $j = 1$), where

$$X_1 = \ln V_1 \tag{7.4}$$

and no transformation was applied to the lubrication indicator variable, which remained as

$$X_2 = V_2 = \begin{cases} 1 & \text{if lubricated,} \\ 0 & \text{if unlubricated.} \end{cases} \tag{7.5}$$

Therefore, the GLL relationship for the Weibull scale parameter η becomes

$$\begin{aligned} \eta(V) &= e^{\alpha_0 + \alpha_1 \ln V_1 + \alpha_2 V_2} \\ &= e^{\alpha_0 + \alpha_2 V_2} V_1^{\alpha_1} \\ &= e^{\alpha_0 + \alpha_2 V_2} V_1^{\alpha_1} \end{aligned} \tag{7.6}$$

Table 7.1: Linear Ball Bushing Representative Failure Times from ALT

				Failure Time Replicates [hours]							
Treatment	A	B	C	X1	X2	X3	X4	Y1	Y2	Y3	Y4
(1)	−1	−1	−1	168 S	168 S	168 S	168 S	168 S	168 S	168 S	168 S
a	+1	−1	−1	160 S	160 S	160 S	160 S	160 F	160 S	160 S	160 S
b	−1	+1	−1	128 S	128 S	128 S	128 S	128 S	128 F	128 S	128 S
ab	+1	+1	−1	113 S	113 S	113 S	113 S	113 F	113 S	113 S	113 S
c	−1	−1	+1	168 S	168 S	168 S	168 S	168 S	168 S	168 S	168 S
ac	+1	−1	+1	154 S	154 S	154 S	154 S	154 S	154 F	154 S	154 S
bc	−1	+1	+1	126 S	126 S	126 S	126 S	126 S	126 F	126 S	126 S
abc	+1	+1	+1	106 S	106 S	106 S	106 S	106 F	106 S	106 S	106 S

Note: S = Suspension, F = Failure

Table 7.2: Linear Ball Bushing Representative Accumulated Travel at Failure from ALT

				Accumulated Travel at Failure Replicates [km]															
Treatment	A	B	C	X1		X2		X3		X4		Y1		Y2		Y3		Y4	
(1)	−1	−1	−1	42.93	S	42.93	S	42.93	S	42.93	S	63.61	S	63.61	S	63.61	S	63.61	S
a	+1	−1	−1	40.89	S	40.89	S	40.89	S	40.89	S	60.58	F	60.58	S	60.58	S	60.58	S
b	−1	+1	−1	32.71	S	32.71	S	32.71	S	32.71	S	48.47	S	48.47	F	48.47	S	48.47	S
ab	+1	+1	−1	28.88	S	28.88	S	28.88	S	28.88	S	42.79	F	42.79	S	42.79	S	42.79	S
c	−1	−1	+1	42.93	S	42.93	S	42.93	S	42.93	S	63.61	S	63.61	S	63.61	S	63.61	S
ac	+1	−1	+1	39.35	S	39.35	S	39.35	S	39.35	S	56.04	S	56.04	F	56.04	S	56.04	S
bc	−1	+1	+1	32.20	S	32.20	S	32.20	S	32.20	S	46.20	S	46.20	F	46.20	S	46.20	S
abc	+1	+1	+1	27.09	S	27.09	S	27.09	S	27.09	S	37.87	F	37.87	S	37.87	S	37.87	S

Note: S = Suspension, F = Failure

Substituting (7.6) into the 2-parameter Weibull CDF and PDF yields

$$\begin{aligned} F(t) &= 1 - \exp\left(-\left(\frac{t}{\eta}\right)^{\beta}\right) \\ &= 1 - \exp\left(-\left(\frac{t}{e^{\alpha_0+\alpha_2 V_2} V_1^{\alpha_1}}\right)^{\beta}\right) \\ &= 1 - \exp\left(-\left(\frac{t}{V_1^{\alpha_1}}\right)^{\beta} e^{-\beta(\alpha_0+\alpha_2 V_2)}\right) \end{aligned} \tag{7.7}$$

$$\begin{aligned} f(t) &= \frac{\beta}{\eta}\left(\frac{t}{\eta}\right)^{\beta-1} \cdot \exp\left(-\left(\frac{t}{\eta}\right)^{\beta}\right) \\ &= \frac{\beta}{e^{\alpha_0+\alpha_2 V_2} V_1^{\alpha_1}}\left(\frac{t}{e^{\alpha_0+\alpha_2 V_2} V_1^{\alpha_1}}\right)^{\beta-1} \cdot \exp\left(-\left(\frac{t}{e^{\alpha_0+\alpha_2 V_2} V_1^{\alpha_1}}\right)^{\beta}\right) \\ &= \beta\left(\frac{t}{V_1^{\alpha_1}}\right)^{\beta-1} e^{-\beta(\alpha_0+\alpha_2 V_2)} \cdot \exp\left(-\left(\frac{t}{V_1^{\alpha_1}}\right)^{\beta} e^{-\beta(\alpha_0+\alpha_2 V_2)}\right) \\ &= \beta\left(\frac{t}{V_1^{\alpha_1}}\right)^{\beta-1} \cdot \exp\left(-\beta(\alpha_0+\alpha_2 V_2) - \left(\frac{t}{V_1^{\alpha_1}}\right)^{\beta} e^{-\beta(\alpha_0+\alpha_2 V_2)}\right) \end{aligned} \tag{7.8}$$

Using statistical analysis software ALTA PRO by Reliasoft and the MLE method for parameter estimation, the following best fit values are found for the data:

$$\widehat{\beta} = 61.1 \tag{7.9}$$
$$\widehat{\alpha}_0 = 4.0657 \tag{7.9a}$$
$$\widehat{\alpha}_1 = -0.10106 \tag{7.9b}$$
$$\widehat{\alpha}_2 = 0.34938 \tag{7.9c}$$

resulting in the unreliability function $F(t)$ of

$$\begin{aligned} F(t) &= 1 - \exp\left(-\left(\frac{t}{V_1^{-0.10106}}\right)^{61.1} e^{-61.1(4.0657+0.34938 V_2)}\right) \\ &= 1 - \exp\left(-t^{61.1} V_1^{6.175} e^{-248.41-21.35 V_2}\right) \end{aligned} \tag{7.10}$$

and reliability function $R(t)$ of

$$R(t) = \exp\left(-t^{61.1} V_1^{6.175} e^{-248.41-21.35 V_2}\right) \tag{7.11}$$

Figure 7-1 is the Weibull plot of the accumulated travel at failure data at the *use stress levels* of $V_1 = 1.8\,\text{kg}$ load (mass of the extruder) and $V_2 = 1$ (lubricated as per standard procedure).

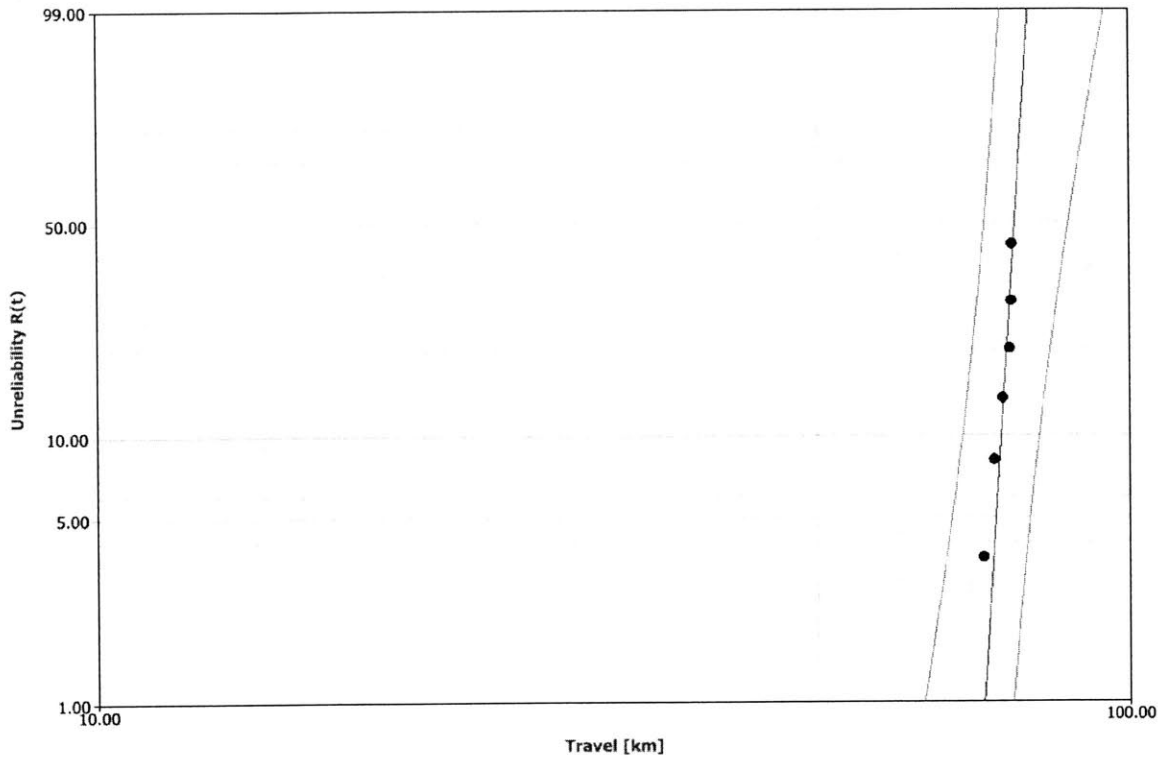

Figure 7-1: Weibull plot of accumulated linear bearing travel at failure at the use stress levels of $V_1 = 1.8\,\text{kg}$ and $V_2 = 1$. $\beta = 61.1$ and $\eta = 77.91$. This plot was created using ALTA PRO software by Reliasoft and using the representative data generated in this section for illustrative purposes.

Table 7.3: Conservative assumptions about a typical print and printer usage

Assumption	Units	Value	Comments
Duration of average print	hr	1	Based on observation
Duty cycle	%	100	Worst case scenario with no downtime
Prints per day		24	Due to 100% duty cycle
Y bearing travel per print	mm	2000	Based on observation
Travel per hour	mm/hr	2000	
Travel per year	km/year	17.52	24×365 hours per year

7.1.3 B_x Life

Estimates of the B_x life at use stress levels $V_1 = 1.8\,\text{kg}$, $V_2 = 1$ and at a given unreliability levels $0 < x < 100\%$ can be obtained by substituting the desired reliability value $R = 1 - x$ into (7.11) and solving for t. For example, the B_1 life is

$$\begin{aligned} R(t) &= \exp\left(-t^{61.1} V_1^{6.175} e^{-248.41-21.35V_2}\right) \\ \Rightarrow t &= \left(-\frac{\ln R}{V_1^{6.175} e^{-248.41-21.35V_2}}\right)^{1/\beta} \\ &= \left(-\frac{\ln 0.99}{(1.8)^{6.175} e^{-248.41-21.35(1)}}\right)^{1/61.1} \\ &= 72.2668\,\text{km} \end{aligned} \tag{7.12}$$

A B_1 life of 72.2668 km means that at use conditions, 1% of linear bushings are expected to fail after accumulating 72.2668 km of travel. Making the assumptions about a typical print and printer usage detailed in Table 7.3, this equates to a linear bushing life of 4.12 years before failure.

The B_{99} life is when 99% of linear bushings are expected to fail at use conditions. This is found it be $B_{99} = 79.8898\,\text{km}$ or 4.56 years before failure, making the same assumptions as before.

This indicates that there is a very small duration during which rapid failures occur. The extremely high Weibull slope parameter of $\beta = 61.1 \gg 1$ also indicates an increasing failure rate with time and rapid failure near end of life.

7.1.4 Reliability at End of Lease

The NVPro lease is a 5 year term. Using the same assumptions used to calculate the B_1 life, outlined in Table 7.3, this equates to 87.6 km of travel. (7.11) can once again

be used, this time to determine the reliability R at use conditions and $t = 87.6$.

$$\begin{aligned} R(t) &= \exp\left(-t^{61.1}V_1^{6.175}e^{-248.41-21.35V_2}\right) \\ &= \exp\left(-(87.6)^{61.1}(1.8)^{6.175}e^{-248.41-21.35(1)}\right) \\ &\approx 0 \end{aligned} \tag{7.13}$$

Therefore, there is 100% probability that all bearings would have failed by the end of the 5 year lease. This is obviously an alarming conclusion, but one that should be taken with caution as the result is very sensitive to the assumptions in Table 7.3 due to the extremely narrow failure region, approximately 72.2668 km to 79.8898 km or 4.12 years to 4.56 years. It is also based on representative data only.

7.2 Summary

This chapter presented representative life data that would be collected if the ALT detailed in Chapter 6 were executed. The data was subsequently analyzed for illustrative purposes. Load and lubrication were the only two factors assumed to be statistically significant. A general log-linear life-stress relationship with those two stresses was combined with the 2-parameter Weibull distribution to model the ALT results. A statistical software package was used to employ the maximum likelihood estimation (MLE) method and obtain model parameter estimates.

The resulting reliability function was used to determine the B_1 and B_{99} lives at use stress conditions to be 72.2668 km and 79.8898 km of accumulated travel respectively. These use conditions accumulated travel were converted to a life estimates in years following a set of assumptions about the typical print and printer duty cycle. Assuming a typical print lasts 1 hour, accumulates 2000 mm of travel on the Y bearings, and the printer is operating on a 100% duty cycle 24/7, the B_1 and B_{99} lives at use stress conditions were 4.12 years and 4.56 years respectively. The same assumptions and the reliability function were also used to determine the reliability of the printer at the end of the 5 year NVPro lease to be 0%, *i.e.* 100% of the linear bushings would have failed by end of lease.

It should be noted that the results were based on representative data only, generated using the author's engineering judgement, intuition, and basic calculations. Any subsequent analysis was also based on a series of assumptions about the results, the statistical model, and the typical usage of the NVPro. The analysis in this chapter was merely meant to illustrate the analysis techniques and procedures that should be implemented by NVBOTS upon collection of actual life data.

Chapter 8

Conclusions, Recommendations, and Future Work

8.1 Conclusions

The purpose of the overall MEngM-NVBOTS collaborative project was to introduce process improvements to match production scale-up at NVBOTS with the scale-up of startup itself. This was accomplished through three sub-projects completed by the MEngM team. Chawla focused on developing a framework for incoming part quality control and inspection procedures, the details of which can be found in his thesis [11]. Straub focused on failure tracking during the development effort, the details of which can be found in his thesis [12]. This thesis focused on improving product reliability through systematic failure analysis and a quantitative understanding of product life through accelerated life testing (ALT). The objectives of the thesis were the creation and implementation of Failure Modes and Effects Analysis (FMEA), and the complete design of an ALT including the theoretical background and experimental hardware design required to estimate the life of a product.

The following conclusions are drawn from the work performed on product reliability:

Importance of product reliability The importance of product reliability to a high-technology manufacturing cannot be understated. The difference between successful scale-up and business failure hinges on delivering a complete, high-quality, and reliable customer experience and this begins with a robust manufacturing during scale-up. The company's image, brand reputation, and financial bottom-line revolves around a reliable product. Specific to NVBOTS, the 5-year lease of the NVPro printer to customers means any service, repair, and replacement costs are directly burdened by NVBOTS. Ensuring a reliable product will reduce the risk of excessive service costs and potential insolvency.

Reliability in design and manufacturing Product design and manufacturing determine the product's reliability, and thus, should be at the forefront of both design and manufacturing engineers minds from early development stages. Ensuring reliability begins with a thorough understanding of how the product will

fail, estimating the impact of these failures and the resulting product life, and mitigating these risks moving forward.

Systematic failure analysis: FMEA Failure Modes and Effects Analysis (FMEA) is a systematic approach to failure analysis through a combination of inductive reasoning and deductive analysis. It involves a comprehensive review of potential failure modes of components, assemblies, and subsystems within a system or product and their underlying failure mechanisms. An FMEA worksheet was developed and used as a tool to evaluate all critical components in the NVPro printer and identify the top priority risk item for further analysis.

Top priority risk: linear ball bushings The linear ball bushings using in the NVPro to enable precise X and Y linear movement of the extruder within the gantry system were identified as the top priority risk. If these bushings were to fail, it would have a catastrophic impact on the printer and would require an immediate swap at the customer site. Therefore, a better understanding of its component life was required, and its life was used to approximate overall printer life. However, before life testing was conducted, potential failure modes of linear bushings were investigated in depth to establish a baseline understanding of degradation of life mechanisms. These failure modes included: adhesive wear, abrasive wear, corrosion, fretting corrosion, false brinelling, and spalling.

Accelerated life testing (ALT) In order to quantitatively estimate the life of the linear bushings with statistical rigor, an accelerated life test was designed. ALT allows for accurate estimation of product life through a special experiment specifically designed to cause failure in a shorter period of time. Background literature on statistical modelling and design techniques of ALT was presented. The general log-linear (GLL) life-stress relationship and the 2-parameter Weibull distribution was selected to model the life of the linear bushings.

Design of Experiment (DOE) A traditional DOE approach was taken in the statistical design of the ALT. The response of the test was the life of the bearings in hours, later converted to travel in kilometers. The control factors varied in the test were mechanical load (in the form of additional weight added to the moving system), bearing lubrication, and degree of misalignment of the Y shafts the bearings travel along. It was unknown at the time of beginning of the experiment which factors would actually be statistically significant. A full factorial 2^3 experiment with a single center point and eight replicates per treatment was employed. A test apparatus was design using product NVPro components, barbell plates for additional loading, and a mechatronic control system for continuous operation during the ALT.

ALT results Though the ALT was completely designed and ready to operate, the experiment could not be run due to project time constraints. However, representative data was presented to illustrate ALT statistical analysis techniques. Using the GLL-Weibull model, it was determined the NVPro's linear bushings

B_1 life, when 1% of all linear bushings in NVPros were expected to fail, was approximately 72.2668 km of accumulated bearing travel or 4.12 years of printer usage, assuming a 100% printer duty cycle, an average print duration of 1 hour, and an accumulation of 2000 mm of travel per Y bearing per print. These results merely illustrate the analysis methodology.

8.2 Recommendations

Based on the work presented, the following recommendations are made regarding continued reliability improvement:

Iterative FMEA use FMEA is an essential reliability engineering tool that should be used iteratively throughout the entire product development process from concept through production and sustaining. The true value of FMEA stems from continued usage to identify, understand, and retire risks. In the immediate future, it should be used to study other critical components more extensively for similar ALT analysis. However, moving forward it should also be used at the system level to systemically analyze printer-level failures. A template worksheet to do so has been provided to NVBOTS.

Execution of ALT The ALT for linear bushings was completely designed and setup, and all necessary background information of statistical analysis was presented. It is recommended that the experiment now be executed to obtain actual estimates of reliability.

Degradation analysis Due to the low number of failures per treatment (1 out of every 8 bearings), it is recommended that degradation analysis also be performed as a secondary reliability calculation. The response should be measurement of bearing wear, characterized by change in inner bearing radius or mass lost to wear debris.

ALT of other critical components Overall product reliability is the product of individual component reliability. Therefore, similar ALT experiments should be conducted for all critical components, identified by a *Unacceptable* risk priority index to obtain an accurate system level understanding of reliability. The test apparatus was designed to accommodate future ALT experiments of XY gantry components.

Hardware build coordination One of the primary reasons the ALT was not executed was lack of time and resources. The mechatronic design of the testing hardware proved to have many unexpected errors and required troubleshooting by an electrical engineer. Though help was available when needed, it put unforeseen pressure on the only electrical engineer on staff at NVBOTS. Early incorporation of both mechanical and electrical engineers into an ALT project with a mechatronic hardware system would ensure correct design and timely troubleshooting, resulting in faster time-to-execution.

Adopting a reliability culture The importance of product reliability has continuously been stressed and demonstrated throughout the work presented. However, it is crucial that a culture of reliability is embraced and adopted at high-technology manufacturing startups. Design engineers should constantly be evaluating designs based on reliability, and should collaborate with manufacturing engineers as early as possible to ensure the reliability carries forward through manufacturing. On an strategic level, the startup should plan personnel hiring and operational procedures in anticipation of reliability risks. This can include hiring an experienced manufacturing and reliability engineer, or consulting contract manufacturers as early as possible. The cost of shipping unreliable product can cripple the startup during the scale-up phase before it even has a chance to flourish.

8.3 Future Work

The work performed by the author provides a starting point for NVBOTS and similar high-technology startups in improving their product reliability during manufacturing scale-up. However, the following ideas present a road-map for future work by NVBOTS or other researchers:

In-depth failure modes investigation The failure modes identified through FMEA were based on prior experience of the NVBOTS engineering staff and the author, literature review of common failure modes, and inductive reasoning. A long-term study of failures observed in the field would characterize the system and provide a better understanding of which risks to focus reliability efforts on. A failure tracking system similar to one developed by Straub in [12] can be used.

Maintaining a statistical reliability library As the company grows, it may prove impractical to always run an ALT to gather basic statistical data such as model parameter values. Therefore, careful execution and documentation of any future ALTs will result in a rich library of application specific statistical parameters, allowing for quick and easy reliability analysis in the future for the same or similar components.

Financial impact of reliability and warranty Due to time constraints, the author was unable to execute the designed ALT and perform actual financial analysis based on the results. Once this data has been collected, a cost model could be developed or modified based on work done by Straub [12] to analyze the financial impact of service costs, repairs, and replacements. Once enough units are in the field, product warranty plans could be developed and implemented using field life data and ALT data along with rigorous statistical analysis similar to that presented here.

Bibliography

[1] A. Hirai, "What Kills Startups?" *Cayenne Consulting*, 2010. [Online]. Available: http://www.caycon.com/downloads/What-Kills-Startups.pdf

[2] M. Less, "Startupedia: What Does Scaleup Mean?" [Online]. Available: http://blog.startupinstitute.com/2015-3-24-what-is-a-scaleup/

[3] S. Berger, "Scaling up Startups to Market," in *Making in America: From Innovation to Market.* Cambridge, MA: MIT Press, 2013, ch. 3, pp. 65–89.

[4] National Venture Capital Association, "Annual Venture Capital Investment Tops $48 Billion in 2014," 2015. [Online]. Available: http://nvca.org/pressreleases/annual-venture-capital-investment-tops-48-billion-2014-reaching-highest-level-decade-according-moneytree-report/

[5] T. Kurfess, "Why Manufacturing Matters," *American Society of Mechanical Engineers*, no. November, 2013. [Online]. Available: https://www.asme.org/engineering-topics/articles/manufacturing-processing/why-manufacturing-matters

[6] C. Banden-Fuller and I. MacMillan, "3 Mistakes Made in Scaling up New Ventures," *Harvard Business Review*, Aug. 2010. [Online]. Available: http://blogs.hbr.org/2010/08/3-mistakes-made-in-scaling-up/

[7] M. Barros, "Poor Quality Will Kill You." [Online]. Available: http://marcbarros.com/poor-quality-will-kill-you/

[8] E. R. Reynolds and H. Samel, "Invented in America, Scaled Up Overseas," *ASME Mechanical Engineering Magazine*, no. November, Nov. 2013. [Online]. Available: https://www.asme.org/engineering-topics/articles/manufacturing-processing/invented-america-scaled-up-overseas

[9] K. Weisul, "Everything Your Startup Needs to Know About Manufacturing," 2015. [Online]. Available: http://www.inc.com/kimberly-weisul/five-lessons-from-the-manufacturing-trenches.html

[10] NVBOTS, "About Us." [Online]. Available: http://nvbots.com/about/

[11] R. Chawla, "Scale-Up of a High Technology Manufacturing Startup: Framework for Analysis of Incoming Parts, Inspection Procedure and Supplier Capability," M.Eng. Thesis, Massachusetts Institute of Technology, 2015.

[12] D. Straub, "Scale-Up of a High Technology Manufacturing Startup: Failure Tracking, Analysis, and Resolution through a Multi-Method Approach," M.Eng. Thesis, Massachusetts Institute of Technology, 2015.

[13] T. Wohlers and T. Caffery, *Wohlers Report 2015: Additive Manufacturing and 3D Printing State of the Industry : Annual Worldwide Progress Report.* Fort Collins: Wholers Associates, Inc, 2015.

[14] I. Gibson, D. W. Rosen, and B. Stucker, *Additive Manufacturing Technologies*, second edi ed. New York: Springer, 2015.

[15] ASTM International, "F2792-12a - Standard Terminology for Additive Manufacturing Technologies," pp. 10–12, 2013.

[16] MIT Lincoln Laboratory, "Additive Manufacturing Methods Schematics," MIT Lincoln Laboratory, Lexington, MA, Tech. Rep., 2014.

[17] NVBOTS, "Pricing." [Online]. Available: http://nvbots.com/pricing/

[18] ——, "NVPRO." [Online]. Available: http://nvbots.com/nvpro/

[19] ——, "MYNVBOTS." [Online]. Available: http://nvbots.com/mynvbots/

[20] ——, "NVLIBRARY." [Online]. Available: http://nvbots.com/nvlibrary/

[21] M. A. Cusumano, "Evaluating a startup venture," *Communications of the ACM*, vol. 56, no. 10, p. 26, 2013. [Online]. Available: http://dl.acm.org/citation.cfm?doid=2507771.2505337

[22] R. Dobbs, J. Manyika Yougang Chen, M. Chui, and S. Lund, "McKinsey Global Institute The McKinsey Global Institute," no. May, 2013.

[23] United States Department of Defense, "MIL-STD-1629A Procedures for Performing a Failure Mode, Effects and Criticality Analysis," United States Department of Defense, Washington, DC, Tech. Rep., 1980.

[24] ——, "MIL-STD-882E System Safety," United States Department of Defense, Washington, DC, Tech. Rep., 2012.

[25] E. E. Bisson, "Various Modes of Wear and Their Controlling Factors," in *American Society for Testing and Materials*, National Aeronautics and Space Administration. Cleveland, OH: NASA, 1968.

[26] C. Horst, T. Saito, and L. Smith, "Friction and Wear," in *Springer Handbook of Materials Measurement Methods.* Würzburg, GE: Springer Science+Business Media, Inc, 2006, ch. 13, pp. 685–710.

[27] National Aeronautics and Space Administration, "Lubrication, Friction, and Wear," National Aeronautics and Space Administration, Springfield, VA, Tech. Rep., 1971.

[28] SKF Bearings Corporation, "Bearing Failures and Their Causes," SKF Bearings Corporation, Sweden, Tech. Rep., 1994.

[29] The Barden Corporation, "Bearing Failure: Causes and Cures," The Barden Corporation, Danbury, CT, Tech. Rep., 2007.

[30] The Timken Company, "Timken Bearing Damage Analysis with Lubrication Reference Guide," The Timken Company, Tech. Rep., 2014. [Online]. Available: http://www.timken.com/EN-US/Knowledge/ForMaintenanceProfessionals/Documents/Bearing-Damage-Analysis-Reference-Guide.pdf

[31] S. Shaffer and W. Glaeser, "Fretting Fatigue," in *ASM Metals Handbook Volume 19: Fatigue and Fracture.* ASM International, 1996, pp. 801–824.

[32] H. Rinne, *The Weibull Distribution: A Handbook.* Boca Raton, FL: CRC Press, 2009.

[33] W. Nelson, *Accelerated Testing: Statistical Models, Test Plans, and Data Analysis.* Hoboken, NJ: John Wiley & Sons, Inc., 2004.

[34] Reliasoft Corporation, "Life Data Analysis Reference," Reliasoft Corporation, Tuscon, AZ, Tech. Rep., 2015.

[35] ——, "Accelerated Life Testing Reference," Reliasoft Corporation, Tuscon, AZ, Tech. Rep., 2015.

[36] D. C. Montgomery, *Introduction to Statistical Quality Control*, 6th ed. Jefferson City, MO: John Wiley & Sons, Inc., 2009.

[37] Calimo, "Weibull distribution," 2010. [Online]. Available: https://en.wikipedia.org/wiki/Weibull_distribution

[38] P. commonswiki, "Lognormal Distribution PDF," 2005. [Online]. Available: https://commons.wikimedia.org/wiki/File:Lognormal_distribution_PDF.png

[39] Reliasoft Corporation, "Experiment Design and Analysis Reference," Reliasoft Corporation, Tuscon, AZ, Tech. Rep., 2015.

[40] R. E. DeVor, T.-h. Chang, and J. W. Sutherland, *Statistical Quality Design and Control: Contemporary Concepts and Methods.* New York, NY: Macmillan Publishing Company, 1992.

[41] Reliasoft Corporation, "Using DOE Results in the Design of an Accelerated Life Test," 2015. [Online]. Available: http://www.reliasoft.com/newsletter/v10i2/doe_results.htm

[42] S. Strzelecki, "Operating Characteristics of Heavy Loaded Cylindrical Journal Bearing with Variable Axial Profile," *Materials Research*, vol. 8, no. 4, pp. 481–486, 2005.

[43] F. Campbell, *Elements of Metallurgy and Engineering Alloys.* Materials Park, Ohio: ASM International, 2008.

[44] R. G. Budynas and J. K. Nisbett, *Shigley's Mechanical Engineering Design*, 9th ed. Singapore: McGraw Hill, 2011.

[45] MISUMI USA Inc., "Calculation of Lifespan of Linear Systems," MISUMI USA Inc., Tech. Rep., 2015.

[46] E. V. Zaretsky, "A. Palmgren Revisited: A Basis for Bearing Life Prediction," in *Society of Tribologists and Lubrication Engineers Annual Meeting.* Cleveland, OH: National Aeronautics and Space Administration, 1997.

[47] K. S. Sollmann, M. K. Jouaneh, and D. Lavender, "Dynamic modeling of a two-axis, parallel, H-frame-type XY positioning system," *IEEE/ASME Transactions on Mechatronics*, vol. 15, no. 2, pp. 280–290, 2010.